Multitrait analysis of *Arabidopsis thaliana* and two *Chenopodium* species under different stress regimes

I n a u g u r a l - D i s s e r t a t i o n

zur

Erlangung des Doktorgrades

der Mathematisch-Naturwissenschaftlichen Fakultät

der Universität zu Köln

vorgelegt von

Barbara Annemarie Marlene Paffendorf

aus Bergisch Gladbach

Köln, 2024

Berichterstatter/in:	Prof. Dr. Martin Hülskamp
	Prof. Dr. Ute Höcker
Prüfungsvorsitzender:	Prof. Dr. Michael Bonkowski

Tag der mündlichen Prüfung: 04.11.2024

Table of Contents

List of Figures

List of Tables

List of Abbreviations

AC	active complex
ACT2	ACTIN2
AD	activator-depletion
AI	activator-inhibitor
AM	Anna Marxer
AST	Alexandra Steffens
AT4G33380	dimethylallyl, adenosine tRNA methylthiotransferase
A. thaliana	*Arabidopsis thaliana*
A. tumefaciens	*Agrobacteria tumefaciens*
BC	bladder cell
bHLH	basic helix–loop–helix
bp	base pairs

BP	Barbara Paffendorf
cbp20	*cap-binding protein 20*
°C	degrees Celsius
cDNA	complementary DNA
Cl^-	chlorid
COP1	CONSTITUTIVE PHOTOMORPHOGENIC 1
CP	crossing point
CPC	CAPRICE
d	day
ddH_2O	double distilled water
DNA	deoxynucleotide acid
DNase	deoxyribonuclease
E	efficiency
ebcf	*epidermal bladder cell-free*
EC	epidermal cell
E. coli	*Escherichia coli*
EDTA	Ethylenediaminetetraacetic acid
eFP	electronic Fluorescent Pictograph
EGL3	ENHANCER OF GLABRA 3
EIF4α	EUKARYOTIC TRANSLATION INITIATION FACTOR 4A1
EMS	ethyl methanesulfonate
EP	Eva Koebke Primer

EtBr	ethidium bromide
ETC1, 2, 3	ENHANCER OF TRY AND CPC 1, 2, 3
EtOH	ethanol
F	forward
GL1, 2, 3	GLABRA 1, 2, 3
GIS	GLABROUS INFLORESCENCE STEMS
GLK1	GOLDEN2-LIKE 1
h	hour
HCF	HIGH CHLOROPHYLL FLUORESCENCE 164
HCl	hydrochloric acid
HY5	ELONGATED HYPOCOTYL 5
IC	inactive complex
IUCN	International Union for Conservation of Nature
JP	Jessica Pietsch
JS	Julian Schiffner
K^+	potassium
kb	kilo base pairs
KCl	potassium chloride
KOH	potassium hydroxide
l	liter
LD	long-day (16 h light, 8 h darkness)
m	meter

mA	milliampere
$MgCl_2$	magnesium chloride
$MgSO_4$	magnesium sulfate
min	minute
ml	milliliter
mm	millimeter
mM	millimole
MS	Murashige and Skoog
R2R3-MYB	Repeat 2 Repeat 3 MYELOBLASTOSIS ONCOGENE
MYB5, 23, 82	MYELOBLASTOSIS ONCOGENE 5, 23, 82
MYC1	MYELOCYTOMATOSIS ONCOGENE 1
Na^+	Sodium
NaCl	sodium chloride
NaClO	sodium hypochlorite
NaOH	sodium hydroxide
nm	nanometer
OE	overexpression
PAP1, 2	PRODUCTION OF ANTHOCYANIN PIGMENT 1, 2
pH	pondus Hydrogenii
PK	Patrizia Kroll
PSB33	PHOTOSYSTEM B PROTEIN33
R	reverse

R^2	coefficient of determination
RD29A	RESPONSE-TO-DEHYDRATION29A
REBC	REDUCED LEVELS OF EBCs
RNA	ribonucleic acid
rRNA	ribosomal RNA
RNase	ribonuclease
rpm	revolutions per minute
RT	room temperature
s	second
SAND	SAND family protein
SC	stalk cell
SD	short-day (8 h light, 16 h darkness)
sec	second
18S rRNA	18S ribosomal RNA
TAE	Tris-acetate-EDTA
TC	trichome cell
TCL1, 2	TRICHOMELESS 1, 2
TI	trichome initial cell
TIP41	TAP42 INTERACTING PROTEIN OF 41 KDA
TRY	TRIPTYCHON
TT2, 8	TRANSPARENT TESTA 2, 8
TTG1	TRANSPARENT TESTA GLABRA 1

TUA5	TUBULIN ALPHA-5
U	enzyme unit
UBC/UBC21/PEX4	UBIQUITIN CARRIER PROTEIN 21/PEROXIN-4
UBQ10	UBIQUITIN 10
UV	ultraviolet
V	volt
WD40	tryptophan aspartate 40
WER	WEREWOLF
YEB	Yeast Extract Beef
µl	microliter
µmol	micromole

Zusammenfassung

Der Klimawandel ist ein schwerwiegendes globales Problem, das weitreichende Folgen für die Pflanzenentwicklung hat. Die genauen Mechanismen, durch die der Klimawandel die physiologischen und genetischen Prozesse von Pflanzen beeinflusst, sind in vielen Bereichen noch nicht vollständig verstanden. Um umfassendere Einblicke in dieses komplexe Thema zu erhalten, wurde für diese Arbeit der Modellorganismus *Arabidopsis thaliana* ausgewählt. *A. thaliana* eignet sich aufgrund seiner einfachen Genetik und seines kurzen Lebenszyklus ideal für experimentelle Studien. In den durchgeführten Experimenten wurde *A. thaliana* verschiedenen Stressbedingungen ausgesetzt, darunter unterschiedlichen Lichtintensitäten und erhöhter Temperatur. Diese Stressfaktoren sind im Zusammenhang mit dem Klimawandel besonders relevant, da in vielen Regionen mit steigenden Temperaturen zu rechnen ist. Ein zentraler Schwerpunkt dieser Studie ist das MBW (MYB-bHLH-WD40) Netzwerk, in dem TRANSPARENT TESTA GLABRA1 (TTG1) als wesentlicher Interaktionspartner bei der Regulierung von Pflanzenmerkmalen wie der Trichomentwicklung fungiert. Zu verstehen, wie das MBW-Netzwerk auf externe Stressfaktoren reagiert und wie es diese auf Expressionsebene integriert, könnte entscheidende Erkenntnisse darüber liefern, wie sesshafte Organismen mit den Herausforderungen des Klimawandels umgehen. Durch die Analyse der Genexpression innerhalb des MBW-Netzwerks und die Auswertung der phänotypischen Reaktionen auf verschiedene Stressbedingungen, wurden in dieser Studie wertvolle Informationen gewonnen, die das Verständnis der Anpassungsmechanismen von Pflanzen verbessern könnten. Es zeigte sich, dass schwache und starke Licht Bedingungen die Entwicklung von Trichomen beeinflussen, wobei starkes Licht eine Erhöhung der Trichomdichte bewirkte, um möglicherweise Schutz vor zunehmender Strahlung zu bieten. Darüber hinaus wurde festgestellt, dass ein kurzer Stresszeitraum zu schnellen Expressionsänderungen auf genetischer Ebene führte, für eine beobachtbare phänotypische Änderung jedoch eine konstante Änderung der Umweltbedingungen erforderlich ist. Ähnliche Trends wurden bei *Chenopodium quinoa* und *Chenopodium suecicum* beobachtet, bei denen Salzstress zu einer erhöhten Trichomdichte auf der adaxialen Blattseite führte. Als salzresistente Pflanzen eignen sich die *Chenopodium*-Arten für die Analyse der Auswirkungen von Salzstress. Diese Erkenntnisse tragen zu einem tieferen Verständnis der Stressreaktion von Pflanzen im Hinblick auf die Herausforderungen des Klimawandels bei.

Abstract

Climate change is a severe global issue that has far-reaching consequences for plant development. The exact mechanisms by which climate change affects the physiological and genetic processes of plants are not fully understood in many areas. To gain more comprehensive insights into this complex topic, the model organism *Arabidopsis thaliana* was selected for this work. *A. thaliana* is ideally suited for experimental studies due to its simple genetics and short life cycle. In the conducted experiments, *A. thaliana* was exposed to different stress conditions, including varying light intensities and elevated temperature. These stress factors are particularly relevant in the context of climate change, as rising temperatures are expected in many regions. A central focus of this study is the MBW (MYB-bHLH-WD40) network, in which TRANSPARENT TESTA GLABRA1 (TTG1) acts as the essential interaction partner in the regulation of plant traits such as trichome development. Understanding how the MBW network responds to external stress and integrates these responses at the gene expression level could provide crucial insights into how sessile organisms cope with climate change challenges. By analyzing the expression of genes within the MBW network and evaluating the phenotypic responses to various stress conditions, valuable information was obtained in this study that could improve the understanding of plant adaptation mechanisms. It was shown that low- and high-light conditions affect the development of trichomes, with high light causing an increase in trichome density, to potentially protect against higher radiation levels. Additionally, it was found that a short period of stress stimulus led to rapid expression changes at the genetic level, but a constant change of the environmental conditions was required for an observable phenotypic change. Similar trends were observed in *Chenopodium quinoa* and *Chenopodium suecicum*, where salt stress led to an increased trichome density on the adaxial leaf side. As salt-resistant plants, the *Chenopodium* species are suitable for the analysis of the effects of salt stress. These insights contribute to a deeper understanding of how plants respond to stress, particularly in the face of climate change challenges.

1 Introduction

The ongoing global climate change is leading to weather extremes that can adversely affect ecosystem health and food security (Lee et al., 2023). In particular, plants are more frequently exposed to heat and drought stress, which not only limit plant growth and grain yield, but can also promote soil salination (Dreesen et al., 2012; Rizza et al., 2004; Schofield & Kirkby, 2003). In addition to heat and drought, the increasing occurrences of unusual cold snaps, heavy rainfall, and flooding have profound effects on the environment (Cameron & Scrosati, 2023; Trenberth, 2011). Such weather events can disrupt ecosystems and potentially result in the decline of biodiversity, including species within the plant kingdom (Cameron & Scrosati, 2023; Talbot et al., 2018). For instance, Cameron and Scrosati documented that a cold snap in February 2023 in eastern Canada led to a mass disappearance of mussels. Furthermore, according to the International Union for Conservation of Nature (IUCN) Red List, which includes more than 163000 species, 45300 species are threatened with extinction, including 41 % of amphibians, 36 % of reef corals, 34 % of conifers and also 26 % of mammals and 12 % of birds (IUCN, 2024). Additionally, heat waves and cold snaps are also dangerous for humans and can lead to loss of life among vulnerable individuals (Shetty, 2024; Tigue, 2024). Moreover, plants are exposed to varying light intensities (Kataria et al., 2014), which can also be negatively affected by climate change (Valladares & Niinemets, 2008). Marine plants are experiencing reduced light intensities as a result of rising sea levels, while at the same time, plants that endure extended periods of heat and drought stress, also caused by prolonged sun exposure, are impacted by increased light intensities (Chaves & Pereira, 1992; Koubouris et al., 2015; Short & Neckles, 1999). These effects also have far-reaching consequences for people, food security and habitats (Agbogidi, 2011; Kahle et al., 2022). Since climate change is more than 50 % man-made, it is our responsibility to develop strategies to counteract the challenges posed by this global change (Lee et al., 2023)

As sessile organisms, plants must adapt to these rapidly changing environmental conditions. One strategy of plant adaption is phenotypic plasticity, meaning the ability of a given genotype to express several phenotypes in response to different stress conditions (Sultan, 2000). It is assumed that phenotypic plasticity is one of the crucial strategies of plants to withstand the pressures of climate change (Merila & Hendry, 2014). Overall, these versatile stress factors

highlight the importance of understanding the resilience of plants to the challenges of climate change and developing strategies to improve their adaptability.

1.1 *A. thaliana* as a model organism for light and heat stress response

A. thaliana belongs to the taxonomic family of the Brassicaceae. It is a facultative long-day plant, which thrives better under certain light conditions (Goto et al., 1991). A key advantage for extensive scientific analyses that require a lot of plant material is its small size, which allows cultivation in limited spaces (Meinke et al., 1998). In addition, it is easy to cultivate and has a short generation time, *A. thaliana* can grow from germination to flowering within just a few weeks (Arabidopsis Genome Initiative, 2000; Kramer, 2015; Li et al., 1998), therefore, several generations can be analyzed in a short period of time. Its small genome consists of five chromosomes and has a total size of approximately 157 Mbp (Bennett et al., 2003). Due to its properties, *A. thaliana* has been established as an essential model organism in plant research and is widely used to study various aspects of plant development and genetic pathways.

The leaves of *A. thaliana* carry trichomes, which serve a variety of essential functions. Among others, they play a role in light reflection and provide protection against harmful UV-B radiation (Bickford, 2016; Hülskamp et al., 1994; Larkin et al., 1996; Liakoura et al., 1997; Suo et al., 2013; Yan et al., 2012). In this context, Suo and colleagues investigated a glassy trichome mutant (*glh*), characterized by more translucent trichomes, that allow greater light penetration. This change in light transmittance highlights the complex relation between trichome structure and light radiation. Trichomes also serve as protection barrier against herbivores (Handley et al., 2005). In addition, a study has demonstrated that the trichome patterning changes in response to heat stress, suggesting that this trichome plasticity may contribute to the environmental fitness of plants (Okamoto et al., 2020). Investigating this topic of adaptability further, for *A. thaliana* and *Arabidopsis lyrata*, a close relative of *A. thaliana*, it was also shown that trichomes contribute to drought tolerance (Jäger et al., 2011; Sletvold & Ågren, 2012). In particular, Jäger and colleagues investigated a drought-tolerant *Arabidopsis* mutant (*cbp20*), which exhibited a greatly increased trichome density. Since climate change will disturb, among others, temperature and light exposure in many regions, these are important conditions whose effects on plants need to be investigated further (Dreesen et al., 2012; Koubouris et al., 2015; Short & Neckles, 1999). Therefore, the following focuses on light and heat stress response in *A. thaliana*.

1.2 *C. quinoa* and *C. suecicum* as model organisms for salt stress response

C. quinoa and *C. suecicum* are two related species of the genus *Chenopodium*. *C. quinoa*, in particular, has become increasingly important in plant research in recent years due to its reputation as a "superfood" with high nutritional value and its salt and drought resistance (Bhathal et al., 2015; Jacobsen et al., 2003). The seeds contain high concentrations of essential fatty acids and natural antioxidants, furthermore, *C. quinoa* is protein-rich and gluten-free (Bhathal et al., 2015; Kozioł, 1992; Ruales & Nair, 1992; Ruales & Nair, 1993). *C. quinoa* is allotetraploid, which probably resulted from genome duplication through genome fusion of two *Chenopodium* parents (Kolano et al., 2016; Palomino et al., 2008). *C. suecicum* is considered one possible parental line (Heitkam et al., 2020). As a diploid species, *C. suecicum* is genetically more accessible than the tetraploid *C. quinoa* (Mandák et al., 2012). Both belong to the halophytes, which are plants that can grow in saline environments and have adapted to complete their life cycle in ≥ 200 mM salt through different mechanisms (Aronson & Whitehead, 1989; Flowers et al., 2010). Both *Chenopodium* species have a special form of trichomes called bladder cells. In *C. quinoa*, these bladder cells serve primarily to excrete and store salt from the leaves to ensure salt tolerance (Kiani-Pouya et al., 2017; Shabala et al., 2014; Thomson et al., 1988). The observed salt resistance in combination with the specialized trichome cells, make the two *Chenopodium* species suitable organisms to study the effect of salt stress.

1.2.1 Salt tolerance mechanisms in halophytes

Soil salinization is one of the greatest threats to agriculture (Rengasamy, 2010) and is often related to irrigation with saline water, excessive chemical fertilization, and inadequate drainage (Abdel Latef, 2010). It strongly affects physiological and biochemical pathways in plants (Nabati et al., 2011), as high accumulation of salt can lead to nutrient deficiency, oxidative stress, growth retardation, and even cell death (Ahanger & Agarwal, 2017). Furthermore, salt stress affects photosynthesis by inhibiting chlorophyll synthesis and restricting electron transport from photosystem II to photosystem I (He et al., 2021; Qin et al., 2020). Understanding the mechanisms by which halophytes have evolved to thrive in these challenging conditions can play a crucial role in enhancing the resilience of crops against environmental stressors, thus contributing to food security.

Among the halophytes, there are excluders that restrict salt transport into the shoot by active salt exclusion via the roots (Alharby et al., 2014; Flowers & Colmer, 2008). For instance, mangroves have developed such specialized root systems to thrive in seawater (Srikanth et al., 2016). Furthermore, there is a group of succulent halophytes that sequester salt into internal storage vacuoles (Bonales-Alatorre et al., 2013; Naidoo & Rughunanan, 1990; Zeng et al., 2018). Another mechanism that approximately 50 % of halophytes have developed is the formation of salt glands that excrete excess salt, or bladder cells, which are used to externally store excess salt (Dassanayake & Larkin, 2017; Flowers & Colmer, 2008; Shabala & Mackay, 2011; Yuan et al., 2016). In *C. quinoa*, sodium (Na^+) and chloride (Cl^-) are sequestered into the vacuole of the bladder cell, which form on the leaf and stem surface (Böhm et al., 2018; Shabala et al., 2014).

1.3 Trichome development in *A. thaliana* and *C. quinoa*

Comparing the formation of trichomes in *A. thaliana* and *C. quinoa* (Figure 1) provides insights into the morphological developmental differences of trichomes on the leaf surface. The two types differ in their development and structure (Hülskamp, 2004; Shabala et al., 2014; Smaoui et al., 2011; Traas et al., 1998).

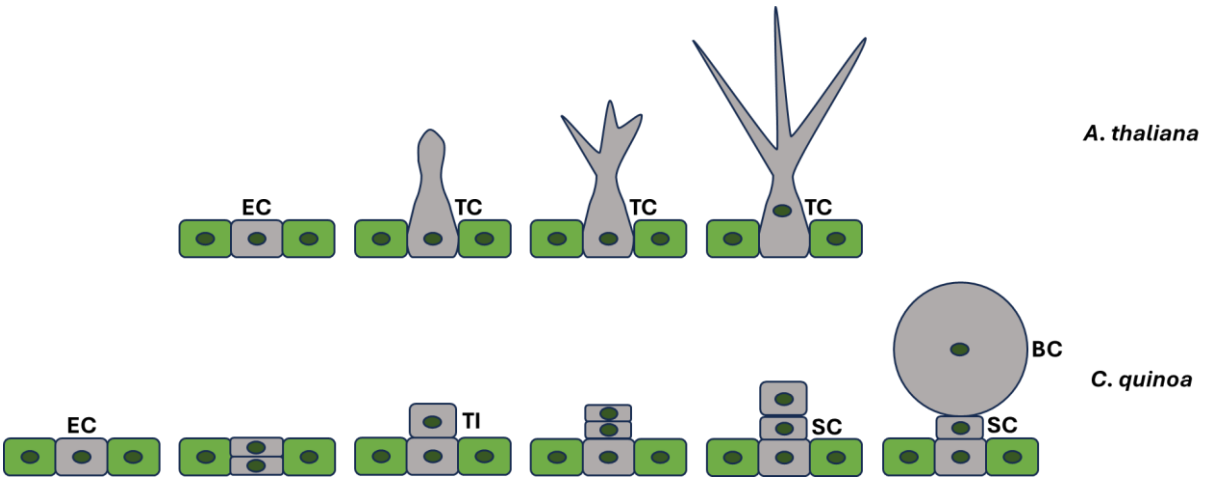

Figure 1: Development of a trichome or bladder cell in *A. thaliana* and *C. quinoa*.From left to right, the step-by-step formation of a trichome (top) or bladder cell (bottom) is shown. In *A. thaliana*, a single trichome cell (TC) is formed from an epidermal cell (EC) by endoreplication and forms into mature trichome with three branches (Traas et al., 1998). A bladder cell in *C. quinoa* is formed by several cell division steps. The epidermal cell divides into two cells, the upper cell develops into the trichome initial cell. This cell divides again. The lower cell develops into the stalk cell, and the upper cell develops into the bladder cell (Shabala et al., 2014). **BC** = bladder cell, **EC** = epidermal cell, **SC** = stalk cell, **TC** = trichome cell, **TI** = trichome initial cell. Modified from Hülskamp, 2004; Shabala et al., 2014 and Smaoui et al., 2011.

In *A. thaliana*, trichomes are unicellular epidermal hairs with typically three branches, which are formed from an epidermal cell (EC) by endoreplication and two branching events

(Hülskamp, 2004; Perazza et al., 1999; Traas et al., 1998). In *C. quinoa,* trichomes are called salt bladders or epidermal bladder cells (EBCs) and are formed by several cell division steps (Shabala et al., 2014; Smaoui et al., 2011). Here, the epidermal cell undergoes two cell division steps, after which the lower cell develops into the stalk cell (SC), and the upper cell increases in size and forms the ballon-shaped bladder cell (BC), containing a large vacuole (Shabala et al., 2014; Smaoui et al., 2011).

It has not yet been studied which genes in *C. quinoa* are responsible for the formation of bladder cells. In contrast, the formation of trichomes and the genetic mechanisms behind it have been researched for decades in *A. thaliana*. Scientists identified an entire network of genes in *A. thaliana* known to be involved in trichome formation and their distribution (Balkunde et al., 2010; Broun, 2005; Pattanaik et al., 2014; Tominaga-Wada et al., 2011; Xu & Min, 2011; Zhang & Schrader, 2017).

1.4 TRANSPARENT TESTA GLABRA1 (TTG1) and the MBW network

The MBW network (Figure 2) controls trichome patterning in *A. thaliana* (Zhang & Schrader, 2017). TRANSPARENT TESTA GLABRA 1 (TTG1) acts as the central component of this regulatory network. The term “transparent testa glabra” originates from phenotypes observed in a loss-of-function *ttg1* mutant (Koornneef, 1981). The mutant seeds have a transparent, yellow seed coat (= TRANSPARENT TESTA) instead of a brownish color and are not able to produce a seed coat mucilage. Furthermore, the leaves have a smooth, glabrous surface without trichomes (= GLABRA), lack anthocyanidin production, and the mutant produces more root hairs (Koornneef, 1981). TTG1 contains four WD40 repeats, which are known to serve as a binding site for protein-protein or protein-DNA interaction (Walker et al., 1999; Xu & Min, 2011). Together with various basic helix-loop-helix (bHLH) and R2R3-myeloblastosis (MYB) transcription factors, TTG1 forms different trimeric MBW complexes, which control five different traits: seed coat mucilage production, proanthocyanidin biosynthesis, anthocyanidin biosynthesis, trichome patterning, and root hair patterning (Koornneef, 1981; Ramsay & Glover, 2005; Walker et al., 1999; Zhang & Schrader, 2017).

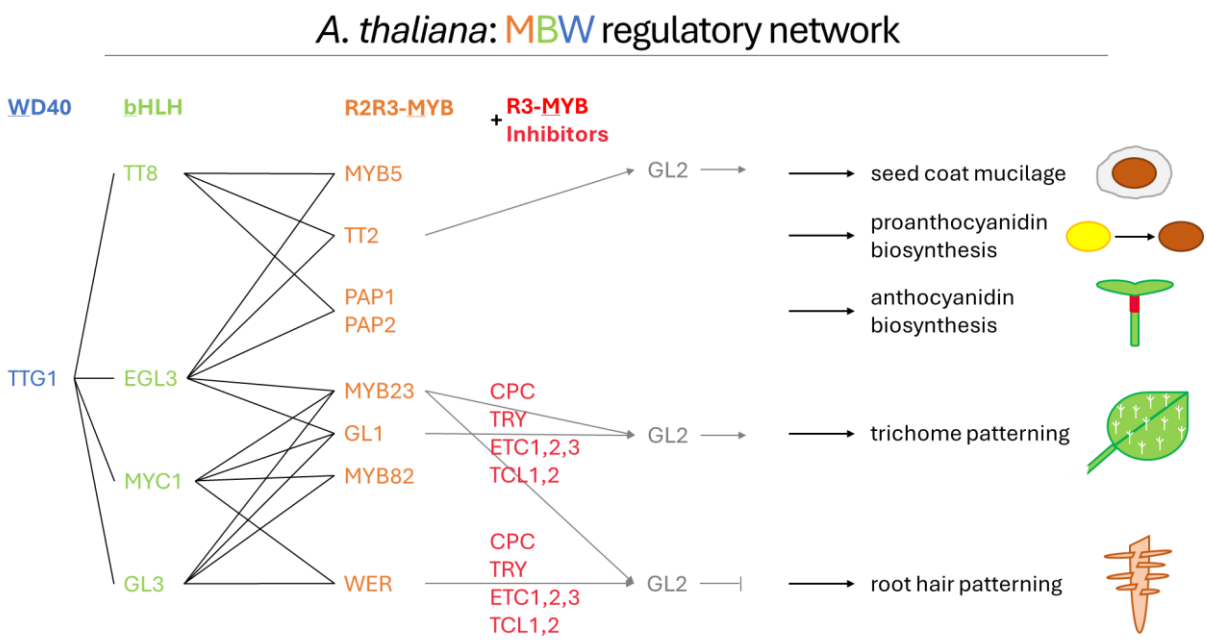

Figure 2: MBW regulatory network: Overview of the TTG1 regulatory network components and the five different traits, which are regulated by trimeric protein complexes. Possible combinations of trimeric complexes are represented by the connecting black lines. The figure does not contain all interaction partners of the different proteins. Each trimeric complex consists of the WD40 protein TTG1 (shown in blue), one bHLH transcription factor (light green) and a R2R3-MYB transcription factor (orange). The black arrows on the right side show which complex formation regulates which trait. The R3-MYB inhibitors (red) are known to inhibit trimeric complexes and therefore are involved in regulating the trichome- and root hair-cell fate. The grey arrows show how GL2 integrates into this network. Modified from Zhang & Schrader, 2017.

The bHLHs include TRANSPARENT TESTA 8 (TT8), ENHANCER OF GLABRA 3 (EGL3), MYELOCYTOMATOSIS ONCOGENE 1 (MYC1) and GLABRA 3 (GL3), each influencing several traits (Morohashi et al., 2007; Nesi et al., 2000; Payne et al., 2000; Zhao et al., 2012). For the regulation of the seed coat mucilage, a complex of TTG1, TT8 or EGL3, and MYB5 is formed (Li et al., 2009). Additionally, the synthesis proanthocyanidin and anthocyanidin is regulated by TTG1 and TT8 or EGL3. For proanthocyanidin synthesis, a complex with TT2 is formed, and for anthocyanidin synthesis, the R2R3-MYBs PRODUCTION OF ANTHOCYANIN PIGMENT 1 and 2 (PAP1, 2) are involved (Debeaujon et al., 2003; Gonzalez et al., 2008). Regarding trichome formation, EGL3, the bHLHs MYC1 and GL3, and several R2R3-MYBs, like MYB23, GL1, and MYB82 are functioning together (Hülskamp et al., 1994; Kirik et al., 2005; Liang et al., 2014). TTG1, MYC1, and GL3 are also forming different trimeric complexes with WEREWOLF (WER) to regulate the root hair patterning (Lee & Schiefelbein, 1999).

The network also includes the inhibitors CAPRICE (CPC), TRIPTYCHON (TRY), ENHANCER OF TRY AND CPC 1, 2, 3 (ETC1, 2, 3) and TRICHOMELESS 1 and 2 (TCL1, 2) (Kirik et al., 2004a; Kirik et al., 2004b; Schellmann et al., 2002; Wang et al., 2007). These R3-MYB transcription factors

are known to affect the trichome- and root hair-cell fate by competing with the R2R3-MYBs for binding to the bHLH transcription factor (Kirik et al., 2004a; Payne et al., 2000).

Additionally, the homeodomain transcription factor GLABRA 2 (GL2) is included in the network, which does not represent a component of an MBW complex but is an important downstream gene of the network (Masucci et al., 1996; Rerie et al., 1994; Wang et al., 2015b). GL2 is known to be involved in trichome and root hair patterning and the regulation of the seed coat mucilage (Koornneef, 1981; Schiefelbein, 2003; Zhang et al., 2003). As a direct target of TTG1, EGL3, and GL3, it plays a crucial role within the network and acts as a positive regulator of the trichome cell fate and as a negative regulator for the root hair cell fate (Masucci et al., 1996; Morohashi et al., 2007; Rerie et al., 1994; Zhang et al., 2003; Zhao et al., 2008).

1.5 Trichome patterning and the MBW network

The formation of trichomes and their distribution pattern is highly complex and involves the interplay of several activators and inhibitors of the MBW network (Balkunde et al., 2010; Pesch & Hülskamp, 2009). In the following (Figure 3), two models are presented that could explain trichome patterning regulation: the activator-inhibitor (AI) and the activator-depletion (AD) model (Balkunde et al., 2010; Bouyer et al., 2008).

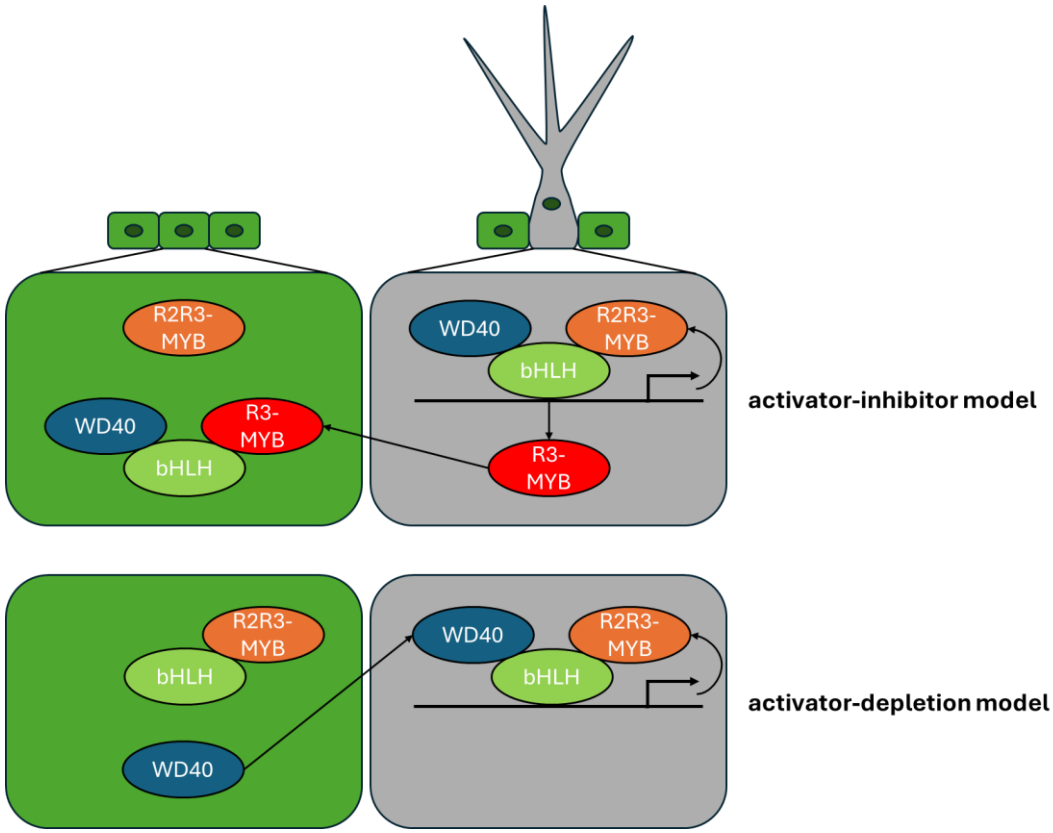

Figure 3: The two trichome patterning models. In the activator-inhibitor model (top), a trimeric activator complex is formed (WD40, bHLH, and R2R3-MYB), which promotes trichome formation by initiating gene expression of a positive feedback loop and inhibitors (R3-MYB). Inhibitors can move to neighboring cells and compete for the binding to the bHLH protein, leading to inhibition of trichome formation. In the activator-depletion model (bottom), the WD40 is recruited to the designated trichome cell and binds to the bHLH to form the activator complex, which regulates trichome formation. Neighboring cells stay in the non-trichome cell fate due to depletion of WD40. Modified from Pesch & Hülskamp, 2009.

According to the activator-inhibitor model, a self-amplifying activator complex is formed consisting of TTG1 (WD40), GL1 (R2R3-MYB), and GL3 or EGL3 (bHLH), which activates the gene expression of downstream genes, such as GL2, to initiate a trichome cell fate (Lin & Aoyama, 2012; Pesch & Hülskamp, 2009; Rerie et al., 1994). Furthermore, the activator complex activates the expression of inhibitors (R3-MYBs) like CPC or TRY (Payne et al., 2000; Pesch & Hülskamp, 2004). It was shown that the inhibitors can move to neighboring cells and compete with R2R3-MYB proteins for binding to the complex (Digiuni et al., 2008; Kurata et al., 2005; Payne et al., 2000; Pesch & Hülskamp, 2004). In such cells, the activator complex is inhibited, and the cell succumbs to a non-trichome cell fate (Pesch & Hülskamp, 2004).

In the activator-depletion model, the trichome cell fate is also regulated by the activator complex. In this case, it is assumed that the WD40 protein TTG1 is recruited to the designated trichome initials from neighboring cells, which leads to depletion of the WD40 and, therefore,

to disruption of the activator complex, resulting in the non-trichome cell fate in the surrounding area (Bouyer et al., 2008; Pesch & Hülskamp, 2009).

Based on a mathematical model developed by Anna Deneer, a new model was created to further determine the operation of the MBW network, which combines components of the activator-inhibitor and activator-depletion model (Balkunde et al., 2020; Deneer, 2022; Pesch & Hülskamp, 2009). The model is based on data of weak *ttg1* alleles (Balkunde et al., 2020). The *ttg1-9* mutant counts as a "weak" mutant and is, in contrast to a "strong" *ttg1* mutant, not glabrous but forms clusters of trichomes at the leaf edges (Koornneef, 1981; Walker et al., 1999). This cluster formation could not be explained with any of the previous models. The new model was able to predict this behavior of "weak" *ttg1* alleles by adapting several components of the TTG1 function in the AD model (Balkunde et al., 2020; Bouyer et al., 2008).

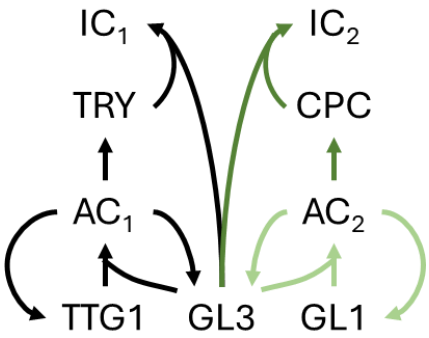

Figure 4: The combined activator-inhibitor and activator-depletion model. Three different components are needed to explain the *ttg1-9* trichome cluster phenotype and TTG1-9 depletion in the surroundings. The colors indicate different adaptions to the model. The black lines indicate the combination of the AI and AD model, TTG1 and GL3 form an active complex (AC_1) that activates TRY, which then binds to GL3 and forms an inactive complex (IC_1). This part of the model alone was not able to explain the lack of depletion of TTG1-9. The light green lines added GL1 to the network, which forms another active complex (AC_2) with GL3. The extended network was able to explain the depletion but disrupted the pattern formation of trichomes. To overcome this issue, CPC was added (dark green lines), which forms another inactive complex together with GL3 (IC2). For simplification, basal production, degradation, and diffusion were omitted. **AC** = active complex; **IC** = inactive complex. Modified from Balkunde et al., 2020.

For the combined model, a three-part model is illustrated (Figure 4). The black lines indicate the simplest combination of the activator-inhibitor and activator-depletion model to predict the observed pattern of the *ttg1-9* mutant (Balkunde et al., 2020). In the first step, TTG1 (WD40) and GL3 (bHLH) form an active complex (AC_1) that activates the inhibitor TRY (R3-MYB) and in a positive feedback loop GL3, which defines the trichome cell fate (Digiuni et al., 2008). TRY, which is considered non-cell autonomous, moves to the surroundings, binds to GL3, and forms an inactive complex (IC_1), which promotes the non-trichome cell fate (Balkunde et al., 2020; Kurata et al., 2005). This model alone could not explain the observed

lack of depletion of TTG1-9 in the *ttg1-9* mutant. Therefore, GL1, an additional patterning compound not depending on TTG1, was added (Balkunde et al., 2020). Since, it was shown that GL2 is not a direct interaction partner of TTG1 (Zhang et al., 2003). In light green (Figure 4) is shown that GL1 forms an active complex (AC_2) with GL3, which activates GL1 and GL3. However, this model could not reproduce the cluster formation of *ttg1-9* either, likely due to TRY activity. Therefore, the inhibitor CPC was added to the model (dark green), which is activated by AC_2 and forms another inactive complex (IC_2) together with GL3 (Balkunde et al., 2020). Since CPC is found to be more stable than TRY, it is assumed that TRY affects short-range distances, while CPC influences long-range distances and is able to preserve the trichome patterning (Balkunde et al., 2020; Tominaga-Wada & Wada, 2017). The final model matched the modeled data with experimentally observed data.

1.6 Intercalating trichomes in *A. thaliana*

In general, trichome development is restricted to the trichome initiation zone, which is located at the leaf base (Larkin et al., 1996). However, Figure 5 shows that intercalating trichomes are produced between already-developed trichomes and are formed outside the initiation zone (Hülskamp et al., 1994).

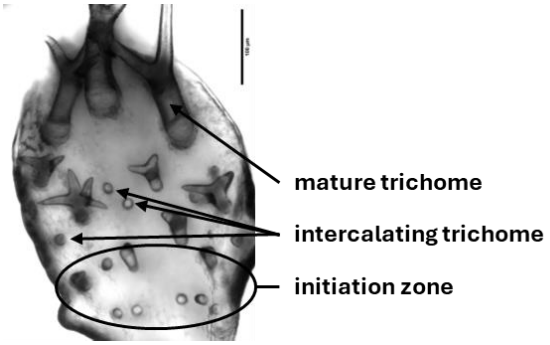

Figure 5: Intercalating trichomes in *A. thaliana* (Col-0). The initiation zone in which trichomes are formed is marked at the leaf base. Intercalating trichomes, which form between existing trichomes, are highlighted. Mature trichomes can also be seen at the leaf tip. The Leica DM5000 B microscope was used to image *A. thaliana* leaves. The scale bar is set to 100 µm.

The mechanisms behind intercalation are still largely unknown. The first clues came from Benjamin Jaegle's doctoral thesis, which investigated various MBW mutants regarding intercalating trichomes. A section of these results can be found in the appendix (supplemental Figure 25). As expected, the *ttg1* mutant showed no intercalating trichomes. Compared to Col-0, the mutation of the activators *EGL3*, *MYC1*, and *GL3* led to a reduction of intercalating trichomes, whereas the mutation of the inhibitors *CPC*, *ETC2*, and *ETC3* induced the formation

of intercalating trichomes. For the *try* mutant, intercalation was negatively affected and the *etc1* mutant hardly differed from the wild-type phenotype. This led to the conclusion that the activators and inhibitors not only regulate trichome patterning but also affect intercalation (Jaegle, 2015).

1.7 Aim of the thesis

In a constantly changing environment, plants are required to adapt to various stressors in order to ensure their survival and reproduction. One aim of this work is to analyze how plants respond to environmental stress at both the phenotypic and genetic levels. In particular, focusing on the expression of genes within the MBW network, which are known to regulate five important traits in *A. thaliana*, including seed coat mucilage production, proanthocyanins and anthocyanins synthesis and the initiation of trichomes and root hairs (Balkunde et al., 2010; Broun, 2005; Lepiniec et al., 2006; Ramsay & Glover, 2005; Tominaga-Wada et al., 2011). These features are suitable for analyzing their resistance to environmental stress. This project seeks to enhance the understanding of how plants adapt to different environmental conditions and how they use phenotypic changes of different traits to do so. Furthermore, the question arises how the MBW network contributes to the regulation of a phenotypic response and how it integrates environmental stresses to enable such a response. This thesis focuses on light and heat stress treatments in *A. thaliana* and particularly investigates the trichome patterning phenotype, in order to understand their role in stress resistance in more detail. In addition, salt stress experiments were conducted in *Chenopodium quinoa* and *Chenopodium suecicum*, the latter is a presumed diploid ancestor of the allotetraploid *C. quinoa* (Jarvis et al., 2017; Marhold, 2006; Storchova et al., 2015). As halophytes, these *Chenopodium* species are particularly suitable for studying the effect of salt stress, since they exhibit a special form of trichomes, called epidermal bladder cells (EBCs), which are important for salt resistance (Kiani-Pouya et al., 2017; Shabala et al., 2014). Overall, these goals aim to provide a more comprehensive understanding of the mechanisms that enable plant adaption to different environmental conditions and a deeper understanding of the genetic and phenotypic changes that contribute to stress resistance.

2 Material and methods

2.1 Materials

2.1.1 Chemicals, enzymes, kits, buffers, and other materials

Table 1: Chemicals, enzymes, kits, and other materials used during this study.

Material	Manufacturer
Chemicals	
Acetic acid (glacial)	Carl Roth
Bacto yeast extract	Carl Roth
BASTA® (183 g/l glufosinate)	Aventis
Meat extract	Merck Millipore
Ethanol absolute (EtOH)	Merck Supelco
EDTA 50 mM	Thermo Scientific™
Ethyl methanesulfonate (EMS)	Sigma-Aldrich
GeneRuler 1 kb DNA-Ladder	Thermo Scientific™
GoTaq® qPCR Master Mix, 2x	Promega
Hydrochloric acid 37 %	Carl Roth
Nuclease-Free Water	Promega
LE Agarose	Biozym
Magnesium sulfate ($MgSO_4$)	Carl Roth
Murashige and Skoog medium including vitamins	Duchefa
Reaction Buffer with MgCl, 10x	Thermo Scientific™
Plant Agar	Duchefa
Potassium hydroxide (KOH)	Carl Roth
Select Agar	Thermo Scientific™
Silwet™ L-77	Loveland Industries
Sodium chloride (NaCl)	Carl Roth
Sodium hydroxide (NaOH)	Carl Roth
Sodium hypochlorite solution, 12 % (NaCLO)	Carl Roth
Sodium thiosulfate ($Na_2S_2O_3 \cdot 5H_2O$)	Carl Roth
Sterican® Safety Needle 20G x 1 ½''	B. Braun
Sucrose	Carl Roth
TriTrack DNA Loading Dye, 6x	Thermo Scientific™
Trypton/Peptone ex casein	Carl Roth
Tween® 20	Carl Roth
Enzymes	
DNase I, RNase-free	Thermo Scientific™
RNase H	Thermo Scientific™
Kits	
RevertAid First Strand cDNA Synthesis Kit	Thermo Scientific™
Other materials	
3M™ Micropore™ adhesive tape	Thermo Scientific™
8-Lid chain, flat	SARSTEDT

96 x 0,2 ml Plate, RP, LF, SUB Sk, 96 well plate	BIOplastics
BioPhotometer plus	Eppendorf
Centrifuge 5418 R	Eppendorf
Centrifuge 5424	Eppendorf
Falcon® 15 ml High-Clarity Polypropylene Conical Tube	Thermo Scientific™
Falcon® 50 ml Polypropylene Conical Tube	Thermo Scientific™
Forceps Dumont #5 (11251-20)	Fine Science Tools
Glass Beads, 2.7 mm	Carl Roth
Inoculation loop 10 µl, blue	SARSTEDT
Light tubes OSRAM Lumilux 58W/840 Cool White	OSRAM
Micro tube 1.5 ml	SARSTEDT
Micro tube 2.0 ml	SARSTEDT
Microscope Leica DM5000 B	Leica
Microscope Leica MZ16 F	Leica
Microscope OLYMPUS SZX16	OLYMPUS
Microscope slide with recess	Carl Roth
Multiply®-µStrip 0.2 ml chain	SARSTEDT
Opti-Seal™ Optical Sealing Sheet	BIOplastics
Perti dishes	SARSTEDT
Pipette tip 1000 µl, blue	SARSTEDT
Pipette tip 200 µl	SARSTEDT
Plant chamber	Johnson Controls
qPCR machine QuantStudio™ 5	Thermo Scientific™
growing pots, 6 cm, round	Pöppelmann TEKU®
growing pots, 9 cm, round	Pöppelmann TEKU®
growing pots, 9 cm, square	Pöppelmann TEKU®
Quality Pipette Tips 0.5 – 20 µl	SARSTEDT
Thermomixer comfort	Eppendorf
SafeSeal micro tube 1.5 ml	SARSTEDT
SafeSeal micro tube 2.0 ml	SARSTEDT
Stereo microscope Leica S6E	Leica
Whatman™ Grade 1 paper 85 mm	GE Healthcare Life Sciences

2.1.2 Oligonucleotides

Table 2: Primers used during this study.

Gen	Primer number	Sequence (5´ → 3´)	Efficiency in %	Correlation R^2	Origin
ACT2	1323 F	CAAGGCCGAGTATGATGAGG			AG Höcker
ACT2	1324 R	GAAACGCAGACGTAAGTAAAAAC	-	-	AG Höcker
AT4G33380	BP068 F	TTGAAAATTGGAGTACCGTACCAA			(Morales et al., 2013)
AT4G33380	BP069 R	TCCCTCGTATACATCTGGCCA	99.30	-0.996	(Morales et al., 2013)
CPC	AST_P0455 F	AAGGCTTCTTGTTCCGAAGAG			Alexandra Steffens, lab collection

CPC	AST_P0456 R	CCTGTCGCCAACG AGTTTAT	100.79	-0.988	Alexandra Steffens, lab collection
EF1α	JP_210 F	CACCACTGGAGGT TTTGAGG			Jessica Pietsch, lab collection
EF1α	JP_211 R	TGGAGTATTTGGG GGTGGT	95.97	-0.998	Jessica Pietsch, lab collection
EGL3	JS07 F	GGTCTGTCTCTGCT TCTCAAC			Julian Schiffner, lab collection
EGL3	JS08 R	GCTCACTTCTCTCA AGACCTAAC	95.79	-0.997	Julian Schiffner, lab collection
EIF4α	BP056 F	AGGTCATGAGGGC CCTTGGT			Anna Marxer, lab collection
EIF4α	BP057 R	CAGCTTGGAGGAT GCGCTGA	105.00	-0.997	Anna Marxer, lab collection
ETC1	PK26 F	CAGCGTAAGTCGA AGCATCTTA			Patrizia Kroll, lab collection
ETC1	PK28 R	TCTTCCTGAGCCAT TGCTATTT	107.74	-0.989	Patrizia Kroll, lab collection
ETC2	JP_208 F	GATCCCGATATGA CTCTGAAGAAGTG AGTAGCATCGAAT GGGAG			Jessica Pietsch, lab collection
ETC2	JP_209 R	CAAGATTTGTTCTA CTTTTATGATTGAA AGCTTTTATTTTG	97.11	-0.993	Jessica Pietsch, lab collection
ETC3	PK30 F	GACCAACTCCATC GTTACTTCT			Patrizia Kroll, lab collection
ETC3	PK32 R	TGCATTCGAGAGA CCAAATCT	96.06	-0.988	Patrizia Kroll, lab collection
GL1	AST_P0467 F	GTGAACAAAGGCA ATTTCACTG			Alexandra Steffens, lab collection
GL1	AST_P0468 R	GTTCTTCCCGGTAC TCTTTTAGC	95.74	-0,995	Alexandra Steffens, lab collection
GL2	AST_P0451 F	AAGCTCGTCGGCA TGAGT			Alexandra Steffens, lab collection
GL2	AST_P0452 R	TTCTCTCGATTTCA CTGTCTGG	90.21	-0.991	Alexandra Steffens, lab collection
GL3	JP_168 F	GATCCGCAACAGA TTCTAGGCG			Jessica Pietsch, lab collection
GL3	JP_169 R	GCCAGCTTTGCAC CTGAGAAGC	98.96	-0.994	Jessica Pietsch, lab collection
HCF	BP058 F	TGGACAACACGAA ATGGGAGCA			Anna Marxer, lab collection
HCF	BP059 R	AGCCTCCCGACCA CATTACCT	94.00	-0.992	Anna Marxer, lab collection
MYB5	BP072 F	TGTGGAAAGAGCT GTCGTCT			this study
MYB5	BP073 R	CCTCGTCCGACGT AATTCCT	91.46	-0.999	this study
MYB23	JP_170 F	CCGAACTCATGGC CAGGGCCAC			Jessica Pietsch, lab collection

MYB23	JP_171 R	GCCGAGGAGCTTG TGGAGTCTG	93.82	-0.995	Jessica Pietsch, lab collection
MYB82	BP064 F	GTGAAGGAAACTG GGCAGAC			this study
MYB82	BP065 R	TGTGGTGACATGC TTCCTCT	99.95	-0.998	this study
MYC1	AST_0463 F	TGGTCGTCTTCACT TACTCAACC			Alexandra Steffens, lab collection
MYC1	AST_0464 R	TTCCTCTTCTTCAT ATCTCCATTGTA	93.03	-0.992	Alexandra Steffens, lab collection
PAP1	BP074 F	ACCGCAAATGACG TCAAGAA			this study
PAP1	BP075 R	GGATCGAGGTCGA GGCTTAT	93.64	-0.999	this study
PAP2	BP076 F	TCCTACAACACCG GTCCAAA			this study
PAP2	BP077 R	TGAGTCCAAGGCA TGAAGGA	96.79	-0.997	this study
PSB33	BP054 F	GTAAGATGCGAG GCGACGGA			Anna Marxer, lab collection
PSB33	BP055 R	ACTCGCCGTTCAC CTTTCGG	92.00	-0.994	Anna Marxer, lab collection
RD29A	BP052 F	CCGATAACGTTGG AGGAAGAGTCG			Alexandra Steffens, lab collection
RD29A	BP053 R	TTTCCAGCTCAGCT CCTGACTCGTCAC C	93.00	-0.997	Alexandra Steffens, lab collection
SAND	-	GGATTTTCAGCTA CTCTTCAAGCTA			AG Kopriva
SAND	-	CTGCCTTGACTAA GTTGACACG	-	-	AG Kopriva
TCL1	AST_P0487 F	GAAATGGGAGTTT ATCAATATGACC			Alexandra Steffens, lab collection
TCL1	AST_P0488 R	ACGTCCCACCACT CTTCTTG	110.55	-0.995	Alexandra Steffens, lab collection
TCL2	AST_P0489 F	GACGGAACAAGA AGAAGATCTCA			Alexandra Steffens, lab collection
TCL2	AST_P0490 R	CTTTGCCTCTCGTC CTACCA	97.55	-0.991	Alexandra Steffens, lab collection
TRY	AST_P0457 F	ACAGACTTGTCGG TGATAGGTG			Alexandra Steffens, lab collection
TRY	AST_P0458 R	CTATCTCCTCTGGT TGTCTTCCA	100.60	-0.994	Alexandra Steffens, lab collection
TT2	BP086 F	GGCGGTTCAATCT GTGGAC			(Jacob et al., 2021)
TT2	BP087 R	CTGTTGGCTCCTCT CTAACG	107.43	-0.991	(Jacob et al., 2021)
TT8	BP088 F	AACAGAGGAGCTT GGACTGA			(Jeong et al., 2010)
TT8	BP089 R	AGGGAGAGTGCTC CATTTGC	100.02	-0.990	(Jeong et al., 2010)

TTG1	JS01 F	CGCCTCAGAGCTG TAAACATA			Julian Schiffner, lab collection
TTG1	JS02 R	CTCCGAACCAGCC GAATAAA	104.42	-0.992	Julian Schiffner, lab collection
TIP41	BP066 F	GTGAAAACTGTTG GAGAGAAGCAA			(Morales et al., 2013)
TIP41	BP067 R	TCAACTGGATACC CTTTCGCA	94.35	-0.993	(Morales et al., 2013)
TUA5	BP062 F	GCCAAGGCTTACC ACGAGCA			Anna Marxer, lab collection
TUA5	BP063 R	TTCCGTGCCTTGG GTCACAC	96.00	-0.997	Anna Marxer, lab collection
UBC21/PEX4	L733	TGCAGTTGACAAT TCGTTCTC			(Skiljaica et al., 2022)
UBC21/PEX4	L734	CGGTCCATTTGAA TATGTTGGT	-	-	(Skiljaica et al., 2022)
UBC	-	CTGCGACTCAGGG AATCTTC			AG Kopriva
UBC	-	TTGTGCCATTGAA TTGAACC	-	-	AG Kopriva
UBQ10	BP060 F	GAGGGTATCCCAC CGGACCA			Anna Marxer, lab collection
UBQ10	BP061 R	ACGCAGACGCAAG ACCAAGT	93.00	-0.997	Anna Marxer, lab collection
18S rRNA	EP0075 F	AAACGGCTACCAC ATCCAAG			Eva Koebke, lab collection
18S rRNA	EP0076 R	GACTCGAAAGAGC CCGGTAT	100.07	-0.998	Eva Koebke, lab collection

2.1.3 Microorganism and plant strains

Table 3: Microorganism and plant strains used during this study, including created overexpression (OE) lines.

Plant strain	**Line name**	**Gene name**	**AGI code**	**Background**	**Origin**
Arabidopsis thaliana	Col-0	-	-	-	-
	ttg1-21	TTG1	AT5G24520	Col-0	(Appelhagen et al., 2014)

OE lines	**Gene name**	**AGI code**	**Plasmid name**	**Method**	**Background**	**Plasmid**
35S:AtPAP1	PAP1	AT1G56650	pAMPAT-35S:AtPAP1	Floral dip	Col-0	Bipei Zhang BP311
35S:AtPAP2	PAP2	AT1G66390	pAMPAT-35S:AtPAP2	Floral dip	Col-0	Bipei Zhang BP312

Plant strain	**Ploidy level**	**Origin**
Chenopodium quinoa	allotetraploid	Jürgen Hintzsche
Chenopodium suecicum	diploid	Prof. Dr. Rainer Hedrich, JMU

Organism	Line name	Origin
Agrobacteria tumefaciens	GV3101: pMP90RK	(Koncz & Schell, 1986)

2.2 Methods *A. thaliana*

2.2.1 Growth conditions and stress treatments in *A. thaliana*

Standard growth conditions

Seeds of Col-0 or *ttg1-21* were sown in round 6 cm pots and stratified in the dark for at least three days at 4-5 °C. The pots were then transferred into a plant chamber (Johnson Controls) set to long-day conditions (16 h light, 8 h dark) at 22 ± 2 °C and 60 % humidity. The light intensity was set to 120 µmol/m^2s. The plants were watered twice a week from below.

Stress treatments

Seeds were sawn in the same way as for standard growth conditions. The plants were either exposed to the different abiotic stresses directly after stratification or after reaching a particular stage under control conditions. If possible, the experiments were carried out in parallel. For the qPCR analysis, a separate control for each stress treatment was harvested if this was not possible due to the time required for sampling (exception: 30 µmol/m^2s short-term experiment). Under constant low-light conditions, the plants grew more slowly, and the desired plant stage was only reached after twelve days. The corresponding control was taken at the same plant stage on day eight. Under constant high-light conditions, the plants grew faster, and the desired plant stage had already been reached after six days. The corresponding control was taken at the same plant stage and day since the high-light plants were stratified for two more days before being transferred to the plant chamber. As before, for harvesting, the cotyledons and the roots were removed, and per sample, the shoot material of 40 plants was pooled. Heat and different light stress treatments were performed as described below (Table 4). The duration and intensity of heat stress were taken from Kilian and colleagues (2007), where sampling for heat stress, 6 hours after onset of stress showed the largest number of genes that were differentially expressed (Kilian et al., 2007). In addition, we based our sampling for light stress on their results of the UV-B treatment. There, too, most expression changes were found 6 hours after the onset of stress (Kilian et al., 2007).

Table 4: Stress treatments performed during this study. After heat stress, the plants were transferred back to control conditions until sampling. 3 or 6 hours (h) of stress is referred to as short-term conditions.

Treatment	Intensity	Start treatment	Duration	Sampling (qPCR)	Purpose
low light	30 µmol/m^2s	day 1	constant	day 12, same time of the day	qPCR
		day 8	6 h	6 h after onset of stress	qPCR; phenotypic analyses
		day 7	constant		phenotypic analyses
low light	60 µmol/m^2s	day 7	constant		phenotypic analyses
low light	90 µmol/m^2s	day 7	constant		phenotypic analyses
control	120 µmol/m^2s	day 1	constant	day 8, same time of the day	qPCR; phenotypic analyses
		day 7	constant		phenotypic analyses
high light	400 µmol/m^2s	day 1	constant	day 6, same time of the day	qPCR
		day 8	6 h	6 h after onset of stress	qPCR; phenotypic analyses
		day 7	constant		phenotypic analyses
heat stress	38 °C	day 8	3 h	6 h after onset of stress	qPCR; phenotypic analyses

2.2.2 Determination of trichome density

One seed was sown per 6 cm pot (*n* = 20) and stratified. The number of trichomes and the leaf area were determined on the adaxial side of leaves three and four under control (120 µmol/m^2s) and different stress regimes (Table 4) to calculate the trichome density. Trichomes were counted when the leaves had reached a suitable length of around 0.3 cm, preventing crowding of trichomes at the leaf base. For leaf three, this was the case when leaf six/seven were developed, and for leaf four, when leaf eight was formed. To speed up the manual counting process, using the Leica S6E stereo microscope, the symmetry of the leaves was used. The number of trichomes was always counted for one leaf side and then doubled. Since the plants grow at different speeds under different light intensities, the same plant stage was examined rather than the same day for all treatments. Overview pictures were taken, using the Sony Xperia 10 III (XQ-BT52), every two three days and additional when the number of trichomes was counted. ImageJ was used to calculate the leaf area. Accordingly, the trichome density was determined in Microsoft Office Excel (2016). The trichome number was analyzed after an additional two weeks to identify any differences. The experiment was performed twice.

2.2.3 Identification of intercalating trichomes

Around 30 seeds were Intercalating trichomes were determined on leaf three of plants grown under control conditions (120 µmol/m^2s) and different light stress regimes (30, 60, 90 and 400 µmol/m^2s). Sample preparation was carried out when leaves one and two were still in the growth phase and leaf three had just formed (300 to 400 µm in size), carrying one to three mature trichomes. Using the fluorescence stereo microscope Leica MZ16 F or the stereo microscope OLYMPUS SZX16, leaf three was separated from the seedling using syringe needles and placed on a depression microscope slide with a droplet of 1 % plant agar (1 g/l plant agar, dissolved in ddH_2O and autoclaved for 20 min at 121 °C, aliquoted in 1.5 ml micro tubes and heated to 99 °C to liquefy before use). The plant agar preserves the leaves during microscopy and keeps them in place. Intercalating trichomes were counted manually on the adaxial side of leaf three using the Leica DM5000 B microscope equipped with the DFC360 FX camera system and the image analysis software: Leica Application Suite Advanced Fluorescence (2.7.0.9329).

2.2.4 Determine dry weight of above-ground material and seed production

One seed per 6 cm pot was sown (*n* = 20). After stratification, the plants grew under different light intensities (30, 60, 90, 120, and 400 µmol/m^2s) until the end of their life cycle. The shoot material was bagged when the first siliques changed color from green to brown. When the seeds were ripe, the shoot material was cut off below the rosette leaves and bagged. After one week in the drying cabinet at 38 °C, the dry weight was determined using a precision scale. 100 seeds were counted and weighed per replicate. The weight of all seeds was then measured, and the total amount of seeds was determined. The experiment was carried out two times.

2.2.5 RNA extraction from plant tissue and DNase I digestion

Total RNA from plant tissue was purified using the TRIzol™ Reagent (Invitrogen™). Seedlings were harvested and collected in a 2 ml SafeSeal micro tube containing at least three glass beads. The samples were snap-frozen in liquid nitrogen immediately and stored at -70 °C until use. For extraction, the samples were cooled down in liquid nitrogen, and then the seedlings were disrupted by a Tissue Lyser (QIAGEN) for three minutes at 30 Hz. The tubes were stored on ice, and 1 ml ice cold TRIzol™ Reagent was added. After the samples were vortexed vigorously for 15 seconds, they were incubated for 3 minutes at RT. Then, 200 µl chloroform

were added and again vortexed vigorously for 15 seconds. Next, the samples were centrifuged at 4 °C and 13000 rpm for 15 minutes. The supernatant was discarded, and the pellet was washed with 500 µl 70 % EtOH. The samples were then centrifuged at RT and 13000 rpm for 5 minutes and washed again with 100 % EtOH. After another 5-minute centrifugation, the pellet was dried for 30 minutes at 37 °C and then resuspended in 30 µl RNase-free water. After 10 minutes of incubation at 37 °C, the DNase I digestion was performed to remove genomic DNA. For this, 30 µl RNA was mixed with 2 µl 10x Reaction Buffer with MgCl2 for DNase I (Thermo Scientific™) and 1 µl RNase-free DNase I (Thermo Scientific™) and incubated for 1 hour at 37 °C. Then, 2.5 µl of 50 mM EDTA were added, and the samples were incubated at 65 °C for 10 minutes. The RNA was stored at -70 °C.

Gel electrophoresis

Gel electrophoresis was performed to separate and visualize RNA or DNA fragments according to their size. To perform gel electrophoresis, a 1 x TAE working solution was prepared by diluting the stock solution with water (50 x TAE buffer: 242 g TRIS diluted in 700 ml ddH_2O, 57.1 ml 100 % acetic acid (glacial) and 100 ml 0.5 M EDTA (pH 8.0), adjusted to a final volume of 1 l). For a 1 % agarose gel, 1 % agarose was dissolved in 1 x TAE buffer and 0.25 µg/ml ethidium bromide (for DNA staining) were added. Samples were mixed with 1 volume of 6x TriTrack Loading Dye (Thermo Scientific™) to 5 volumes of DNA sample and loaded onto the gel. In order to determine the fragment size a DNA ladder (GeneRuler 1 kb or GeneRuler 1 kb Plus; Thermo Scientific™) was loaded additionally. Gels were run at 120 V and 400 mA for 30 to 40 minutes. The INTAS Gel Jet Imager equipped with the Intas GDS Touch 2 version 2.1.4 was used to visualize the DNA and RNA fragments.

RNA integrity test

To test RNA quality, a bleach gel was prepared. The bleach denatures the RNA in its secondary structure, revealing three distinct bands (= high quality) which represent the ribosomal RNAs: 28S rRNA, 18S rRNA and 5.8S/5S rRNA (Aranda et al., 2012). For gel electrophoresis, a 1 % agarose gel was prepared, containing 0.25 µg/ml ethidium bromide and 1 ml 2 % NaClO per 50 ml. Per sample, 2 µl RNA were mixed with 8 µl H_2O (RNase free) and 2 µl loading dye and loaded onto the gel. In addition, 10 µl DNA ladder (GeneRuler 1 kb) were loaded, and the gel was run at 120 V and 400 mA for 35 minutes.

2.2.6 cDNA synthesis

RNA concentration in 1:50 dilutions was measured at a wavelength of 230, 260, and 280 nm using the BioPhotometer Plus (Eppendorf). For use in qPCR the cDNA concentration was set to 2500 ng for all samples and calculated accordingly. For the cDNA synthesis from total RNA, the RevertAid First Strand cDNA Synthesis Kit (Thermo Scientific™) was used with oligo(dT) primers according to the manufacturer's instructions. After cDNA synthesis, the samples were treated with 0.4 µl RNase H 5 U/µl (Thermo Scientific™) for 20 minutes at 37 °C and stored at -20 °C.

2.2.7 Floral dipping with *Agrobacteria tumefaciens*

Transformation of plasmids into *A. tumefaciens*

For Agrobacteria transformation, competent cells of the strain GV3101:pMP90RK were thawed on ice for 10 minutes. On ice, 2 µl of the desired plasmid were added to 50 µl competent cells and mixed by pipetting up and down. The mixture was incubated on ice for 20 minutes and then heat-shocked at 42 °C for 1 minute and 30 seconds. Then, the samples were incubated on ice for 1 minute and 30 seconds, and afterwards, 700 µl YEB medium (5 g/l trypton/pepton ex casein, 5 g/l meat extract, 1 g/l Bacto yeast extract, 5 g/l sucrose, 0.2 M $MgSO_4$, dissolved in ddH_2O and autoclaved for 20 min at 121°C; YEB plates: add 1.6 g/l micro agar) was added. The suspension was incubated at 28 °C and 500 rpm for 1 hour and 30 minutes. The mixture was centrifuged for 2 minutes at 8000 rpm. The supernatant was discarded, and the pellet was resuspended in 100 µl of the remaining medium. These 100 µl of the suspension were plated onto YEB selection medium containing 50 µg/ml Rif, 50 µg/ml Kan, and 100 µg/ml Carb. The plates were incubated for two days at 28 °C.

Floral Dip

Transformed Agrobacteria were incubated in 5 ml YEB medium (Rif 50, Kan 50, Amp 100 µg/ml) in a 100 ml Erlenmeyer flask overnight at 28 °C and 200 rpm. With 2 ml of the overnight culture, 200 ml main culture were inoculated and incubated at 28 °C and 200 rpm for two days. 10 g sucrose and 40 µl Silwet™ were added to the culture and incubated for another 10 minutes. Then, the culture was transferred to a 250 ml beaker, and the flowering plants were dipped headfirst into the Agrobacteria culture for around 30 seconds until everything was well-wetted. The plants were transferred to a tray covered with a lid and

stored without direct sunlight overnight. The next day, the plants were transferred to the greenhouse.

BASTA® selection

The seedlings of the floral dip were treated with BASTA® (0,1 % BASTA®; 0,01 % Tween 20) to identify overexpression lines that are homozygous for the insert. Seedlings that do not carry the desired insert are not resistant and die. For this purpose, seeds were sown on soil in a tray with PREVICUR®. After three days of stratification at 4-5 °C in the dark, the tray was transferred to the greenhouse. Once the first true leaves developed, the seedlings were sprayed with BASTA® twice, at intervals of two days. After seven days the surviving plants were selected and repotted to single pots.

2.2.8 quantitative real-time PCR (qPCR)

Quantitative real-time PCR was used to monitor the amplification of a specific DNA fragment in real-time through the detection of a fluorescent DNA binding dye. Samples for qPCR were harvested after eight days and at the same time of the day to avoid circadian fluctuations. At this plant stage, the first two true leaves were still in the growth phase and leaves three and four had just been formed. Since the thesis focuses on the trichome patterning genes in young leaves that are currently in the patterning phase, the trichome-less cotyledons and the roots were removed. Per sample, the shoot material of 40 plants was harvested.

Identifying suitable reference genes for qPCR

The RefFinder web tool was used to screen for suitable reference genes (Xie et al., 2012). RefFinder integrates the common programs geNorm (Vandesompele et al., 2002), NormFinder (Andersen et al., 2004), BestKeeper (Pfaffl et al., 2004) and the comparative ΔCt method (Silver et al., 2006), which test the stability of reference genes, to assigns them according to the geometric mean of ranking values.

Efficiency testing of qPCR primers

The efficiency and correlation of primer sets used for qPCR were tested to identify suitable primers. Therefore, a dilution series of cDNA was prepared (1:2.5, 1:5, 1:10, 1:20, 1:40, 1:80). For each dilution the mean Ct-value was plotted against the log10 of the dilution factor to calculate the slope and the R^2 (coefficient of determination/correlation) in Microsoft Office

Excel (2016). The slope was then used to calculate the efficiency in percent using the following formula:

$$\mathrm{E} = (-1 + (10^{(-1/\mathrm{slope})})) * 100$$

For all primer pairs the correlation should be between -0.99 and -1 and the efficiency of reference gene primers should be between 90 and 110 % and between 80 and 120 % for genes of interest (Stephan et al., 2019). In addition, the melt curve data (supplemental Figure 28), provided by the QuantStudio™ Design & Analysis Software, were interpreted to identify suitable primer pairs. In the optimal case, the melt curve plots show a single tight peak. Primer dimers would be visible as an additional peak or a wavy shape of the peak. Tested primer sets, efficiency and correlation results are listed in Table 2. Most primer sets were tested by Dr. Jessica Pietsch.

qPCR reaction and program

The used GoTaq® qPCR Master Mix (2x) from Promega contains BRYT Green® Dye. Samples were pipetted into a 96-well plate (0.2 ml; BIOplastics), the plate was sealed (Opti-Seal™; BIOplastics) and spun down. Three biological replicates with three technical replicates each were accomplished. qPCR was performed using the QuantStudioTM 5 qPCR machine equipped with a 96-well block. See Table 5 for the reaction mix and Table 6 for the qPCR program.

Table 5: qPCR reaction mix for one sample.

Compound	Volume in µl
GoTaq®	5
H_2O (RNase free)	3.6
Primer Mix	0.4
cDNA	1
Total	10

Table 6: qPCR program including dissociation stage. Volume: 10 µl, Cover: 105 °C

	Temperature in °C	Time
	50	2 min
	95	10 min
40 times	95	15 sec
	60	1 min
	95	15 sec
	60	1 min
	Dissociation (0.15 °C/s)	
	95	1 sec

Analysis of qPCR data

For evaluation of the qPCR results, the QuantStudio™ Design & Analysis Software (v1.4.3) was used to extract Ct-values. Data analysis was performed in Microsoft Office Excel (2016). Prior to statistical analysis, significant outliers within the raw data were identified by using an online tool for two-sided Grubbs' test (Graph Pad Outlier Calculator; $\alpha < 0.05$) and excluded. Gen expressions were normalized relatively to each other, according to geNorm manual (Vandesompele et al., 2002), with a few adjustments. To determine the quantity, the respective efficiency of the primer pair was taken into account. In addition, normalization factors were determined to normalize the data of each treatment against two different reference genes.

In a first step, the lowest Ct-value of each data set for all genes of interest and the two reference genes was identified separately. Then, the Ct-values of each replicated data set were subtracted with the lowest Ct-value. Afterwards the quantity was determined by using the following formula:

$$quantity = (1 + efficiency)^{-(Ct - Ct_{min})}$$

All expression levels were normalized to two reference genes, by calculating the mean quantity of each biological replicate of the reference genes. From the mean quantities, then, the geometric mean of the respective reference gene set was calculated. The quantity values of the genes of interest were then divided by the calculated geometric mean. After normalization to the reference genes, the mean value of each biological replicate was determined. To log-transform the data and identify the corrected mean and standard deviation, the variance and the coefficient of variation for log-normal data were calculated in the next step:

$$variance = LN\left(1 + \left(\frac{SD^2}{mean^2}\right)\right)$$

$$coefficient\ of\ variation = \sqrt{1 + efficency^{variance} - 1}$$

To then identify the corrected mean and standard deviation the following formulas were used to compare tissues within one species, Cq values were normalized to the overall minimal

Cq value. This resulted in larger differences within the replicates, which were enhanced by subsequent logarithmic calculation of the relative expression:

$$corrected\ mean = (1 + efficiency)^{LN\frac{mean}{\sqrt{1+SD^2/mean^2}}+0.5*variance}$$

$$corrected\ SD = mean * coefficient\ of\ variation$$

2.2.9 Data representation and statistics

Statistical evaluation was conducted in RStudio Version 1.1.383 (RStudioTeam, 2015). The data were tested for variance homogeneity (Levene's Test for Homogeneity of Variance) and normal distribution (Shapiro-Wilk normality test). One-way ANOVA (ANalysis Of Variance) with post-hoc Tukey HSD (Honestly Significant Difference) test was performed if both requirements had been met. If the requirement for normal distribution was not fulfilled, One-way ANOVA was still used as it is robust to non-normal distribution (Blanca et al., 2017; Khan & Rayner, 2003). If no variance homogeneity was given Welch-ANOVA and Games-Howell post-hoc test were performed. Mann-Whitney U test was performed in Microsoft Office Excel (2016) to identify significant differences within the qPCR results. Excel was used to create figures including mean and standard deviation.

2.3 Methods *C. quinoa* and *C. suecicum*

2.3.1 Seed sterilization

Chlorine gas

Chlorine gas sterilization was performed under a fume hood. The required number of seeds were added to 1.5 ml microtubes and placed open in a desiccator. The tubes were filled to a maximum of one-fifth. A 50 ml beaker containing 20 ml of 12 % NaClO was placed next to the seeds in the desiccator, and with a disposable pipette, 7.5 ml of 37 % HCl was added. The desiccator was closed, and the seeds were sterilized for 3 hours.

Sodium hypochlorite

Sodium hypochlorite sterilization was performed under a clean bench. The required number of seeds was added to a 1.5 ml microtube, and 750 µl EtOH was added. Once the seeds sunk to the bottom, the supernatant was removed, and 500 µl 2 % NaClO were added. The tubes were incubated in a thermoshaker for 8 minutes at maximum speed. Afterwards, the tubes

were centrifuged for a few seconds at a maximum speed of 6000-7000 rpm. The supernatant was removed, and the seeds were washed thoroughly twice with sterile water.

2.3.2 Growth conditions and stress treatments in *C. quinoa* and *C. suecicum*

Standard growth conditions

Seeds of *C. quinoa* and *C. suecicum* were either sown in round 9 cm pots or on Whatman paper in petri dishes. The plates were sealed with adhesive tape. The pots/plates were then transferred into a plant chamber (Johnson Controls) set to long-day conditions (16 h light, 8 h dark) or short-day conditions (8 h light, 16 h dark) at 22 ± 2 °C. The humidity was set to 60 %, and the light intensity to 200-250 µmol/m^2s in both chambers. The plants were watered three times a week from below.

Seeds of the EMS mutagenesis in *C. suecicum* were sawn in trays filled with square 9 cm pots and grown in the greenhouse under long-day conditions. For the mutant screen, M2 seeds were sterilized and sown onto 1 % MS plates (4.4 g/l Murashige and Skoog medium (Murashige & Skoog, 1962) and 1 % sucrose dissolved in ddH_2O, pH adjusted to 5.8 with 1 M KOH, 8 g/l plant agar added and autoclaved for 20 min at 121 °C). The plates were sealed with adhesive tape. After stratification in the dark for six days at 4-5 °C, the plates were transferred into a plant chamber set to short-day conditions at 22 ± 2 °C. The humidity was set to 60 % and the light intensity to 200-250 µmol/m^2s. Suitable mutants were transferred to soil (round 9 cm pots) and transferred back to the short-day chamber.

Stress treatments

Seeds were sawn in the same way as for standard growth conditions and transferred to the same long- or short-day chamber. The plants were either exposed to different salt stress conditions (100, 200, 300, 400, 500 mM NaCl) directly after sowing or when the seedlings were one, two, or three weeks old, respectively. If possible, the experiments were performed in parallel. The plants were watered three times a week from below.

2.3.3 EMS mutagenesis of *C. suecicum*

Around 2000 seeds per ethyl methanesulfonate (EMS) treatment were added to a 100 ml glass flask and incubated for 16 hours in 50 ml 0.1 % KCl at 4 °C on a rocking table. Afterwards, the KCl was discarded, and the seeds were washed with 100 ml ddH_2O. Under the fume hood, 30 ml ddH_2O was added to the flask, and with a 1 ml syringe, the desired amount of EMS (1 %,

2 %, or 3 %) was added. Seeds were incubated under the hood for 8 h or 16 h on a rocking table. The EMS solution was discarded into a waste bottle containing 10 % sodium thiosulfate. Seeds were incubated in 20 ml sodium thiosulfate (100mM) for 15 minutes on the rocking table. This step was repeated once. Then 50 ml ddH_2O was added, and the seeds were incubated on a rocking table for 30 minutes. This step was repeated two times. 1000 seeds per tray were sown, and the trays were transferred to the greenhouse. Germination rate of M1 seeds and the amount of plants that fulfilled their whole life cycle were determined.

Production of M2 seeds

The shoot material of around 20 M1 plants was pooled and bagged when the first ripe, dark seeds were visible. When the seeds were ripe, the seed bags were cut and transferred to a drying cabinet at 38 °C for one week. The dry weight was calculated using a precision scale. 100 seeds were counted and weighed per seed pool. Then, the weight of all seeds was measured to calculate the total number of seeds.

Germination rate of M2 plants

In a preliminary experiment, the germination of 50 seeds on soil (round 9 cm pot) or 1 % MS was analyzed. The plate was sealed with adhesive tape. After stratification in the dark for six days at 4-5 °C, the pot and plate were transferred into a plant chamber set to short-day conditions and the germination rate was determined.

Mutant screen

After the seeds of EMS mutagenesis were brought to the next generation, the M2 seeds were sterilized and sown onto 1 % MS plates. Sowing was adjusted, taking the previous germination experiment into account, to get 50 germinating seeds per plate. Seedlings were analyzed using the Leica S6E stereo microscope. The Leica MZ16 F fluorescence stereo microscope (z-stack function) was used to image *C. suecicum* mutants and albinos, the microscope is equipped with the Leica DFC420 C camera system and the Leica Application Suite X (3.4.2 build 18368) image analysis software. Suitable mutants were transferred to soil.

2.3.4 Determination of germination efficiency

The germination rate of *C. suecicum* was analyzed under control conditions (0 mM NaCl) or under exposure to various salt stress conditions (100, 200, 300, 400, 500 mM NaCl). For each treatment, three times 50 seeds per petri dish were sown on Whatman paper, 5 ml of NaCl

solution was added and the plates were sealed with adhesive tape. The plates were then transferred to short-day (SD) or long-day (LD) conditions and the germination rate was checked every two to three days until no new seedlings could be observed. The experiment was repeated three times.

2.3.5 Determination of flowering time and grain yield

Flowering time and the grain yield of *C. quinoa* and *C. suecicum* was analyzed under control conditions (0 mM NaCl) or under exposure to salt stress conditions (100, 200, 300 mM NaCl). Flowering time was analyzed by determining the time of bolting (bolting = first flower bud visible) and for *C. quinoa* also the number of true leaves at the main stem when bolting was recorded. In addition, the height of the plants was measured for both species at the time of bolting. One seed per 9 cm pot was sown (n = 10) and the pots were transferred to short-day conditions. The plants were either exposed to different salt stress conditions directly after sowing or when the seedlings were one, two, or three weeks old. The grain yield was analyzed after the plants completed the life cycle.

2.3.6 Determination of epidermis and bladder cell area

The cell size of epidermis and bladder cells was analyzed under standard growth conditions on the adaxial and abaxial leaf sides of *C. quinoa* and *C. suecicum*. For evaluation of the epidermis cell sizes, three different sections (leaf tip, leaf middle, leaf base) of a young (1.5 cm) and an old leaf (around 3 cm) were evaluated. Per leaf section, ten epidermal cells were analyzed (n = 300). From these, mean values were determined. For determination of the bladder cell size, young leaves with a size of 1 cm were analyzed. The area of the largest expansion of the bladder cells was determined. Per replicate, the sizes of ten bladder cells were analyzed (n = 30). The Leica DM5000 B microscope, equipped with the DFC36-0 FX camera system, was used for image acquisition and ImageJ to determine the cell sizes. These analyses were performed by Anna Marxer during her bachelor thesis.

2.3.7 Determination of bladder cell density

To determine the bladder cell density of *C. quinoa* and *C. suecicum*, five-day-old seedlings were watered with control (0 mM NaCl) or 200 mM NaCl solution three times a week for a duration of two weeks. For another two weeks, plants were watered with water. When leaf three reached a size of around 1.5 (*C. quinoa*) or 2 cm (*C. suecicum*), the amount of bladder cells was determined on the leaf base, the leaf middle, and the leaf tip, since density decreased

from the leaf base to tip. The fluorescence stereo microscope Leica MZ16 F, equipped with Leica DFC420 C digital microscope camera, was used for image acquisition and ImageJ to determine the number of bladder cells for a leaf section of 6 mm^2, respectively. From these values, an average and the amount of bladder cells per mm^2 were calculated in Microsoft Office Excel (2016). Per species, ten replicates were analyzed (n = 30). These analyses were performed by Anna Marxer during her bachelor thesis.

2.3.8 Data representation and statistics

Statistical evaluation was done in RStudio Version 1.1.383 (RStudioTeam, 2015). The data were tested for variance homogeneity (Levene's Test for Homogeneity of Variance) and normal distribution (Shapiro-Wilk normality test). One-way ANOVA (ANalysis Of Variance) with post-hoc Tukey HSD (Honestly Significant Difference) test was performed if both requirements had been met. If no variance homogeneity was given Welch-ANOVA and Games-Howell post-hoc test were performed. For statistical evaluation of the epidermal and bladder cell area and the bladder cell density, two-sided Fisher test and a subsequent two-sided Student t-test ($\alpha = 0.05$) were performed in Microsoft Office Excel (2016). Excel was also used to create figures, including mean and standard deviation.

3 Results

A. thaliana

This work investigates the effects of varying light intensities and heat stress on traits associated with the MBW network, with a particular focus on trichome development. In addition, the dry weight of above-ground material and the seed number of treated plants were quantified as indicators of *A. thaliana*'s adaptive response to light stress. The gene expression of the MBW components was analyzed to determine potential expression changes within the network. By comparing the different light stress expression data and integrating them with available transcriptome data, the results may shed light on the molecular mechanisms behind *A. thaliana's* stress response. Overall, the aim of this project is to better understand the adaptation strategies of *A. thaliana* to changing environmental conditions.

3.1 Varying light intensity affects the dry weight and the number of seeds

To demonstrate that the chosen light stress treatments are sufficient to induce a phenotypic response, the dry weight of above-ground material and the grain yield of Col-0 (wild type) and the *ttg1-21* mutant were determined, to find out whether they change significantly compared to the control. The *ttg1-21* mutant was inspected to investigate how the lack of the MBW regulation affects these proxies for stress response. For this experiment, the plants were grown under different light conditions (30, 60, 90, 120 and 400 µmol/m^2s) from the seed stage and were thus exposed to constant light stress.

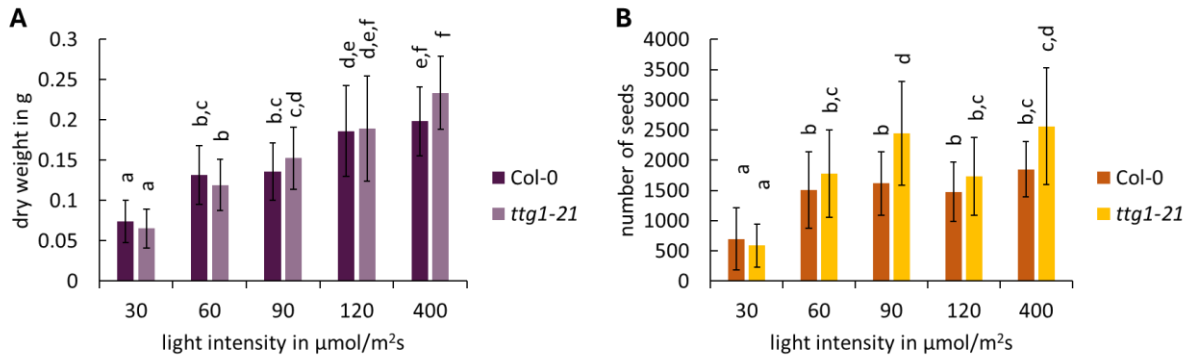

Figure 6: Dry weight and seed production under different light intensities. Plants were either grown under low-light (30, 60, 90 µmol/m²s), control (120 µmol/m²s), or high-light (400 µmol/m²s) conditions after stratification. The graphs show how **A)** the dry weight and **B)** the production of seeds changes under various light intensities. Error bars depict the standard deviation; *n* = 20 replicates; lowercase letters indicate significance groups; significance was tested using Welch-ANOVA and Games-Howell post-hoc test at a level of $p < 0.05$.

Figure 6 A) displays that at 30 µmol/m²s, the dry weight was, on average, about 0.07 g per plant, and at 60 and 90 µmol/m²s, the dry weight almost doubled to 0.15 g. For the higher light intensities of 120 and 400 µmol/m²s, the dry weight reached an amount of around 0.2 g. For the mutant, it was also evident that the dry weight of the low-light treatments (30, 60, 90 µmol/m²s) differed significantly from treatments with high light. Overall, the dry weight was significantly affected under varying light intensities and increased with higher light intensity. However, the dry weight did not differ between the mutant and the wild type.

Seed production was significantly reduced under the lowest light stress treatment compared to all other treatments (Figure 6 B). In this case, seed production only reached an amount of 500 seeds for the mutant and 700 seeds for the wild type. For all other treatments, the number of seeds was around 1500 or higher. Regarding seed production, there were no significant differences between the mutant and the wild type for most light intensities. Only at an exposure of 90 µmol/m²s the mutant produced significantly more seeds, and the seed production rose to a total of 2500 seeds. Here, seed production was also greater than for the 60 µmol/m²s and 120 µmol/m²s treatments. Generally, the seed number seems very variable, which was also reflected in high standard deviations. Nevertheless, it was affected by varying light intensity.

3.2 Varying light intensity affects the phenotypic plasticity of trichomes

To understand how the MBW network reacts to abiotic stress at a phenotypic level, a phenotypic analysis of the trichome patterning trait was performed. To investigate how the trichome phenotype changes under light stress, Col-0 was exposed to different light intensities

(30, 60, 90, 120 and 400 µmol/m²s). For short-term stress, seedlings were grown for eight days at 120 µmol/m²s and long-day conditions. Next, the plants were transferred to light stress for 6 hours (30, 60, 90 and 400 µmol/m²s) and then transferred back to 120 µmol/m²s until analysis. For constant light stress (long-term), the plants were grown under the same five light conditions from the seed stage. The number of trichomes was examined on the adaxial side of leaves three and four and evaluated when the leaves had reached a suitable size (≈ 0.3 cm).

3.2.1 Short-term light stress does not affect trichome number

Since trichomes are assumed to have a light-reflecting property, the question arose whether increased light stress can lead to an increased trichome density (Xiao et al., 2017). The number of trichomes was recorded after the exposure to low- (30 µmol/m²s) or high-light (400 µmol/m²s) stress for 6 h. Ten replicates per treatment and control were analyzed.

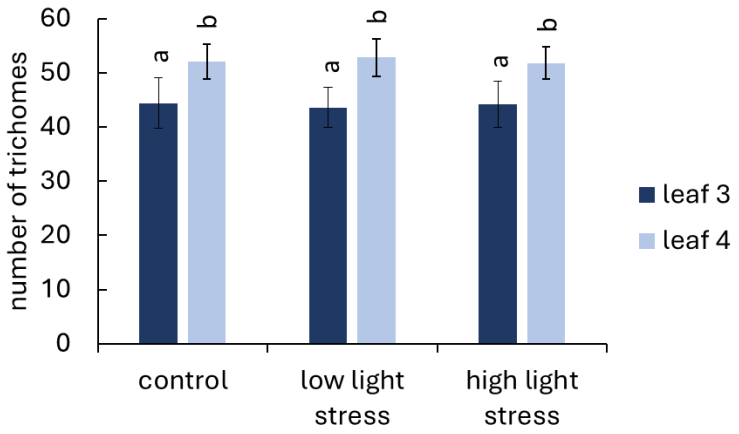

Figure 7: Trichome number under short-term light stress. Plants were grown for 8 d under control conditions (120 µmol/m²s) and then exposed to low- (30 µmol/m²s) or high-light (400 µmol/m²s) stress for 6 h. Error bars depict the standard deviation; *n* = 10 replicates; lowercase letters indicate significance groups; significance was tested using One-way ANOVA with post-hoc Tukey HSD test at a level of $p < 0.05$.

The number of trichomes did not differ between the two extreme light treatments and the control (Figure 7). On leaf three, the number of trichomes was approximately 43, which differs significantly from the number on leaf four, where 53 trichomes were recorded.

3.2.2 Constant light stress affects trichome number

To investigate how trichome density changes under various constant light intensities (30, 60, 90, 120 and 400 µmol/m²s), the leaf area and the number of trichomes on the adaxial side of leaves three and four were recorded to calculate the trichome density. The first analysis was performed when the leaf reached a suitable length of around 0.3 cm. Two weeks after the first

analysis, the number of trichomes was counted again, but did not reveal any significant differences (supplemental Figure 27)

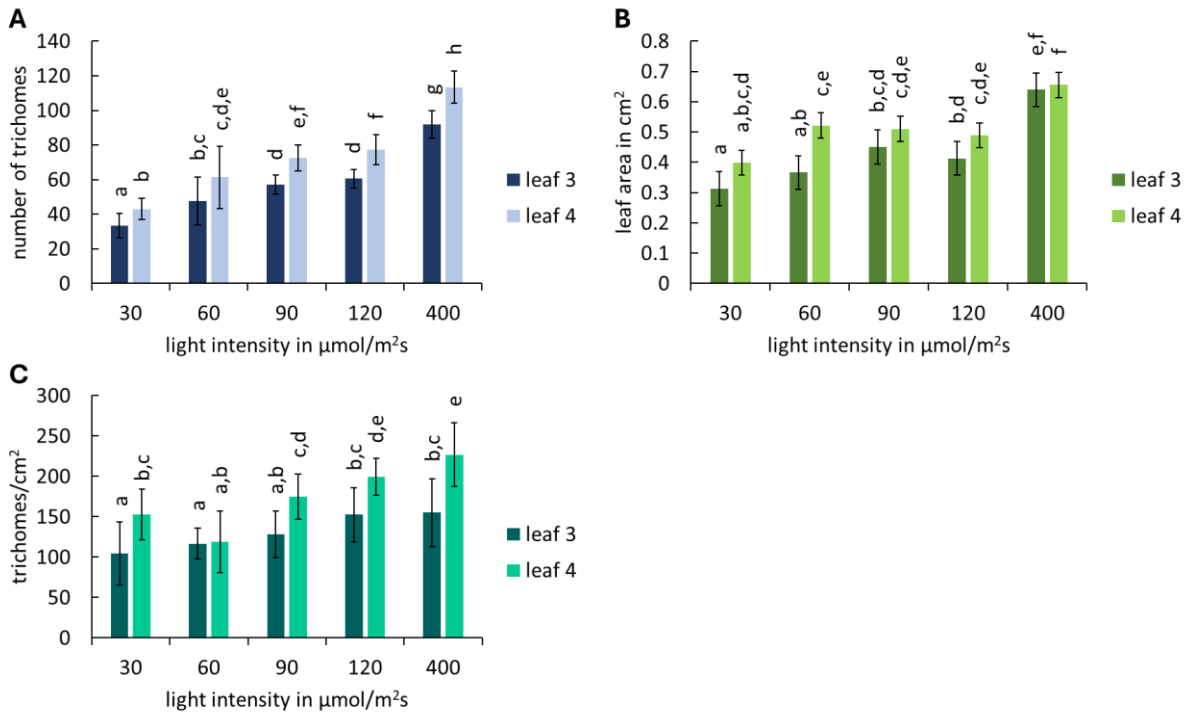

Figure 8: Number of trichomes, leaf area and trichome density under different constant light intensities. Plants were either grown under low-light (30, 60, 90 µmol/m²s), control (120 µmol/m²s) or high-light (400 µmol/m²s) conditions after stratification. The graphs show **A)** the number of trichomes, **B)** the leaf area, and **C)** the trichome density. Error bars depict the standard deviation; *n* = 20 replicates; lowercase letters indicate significance groups; significance was tested using Welch-ANOVA and Games-Howell post-hoc test at a level of $p < 0.05$.

Figure 8 A) displays the number of trichomes. At an intensity of 30 µmol/m²s, leaf three carried, on average, 35 trichomes and leaf four around 45. As the light intensity increased to 60 µmol/m²s, the number rose significantly by about 15 additional trichomes for both leaves. The number of trichomes on leaf three rose significantly with each intensity step except between 90 and 120 µmol/m²s. A very similar result is shown for leaf four, but no significant differences existed between 60 and 90 µmol/m²s. Between the 120 µmol/m²s and 400 µmol/m²s treatments, the number increased again significantly to 95 trichomes on leaf three and 110 trichomes for leaf four. Overall, the number of trichomes rose by more than double from the lowest to the highest light intensity.

To rule out that higher numbers of trichomes are only due to larger leaves, the leaf area was determined (Figure 8 B). A similar developmental stage for analyzing trichomes and leaf area was aimed for all treatments. However, leaf three at an intensity of 30 µmol/m²s was significantly smaller than the 90, 120, and 400 µmol/m²s treatment with an area of 0.3 cm².

Leaves three and four under high-light conditions were significantly larger than all other treatments, with an area of about 0.65 cm^2.

The trichome density (Figure 8 C) was determined from the number of trichomes and the leaf area. Leaves three and four, at a light intensity of 30 and 60 µmol/m^2s, showed significantly reduced trichome density in contrast to higher light intensities of 120 and 400 µmol/m^2s. The trichome density increased by around 50 to 65 trichomes per cm^2. Overall, the graph shows that trichome density rose with higher light intensity.

Intercalation is not the reason for differences in trichome density

This study showed that the density of trichomes rose with increasing light intensity. Understanding the mechanism behind this observation could provide valuable insights into how environmental stress influences plant trichome development and distribution. Two hypotheses can be formulated to explain the higher number of trichomes under high- light stress. Firstly, the increased light intensity could generally increase the expression of genes responsible for the trichome patterning and thus increase the total number of trichomes. Alternatively, another mechanism, known as intercalation, could play a role. Intercalating trichomes develop above the trichome initiation zone of young leaves, between already-formed trichomes (Hülskamp et al., 1994). It is possible that the increased light intensity promotes the formation of intercalating trichomes and thereby raises the total number of trichomes. To test this hypothesis, leaf three was examined under different light conditions, at a size of 300 to 400 µm (Figure 9, supplemental Figure 26).

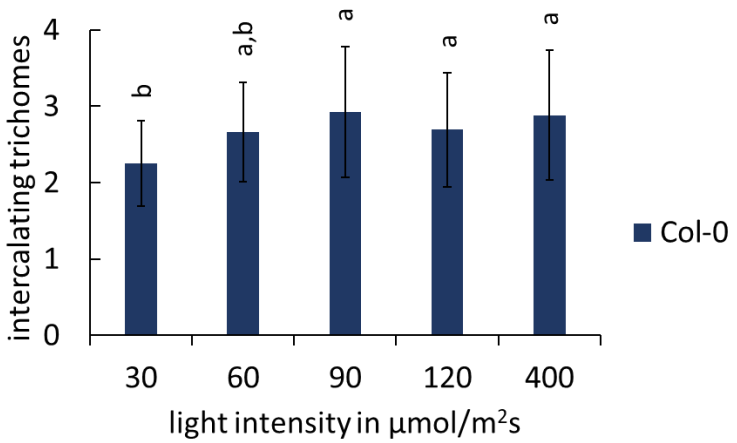

Figure 9: Intercalating trichomes under different light intensities. Plants were either grown under low-light (30, 60, 90 µmol/m²s), control (120 µmol/m²s) or high-light (400 µmol/m²s) conditions after stratification. Newly developing trichomes above the trichome initiation zone were counted. Error bars depict the standard deviation; $n \geq 48$ replicates; lowercase letters indicate significance groups; significance was tested using One-way ANOVA with post-hoc Tukey HSD test at a level of $p < 0.05$.

The number of intercalating trichomes that develop above the initiation zone (Figure 5) ranges from two to three per leaf, indicating a relatively low number of intercalating trichomes. However, a significant reduction of intercalation is shown for the lowest light treatment (30 µmol/m^{2}s) compared to the treatments with higher light intensities of 90, 120 and 400 µmol/m^{2}s. Instead of about three trichomes, there are only two intercalating trichomes present per leaf. Nevertheless, this difference is minimal and cannot explain the difference in trichome density of approximately 50 trichomes observed in the previous experiment (Figure 8 C) between the lowest and the highest light treatment.

3.2.3 Constant high-light stress induced anthocyanin production

Plant development under light stress was tracked every two to three days. The following figure shows overview of representative Col-0 plants under control (120 µmol/m^{2}s) and high-light (400 µmol/m^{2}s) conditions treated with constant light for 14 or 16 days (Figure 10).

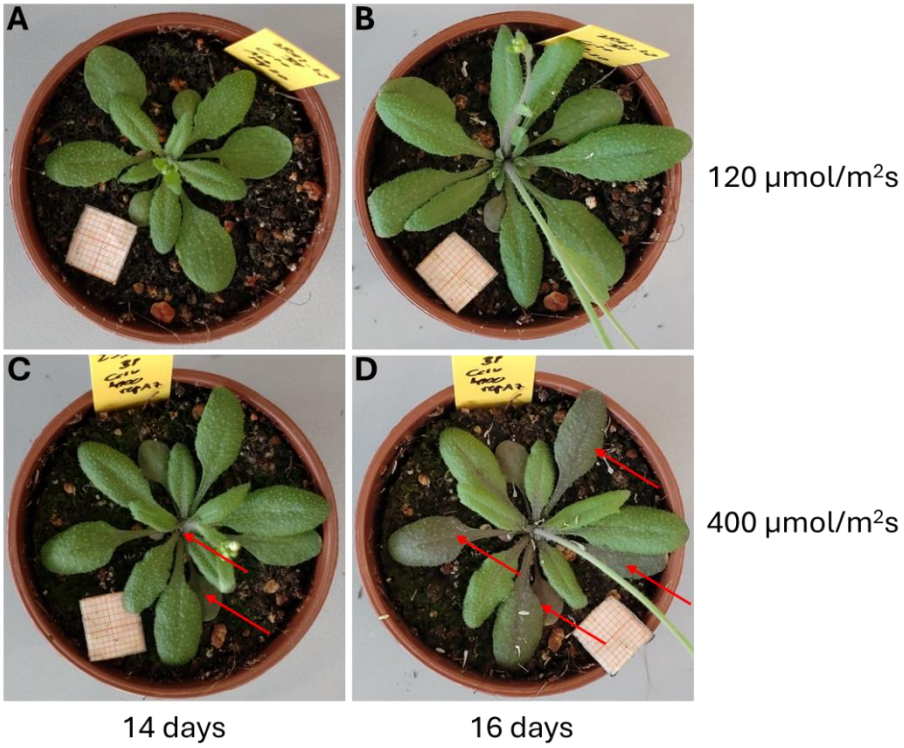

Figure 10: Overview of single Col-0 plants under control and high-light conditions. Plants were either grown under control (120 µmol/m²s) or high-light (400 µmol/m²s) conditions after stratification. **A)** overview control 14 days, **B)** overview control 16 days, **C)** overview high light 14 days, **D)** overview high light 16 days.

When comparing the overview pictures (Figure 10), it was noticeable that after about two weeks, anthocyanin production was visible in the first two true leaves and in the stem of plants exposed to high light (red arrows, Figure 10 C). After 16 days, the anthocyanin production was even more prominent (Figure 10 D). The plants treated with 120 µmol/m²s did not show distinct red coloring.

3.3 Light stress affects MBW gene expression

To understand how the MBW network integrates stress information to regulate a phenotypic response, an expression analysis via quantitative real-time PCR was performed. Based on the previous experiments, where it was shown that the trichome density is significantly reduced under low light and significantly increased under high light, the expression analysis was carried out under these conditions (Figure 8 C). The seedlings were either grown directly under the desired light intensities of 30 or 400 µmol/m²s, which provided a constant light environment, or they underwent a transfer experiment in order to record rapid changes in expression levels due to short-term stress. In the first setup, the seedlings were exposed continuously to the specified light conditions for eight days. In the second setup, the transfer experiment involved

moving the seedlings from 120 µmol/m^2s light intensity to low- or high-light stress for a period of 6 hours.

Since this work particularly focuses on trichome patterning, early leaf stages with developing trichomes were selected and analyzed, as the patterning genes are only switched on in detectable concentrations during trichome formation (Pietsch, 2022). The cotyledons without trichomes and the roots were removed from the young seedlings for sampling. Even though the work focuses on trichome patterning and the sampling was designed accordingly, the genes of the other traits were also analyzed to get an impression of how the entire network reacts to stress and whether conclusions can be drawn about possible phenotypes from the expression analysis. Significant differences were identified, and only those changes were deemed biologically relevant that showed at least a doubling or halving of gene expression. A complete overview of the expression data can be found in the appendix (supplemental Figure 29 to Figure 32 and Table 9).

3.3.1 Expression analysis of MBW genes under constant light stress

The results show how the gene expression of the genes that regulate the five MBW traits changes under constant light stress. The color coding corresponds to that of the MBW network (Figure 2) and distinguishes between the activators WD40, bHLH and R2R3-MYB, the R3-MYB inhibitors as well as *GL2*. The unique genes only associated with the seed coat mucilage trait and the root hair patterning trait did not change under stress conditions: *MYB5*, specific for the seed coat mucilage, and *WER*, specific for root hair patterning, were never significantly affected according to the set requirements. Hence, this section focuses on the genes related to anthocyanin and proanthocyanin production and the formation of trichomes.

<u>Anthocyanidin and proanthocyanidin</u>

Figure 11 shows the expression changes of the constant light experiments regarding the anthocyanidin and proanthocyanidin traits. The two traits were summarized in one figure, as they only differ in a few MYB genes but share the same BHLHs (*TT8*, *EGL3*). The anthocyanin trait is regulated by MBW complexes formed with *PAP1* or *PAP2*. The production of proanthocyanins, on the other hand, is regulated by an MBW complex formed with *TT2*.

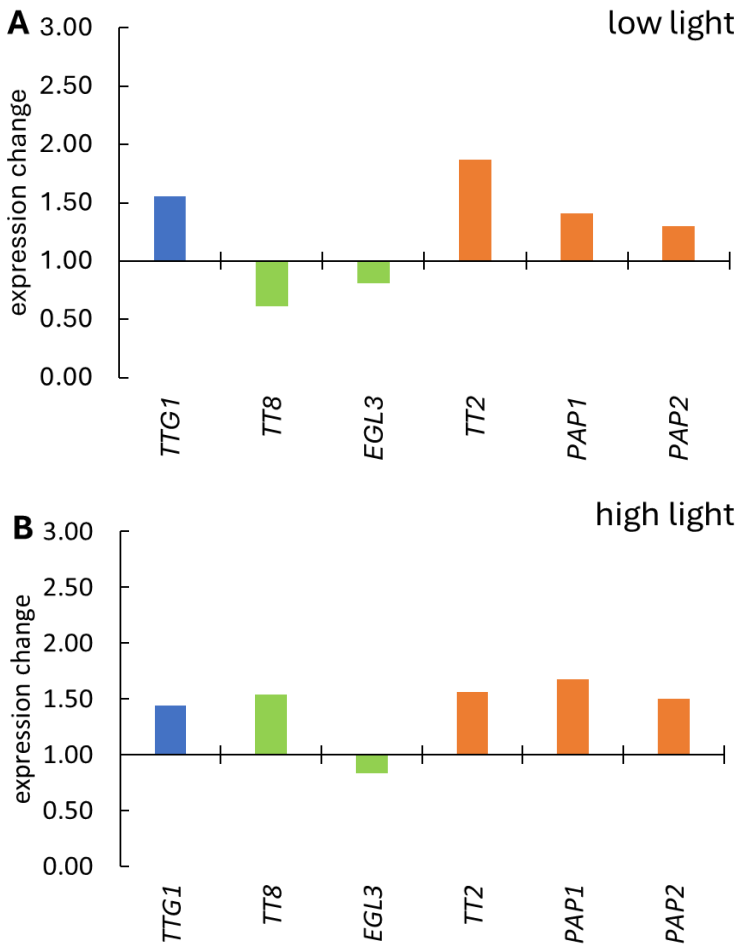

Figure 11: Expression changes of constant light experiments compared to control conditions for anthocyanidin and proanthocyanidin genes. Plants were grown under **A)** low- (30 µmol/m²s) or **B)** high-light (400 µmol/m²s) conditions after stratification. WD40 (blue), bHLH (light green), R2R3-MYB (orange). All values were normalized to the two reference genes *TIP41* and *AT4G33380*. *n* = 3 replicates; significance was tested using Mann Whitney U test at a level of $p < 0.1$.

Under constant low-light conditions (Figure 11 A), the expression of the genes did not differ significantly. *TTG1*, *TT2*, *PAP1,* and *PAP2*, however, appeared to be slightly stronger expressed under low-light conditions than under control conditions. In contrast, *TT8* and *EGL3* expression tended to decrease compared to the control under stress. Under high-light stress (Figure 11 B), the expression of the genes did not differ significantly according to the specified conditions either.

Trichome patterning

The following shows how the expression of the MBW genes of the trichome patterning trait changed under constant low- or high-light conditions (Figure 12).

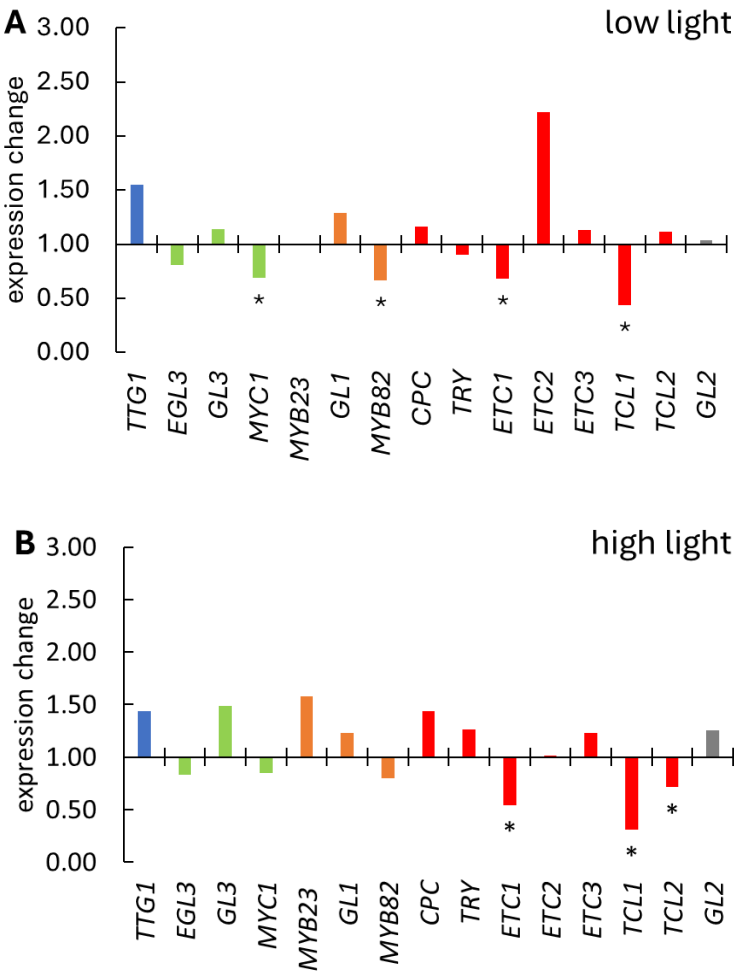

Figure 12: Expression changes of constant light experiments compared to control conditions for trichome patterning genes. Plants were grown under **A)** low- (30 µmol/m²s) or **B)** high-light (400 µmol/m²s) conditions after stratification. WD40 (blue), bHLH (light green), R2R3-MYB (orange), inhibitors (red), *GL2* (grey). All values were normalized to the two reference genes *TIP41* and *AT4G33380*. *n* = 3 replicates; * indicate significant differences; significance was tested using Mann Whitney U test at a level of $p < 0.1$.

When growing under low light (Figure 12 A), most genes did not reach the set threshold. Only *TCL1* was affected significantly at a biologically relevant level under low light. *TCL1* expression was significantly reduced by half. Although not significant, *ETC2* expression was more than twice as high in comparison to control conditions. Under high-light intensity (Figure 12 B), *TCL1* was the only gene that exceeded the set threshold. Intriguingly, *TCL1* showed a similar downregulation in both setups, despite opposite stress conditions. In contrast, *ETC2* expression did not seem to be affected at all under high light. In both experiments, the expression of some of the inhibitors was significantly regulated. However, it did not reach the set biologically relevant levels. It is also noticeable that *MYB23*, *TRY* and *TCL2* expression were influenced in opposite directions, although not significantly. Under low-light conditions, the

expression of *MYB23* and *TRY* tended to be downregulated, whereas *TCL2* tended to be upregulated.

3.3.2 Expression analysis of MBW genes under short-term light stress

The following section shows the expression changes for the short-term light stress experiments. The plants were treated with 30 or 400 µmol m^2s for 6 hours. Expression changes of the MBW genes under rapid environmental changes are displayed for the selected traits.

Anthocyanidin and proanthocyanidin

Figure 13 displays the expression changes related to the anthocyanidin and proanthocyanidin production traits.

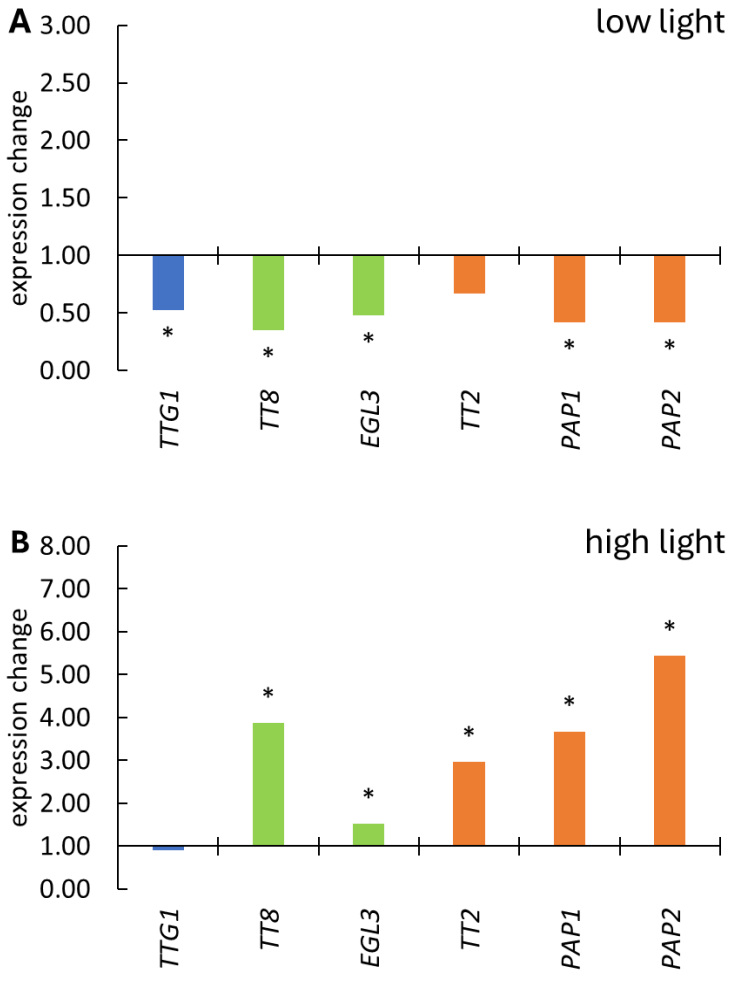

Figure 13: Expression changes of short-term experiments compared to control conditions for anthocyanidin and proanthocyanidin genes. Plants were grown for 8 d under control conditions (120 µmol/m^2s) and then exposed to **A)** low-light (30 µmol/m^2s) or **B)** high-light (400 µmol/m^2s) conditions for 6 h. WD40 (blue), bHLH (light green), R2R3-MYB (orange). All values were normalized to the two reference genes *TIP41* and *AT4G33380*. *n* = 3 replicates; * indicate significant differences; significance was tested using Mann Whitney U test at a level of $p < 0.1$.

Under short-term low light (Figure 13 A), the expression was downregulated for all involved MBW genes, of which the expression of *TT8*, *EGL3*, *PAP1* and *PAP2* significantly fell below the relevant threshold. The expression was reduced by half compared to the control. Except for *TTG1*, the same genes were upregulated under high light (Figure 13 B). Additionally, *TT2* was significantly upregulated in high light. The expression was increased three times for *TT2*, four times for *TT8* and *PAP1,* and even five times for *PAP2*. Overall, the expression of the MBW genes decreased under low-light and increased under high-light conditions.

Trichome patterning

For the trichome patterning trait, expression levels in different short-term light stress experiments were compared to the control treatment (Figure 14).

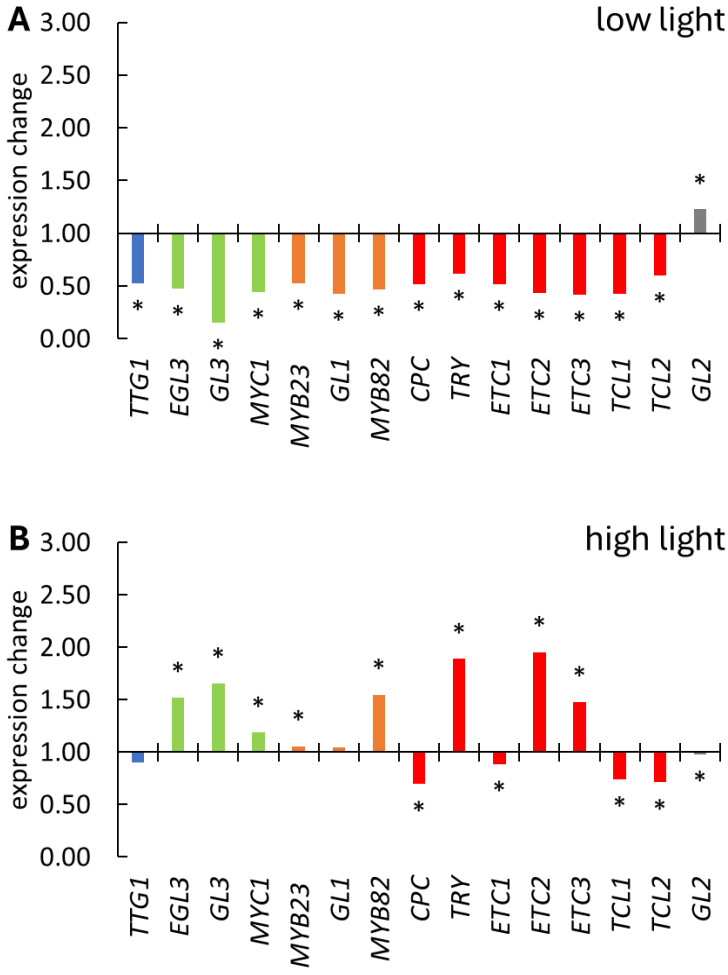

Figure 14 Expression changes of short-term experiments compared to control conditions for trichome patterning genes. Plants were grown for 8 d under control conditions (120 µmol/m²s) and then exposed to **A)** low-light (30 µmol/m²s) or **B)** high-light (400 µmol/m²s) conditions for 6 h. WD40 (blue), bHLH (light green), R2R3-MYB (orange), inhibitors (red), *GL2* (grey). All values were normalized to the two reference genes *TIP41* and *AT4G33380*. *n* = 3 replicates; * indicate significant differences; significance was tested using Mann Whitney U test at a level of $p < 0.1$.

The short-term experiment under low-light conditions (Figure 14 A) shows that the expression of all MBW genes tended to be downregulated except for *GL2*. *GL2* was slightly upregulated but did not fulfill the set requirements. A significant expression reduction by more than half was shown for *EGL3*, *GL3*, *MYC1*, *GL1*, *MYB82* and the inhibitors *ETC2*, *ETC3* and *TCL1*. For the short-term experiment under high-light conditions (Figure 14 B), there were no significant differences that fulfilled the set requirements. However, there was a tendency that most genes were upregulated under high-light stress and thus stand in contrast to the low-light treatments. Only *TTG1*, *GL2* and the inhibitors *CPC*, *ETC1*, *TCL1* and *TCL2* seemed to be downregulated. Overall, the short-term experiments (Figure 13 and Figure 14) showed more expression differences than the constant stress experiments (Figure 11 and Figure 12).

3.4 Comparison of the various light stress experiments

In order to determine significant expression changes between the various light stress experiments, as opposed to a comparison to standard conditions, the data were analyzed accordingly. The following table shows how the expression of the MBW genes changed comparing the low-light (30 µmol/m^{2}s) experiments with the high-light (400 µmol/m^{2}s) stress experiments, and how the expression in constant light experiments differed from the short-term light stress (6 h) experiments. Significant differences, with a cut-off at differences that show at least a doubling or halving of gene expression, are marked. An overview of the expression data is appended (Figure 29 to Figure 32).

Table 7: Expression changes within the various light stress experiments. WD40 (blue), bHLH (light green), R2R3-MYB (orange), inhibitors (red), *GL2* (grey), green background = significant differences and at least doubling of expression, light red background = significant differences and at least halving of expression. *n* = 3 replicates; significance was tested using Mann Whitney U test at a level of $p < 0.1$.

expression change	constant light 30 vs 400	short-term light 30 vs 400	constant vs short-term 30	constant vs short-term 400
TTG1	1.195	1.322	0.636	0.841
TT8	3.178	5.263	1.395	7.343
EGL3	1.287	2.130	1.282	2.731
GL3	1.640	4.384	0.496	2.175
MYC1	1.240	0.337	2.016	0.679
MYB5	1.411	1.608	0.547	0.880
TT2	1.082	10.871	0.044	0.475
PAP1	1.475	11.292	0.533	6.018
PAP2	1.447	21.570	0.062	1.348
MYB23	1.980	1.834	1.062	1.947
GL1	1.195	1.770	1.355	2.398

MYB82	1.525	2.194	1.079	2.368
WER	1.041	1.183	0.894	1.057
CPC	1.568	4.099	1.136	4.658
TRY	1.778	4.279	0.905	3.870
ETC1	1.047	1.512	1.016	1.536
ETC2	0.572	16.117	0.238	3.836
ETC3	1.362	4.259	0.548	2.335
TCL1	0.941	2.008	1.013	2.034
TCL2	0.804	1.189	1.019	1.212
GL2	1.487	0.758	2.151	1.631

Comparing the two constant light stress experiments (Table 7), with each other, it was shown that *TT8* expression is significantly increased by three-fold from low to high light. *TT8* is involved in the production of the seed coat mucilage, anthocyanidin, and proanthocyanidin.

Comparing the two short-term experiments, significant expression differences emerged for various MBW network components. Most of the genes were significantly upregulated when exposed to high-light stress. Only the expression of *MYC1*, which is involved in trichome and root hair patterning, was reduced by three-fold when exposed to high light. In contrast, the expression of *TT8*, *EGL3*, *GL3*, *TT2*, *PAP1*, *PAP2*, *MYB82*, and of the inhibitors *CPC*, *TRY*, *ETC2*, *ETC3* and *TCL1* was increased under high light. The expression was particularly increased for the bHLHs, *TT8* (five-fold) and *GL3* (four-fold). Also, the expression of the R2R3-MYBs, *TT2* and PAP1 increased significantly by eleven-fold, and *PAP2* expression increased especially by twenty-one-fold. Furthermore, the expression of the inhibitors *CPC*, *TRY* and ETC3 was increased by four-fold, and for ETC2, even by sixteen-fold. The different genes cover all five traits of the MBW network.

Regarding the constant versus short-term low-light experiments, *GL3*, *TT2*, *PAP2,* and *ETC2* showed significantly reduced expression under short-term conditions. In particular, the expression of *TT2* and *PAP2* was affected. *TT2* expression was reduced by twenty-three-fold and *PAP2* expression by sixteen-fold. *GL3* expression was reduced by half and *ETC2* expression by four-fold. In contrast, for *MYC1* and *GL2*, a rise in expression of about two times was observed under short-term exposure at 30 µmol/m^{2}s. The different MBW genes are involved in the production of anthocyanidin and proanthocyanidin as well as in the formation of trichomes and root hairs. With *GL2* the seed coat mucilage trait was also covered.

Comparing constant high light (400 µmol/m²s) with short-term high light, *TT8*, *EGL3*, *PAP1*, *GL1*, *MYB82* expression and the expression of the inhibitors *CPC*, *TRY*, *ETC2*, *ETC3* and *TCL1* was significantly upregulated under short-term conditions. For most of these genes, expression was significantly upregulated two- to three-fold. *CPC*, *TRY* and *ETC2* expression rose by around four-fold under short-term exposure to high light. The expression level of *TT8* increased even seven-fold and that of *PAP1* six-fold when comparing the two high-light experiments. All five traits were affected by the expression changes of these MBW genes. Overall, gene expression was significantly more impaired after a short period of exposure to stress.

3.5 Short-term heat stress does not affect trichome number

In a previous study it was shown that mild heat treatments of 26 or 30 °C influence the trichome distribution pattern (Okamoto et al., 2020). Here, the number of trichomes was recorded under heat stress to find out whether short-term heat stress has an influence on trichome density. The number of trichomes was examined on the adaxial side of leaves three and four after exposure to heat stress (38 °C) for 3 h. The number of trichomes was evaluated when leaves three and four had reached a suitable size (around 0.3 cm), ten replicates per treatment and control were examined.

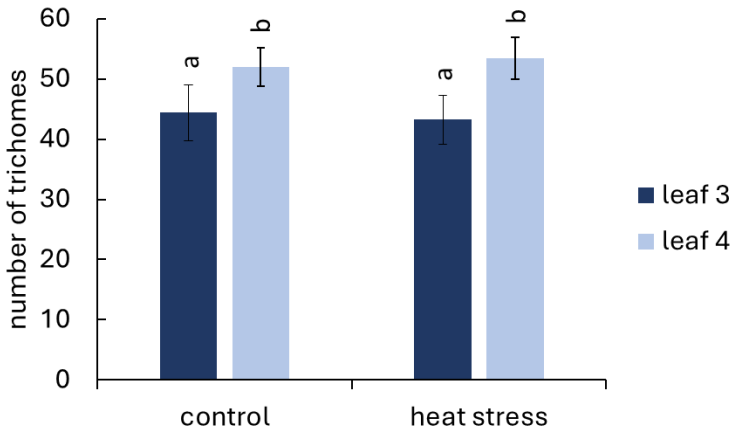

Figure 15: Trichome number under short-term heat stress. Plants were grown for 8 d under control conditions (120 µmol/m²s) and then exposed to heat stress (38 °C) for 3 h. Error bars depict the standard deviation; *n* = 10 replicates; lowercase letters indicate significance groups; significance was tested using One-way ANOVA with post-hoc Tukey HSD test at a level of $p < 0.05$.

Compared to the control, the number of trichomes did not increase or decrease when the plants were exposed to heat stress (Figure 15). The amount remained the same. On average, leaf three carried about 43 trichomes, while leaf four had about 53 trichomes. This difference

in the number of trichomes between leaves three and four is significant, leaf four carried, on average, 10 more trichomes than leaf three.

3.6 Heat stress affects MBW gene expression

For heat stress treatments, the seedlings were grown under control conditions (120 µmol/m^2s) for eight days and then exposed to heat stress for 3 hours at 38 °C in an incubator (modified from Kilian et al., 2007). After another 3 hours under control conditions, samples were collected. In a first step, new reference genes for heat stress were tested and defined. These reference genes were included to evaluate the qPCR data. Calculated expression changes of the MBW genes between heat stress and the control are shown below. A complete overview of the expression data is appended (supplemental Figure 33 and Table 9).

3.6.1 Establishment of heat stress reference genes

A challenging task was to find suitable reference genes for heat stress. Twelve different reference gene candidates were tested on cDNA of *A. thaliana* shoot material grown under control and heat stress conditions. The RefFinder tool (Xie et al., 2012) was used to identify matching reference genes. The tool displays the ranked results of common reference gene testing programs such as geNorm (Vandesompele et al., 2002), BestKeeper (Pfaffl et al., 2004), and NormFinder (Andersen et al., 2004). It was found that some of the standard reference genes for qPCR, such as UBQ10, Actin, or 18S rRNA, are not suitable candidates since their expression is affected by heat stress.

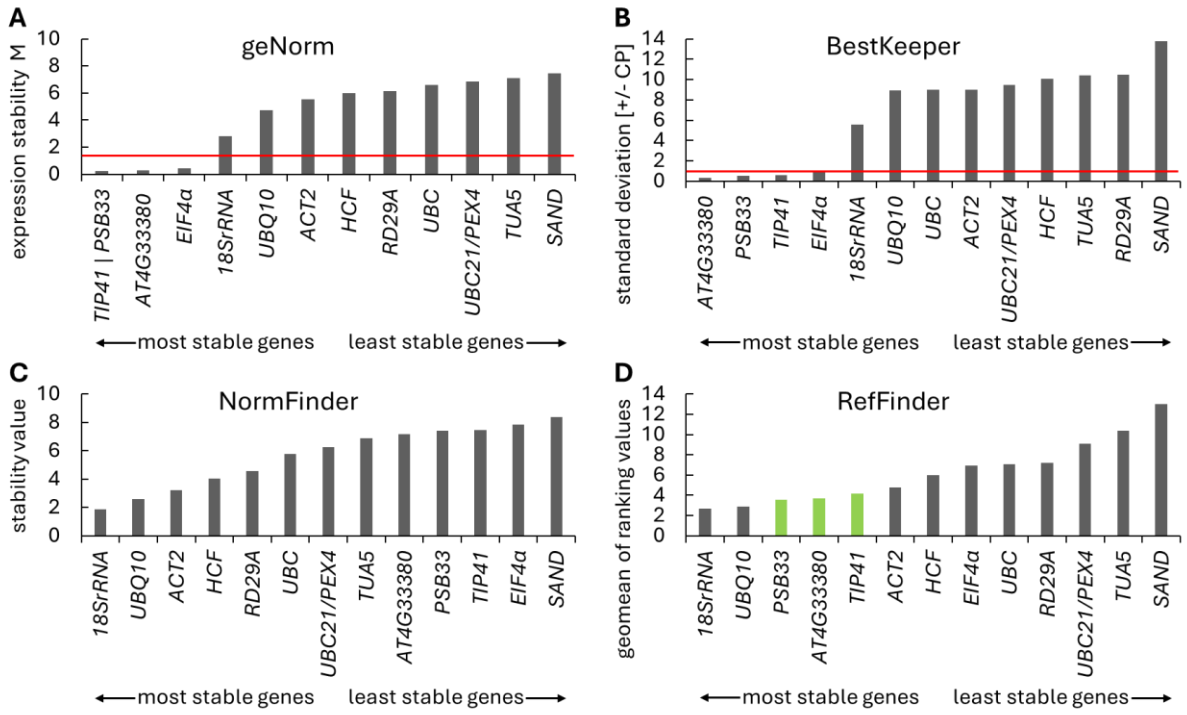

Figure 16: Determination of stable reference genes under heat stress conditions according to different programs. The expression of the reference gene candidates was tested under control and heat stress conditions. Plants were grown for 8 d under control conditions (120 µmol/m²s) and then exposed to heat stress (38 °C) for 3 h. The Ct values were entered into the web tool and analyzed with **A)** geNorm (red line specifies geNorm cut-off value = 1.5), **B)** BestKeeper (red line specifies BestKeeper cut-off value = 1; CP **=** crossing point) and **C)** NormFinder. **D)** RefFinder ranks the genes according to the stability output values from the different programs, suitable primer sets are shown in green.

Figure 16 A and B show the results of the geNorm and BestKeeper analysis, the genes were sorted from left to right according to their stability. The cut-off value for geNorm corresponds to 1.5 and for BestKeeper to 1. Therefore, only *PSB33*, *TIP41*, *ATG4G33380* and *EIF4α* could be considered stable reference genes. For expression stability analysis with NormFinder (Figure 16 C), 18SrRNa and UBQ10 displayed the highest stability. The RefFinder (Figure 16 D) identified the most stable reference genes from the various programs by comparing the ranks and establishing its own order accordingly. Considering the cut-off values of geNorm and BestKeeper, the three best reference genes identified were *PSB33*, *AT4G33380* and *TIP41*. Among these, *PSB33* and *AT4G33380* were used as reference genes for heat stress in this study.

3.6.2 Expression analysis of MBW genes under heat stress

In the following, the expression change of the various MBW genes under heat stress is shown. The traits regulated by the MBW network were categorized according to the genes associated with the selected trait.

Anthocyanidin and proanthocyanidin

Expression changes of the genes involved in the anthocyanidin and proanthocyanidin traits under heat stress are shown in Figure 17.

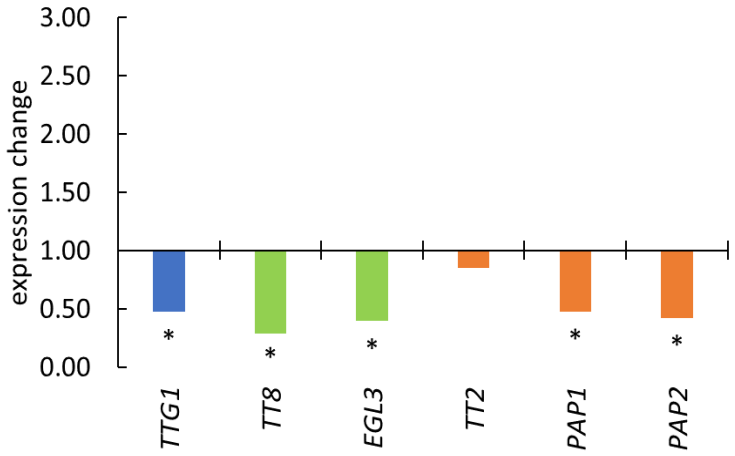

Figure 17: Expression changes of heat stress experiment compared to control conditions for anthocyanidin and proanthocyanidin genes. Plants were grown for 8 d under control conditions (120 µmol/m²s) and then exposed to 38 °C for 3 h. WD40 (blue), bHLH (light green), R2R3-MYB (orange). All values were normalized to the two reference genes *PSB33* and *AT4G33380*. *n* = 3 replicates; * indicate significant differences; significance was tested using Mann Whitney U test at a level of $p < 0.1$.

For the anthocyanin and proanthocyanin traits, the expression of the MBW genes decreased under heat stress conditions. The heat stress experiment showed that the expression of *TTG1*, *TT8*, *EGL3*, *PAP1* and *PAP2* was significantly downregulated. The expression was reduced by half compared to the control. *TT2*, which forms a trimeric complex with *TTG1* and *TT8* or *EGL3* to regulate proanthocyanidin production, showed no significant change in expression compared to the control.

Trichome patterning

The following figure shows how the expression of the MBW genes of the trichome patterning trait changed under heat stress conditions (Figure 18).

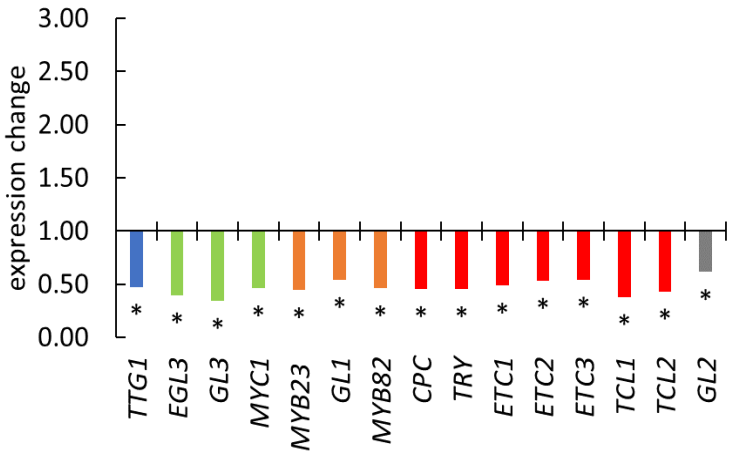

Figure 18: Expression changes of heat stress experiment compared to control conditions for trichome patterning genes. Plants were grown for 8 d under control conditions (120 µmol/m²s) and then exposed to 38 °C for 3 h. WD40 (blue), bHLH (light green), R2R3-MYB (orange), inhibitors (red), *GL2* (grey). All values were normalized to the two reference genes *PSB33* and *AT4G33380*. *n* = 3 replicates; * indicate significant differences; significance was tested using Mann Whitney U test at a level of $p < 0.1$.

Under exposure to heat stress, all MBW genes were negatively affected. For most genes the expression was downregulated to about half compared to the control. The exceptions were *GL1*, *ETC2*, *ETC3* and *GL2*. Although they showed a tendency towards reduced expression, these differences did not meet the set requirements. In general, the heat stress treatment negatively affected gene expression for the selected traits.

3.7 Comparison of expression data to available transcriptome data

In Table 8, the qPCR results of this work are compared with published transcriptomic data. However, not all MBW genes were covered by these studies (Huang et al., 2019; Kilian et al., 2007; Winter et al., 2007). The heat stress experiment, in this thesis, was conducted according to the method outlined by Kilian and colleagues, seedlings were exposed to 38 °C for 3 hours, and samples were collected after a total period of 6 hours (Kilian et al., 2007). In a separate study, Huang and colleagues compared expression data from low-light and high-light treatments, however, the intensities differed from those in this thesis. Specifically, high-light stress was conducted at an intensity of 1200, while the low-light treatment corresponded to an intensity of 60 µmol/m²s, with samples taken after 6 hours (Huang et al., 2019).

Table 8: Expression changes within the different short-term stress experiments. The Arabidopsis electronic Fluorescent Pictograph (eFP) Browser was used to extract heat stress data from Kilian and colleagues (Kilian et al., 2007; Winter et al., 2007). The expression change in comparison to standard growth conditions was determined. Fold change data regarding light stress were obtained from the supplemental material of Huang et al., 2019. The respective experimental data were classified according to their expression using an automatic color scaling in Excel. The color intensity reflects the strength of the expression change. WD40 (blue), bHLH (light green), R2R3-MYB (orange), inhibitors (red), *GL2* (grey). Color scale: red = values below one/downregulation, green = values above one/upregulation. x = not analyzed.

expression change	heat stress this thesis	heat stress Kilian et al., 2007	30 vs 400 (6 h) this thesis	90 vs 1200 (6 h) Huang et al. 2019
TTG1	0.474	0.926	1.322	x
TT8	0.290	0.654	5.263	1.961
EGL3	0.394	1.009	2.130	x
GL3	0.342	x	4.384	x
MYC1	0.459	0.838	0.337	x
MYB5	0.467	1.017	1.608	x
TT2	0.852	0.749	10.871	x
PAP1	0.477	0.560	11.292	2.782
PAP2	0.424	1.067	21.570	6.224
MYB23	0.442	0.741	1.834	x
GL1	0.538	0.789	1.770	x
MYB82	0.460	x	2.194	x
WER	0.524	0.151	1.183	x
CPC	0.452	0.535	4.099	x
TRY	0.452	1.014	4.279	x
ETC1	0.484	0.685	1.512	x
ETC2	0.530	x	16.117	0.720
ETC3	0.541	x	4.259	2.291
TCL1	0.377	x	2.008	0.324
TCL2	0.430	x	1.189	x
GL2	0.612	0.564	0.758	x

When comparing the generated heat stress data from this study with the published transcriptome data (Table 8), it was noticeable that all genes tend to be downregulated under heat stress in this study. For most genes, the expression change was slightly below 0.5. As reflected by the color scale, *TT8* and *GL3* were downregulated the most. In comparison, for *TT2* the expression change was above 0.8 and therefore was least affected by heat stress, in this setup. In the published data, most MBW genes also tend to be downregulated under heat stress, except for *EGL3*, *MYB5*, *PAP2* and *TRY*, whose expression differed only slightly from the control. In particular, *WER* expression was strongly downregulated (0.151) compared to the control. This differed from the results of this study, in which *WER* did not reach the two-fold threshold. Overall, the data were not identical, but for most genes, the expression tend to be downregulated.

Comparing the low-light stress treatments to the high-light stress experiments, it was noticeable that in the published data, of the few MBW genes analyzed, *PAP2* was most strongly upregulated under high-light stress. In this thesis, *PAP1* and additionally *ETC2* were also significantly affected. Furthermore, high light led to an upregulation of *TT8*, *PAP2* and *ETC3* in the published data, even though the expression differences were not as large as in this thesis, a similar direction of regulation was observed. For *ETC2* and *TCL1*, contradictory results were obtained, in the published data, expression was reduced compared to low light, while in this study, gene expression was significantly upregulated under high light. These differences in expression could be due to the different light intensities.

C. quinoa and C. suecicum

In order to introduce *C. suecicum* as a model organism, initial analyses were carried out on this diploid presumed ancestor of *C. quinoa* (Jarvis et al., 2017; Marhold, 2006). An EMS screen was designed in *C. suecicum*, to identify bladder cell mutants that may affect salt stress resistance. Furthermore, since *C. suecicum* has hardly been researched yet, in a first approach the salt resistance of *C. suecicum* seeds was determined under various salt concentrations (100 to 500 mM NaCl). In a follow-up experiment, flowering time and grain yield were determined under exposure to salt stress for *C. quinoa* and *C. suecicum*. Also, morphological differences between *C. quinoa* and *C. suecicum*, regarding epidermal- and bladder-cell size and density, were analyzed under salt stress conditions.

3.8 EMS mutant screen

An EMS mutagenesis with different durations (8 h or 16 h) and EMS concentrations (1-3 %) was performed in *C. suecicum* to identify bladder cell mutants. As a diploid species, *C. suecicum* is genetically more accessible compared to the tetraploid *C. quinoa* (Mandák et al., 2012). Hence, identifying a homozygous EMS mutant in *C. suecicum* would be more straightforward while the investigation of bladder cell mutants in *C. suecicum* could still provide valuable insights about the bladder cells in *C. quinoa*. The genes behind the formation of bladder cells have not yet been fully identified. Therefore, a glabrous mutant could enable the identification of genes involved in bladder formation through whole genome sequencing, thereby enhancing the understanding of the mechanism behind bladder cell formation.

3.8.1 EMS concentration affects germination rate and grain yield of M1 plants

In a first experiment, the germination rate of EMS treated M1 seeds was analyzed (Figure 19 A) since it is known that EMS treatment affects germination success (Cox, 2020; Martin et al., 2009). While bagging and collecting the M1 plants, it was found that not all germinated seedlings were able to survive and fulfill their whole life cycle, therefore, the number of bagged M1 plants was determined (Figure 19 B). Additionally, the number of M2 seeds and the corresponding germination rates on 1 % MS and soil were documented, to determine a suitable setup for the mutant screen (Figure 19 C-D).

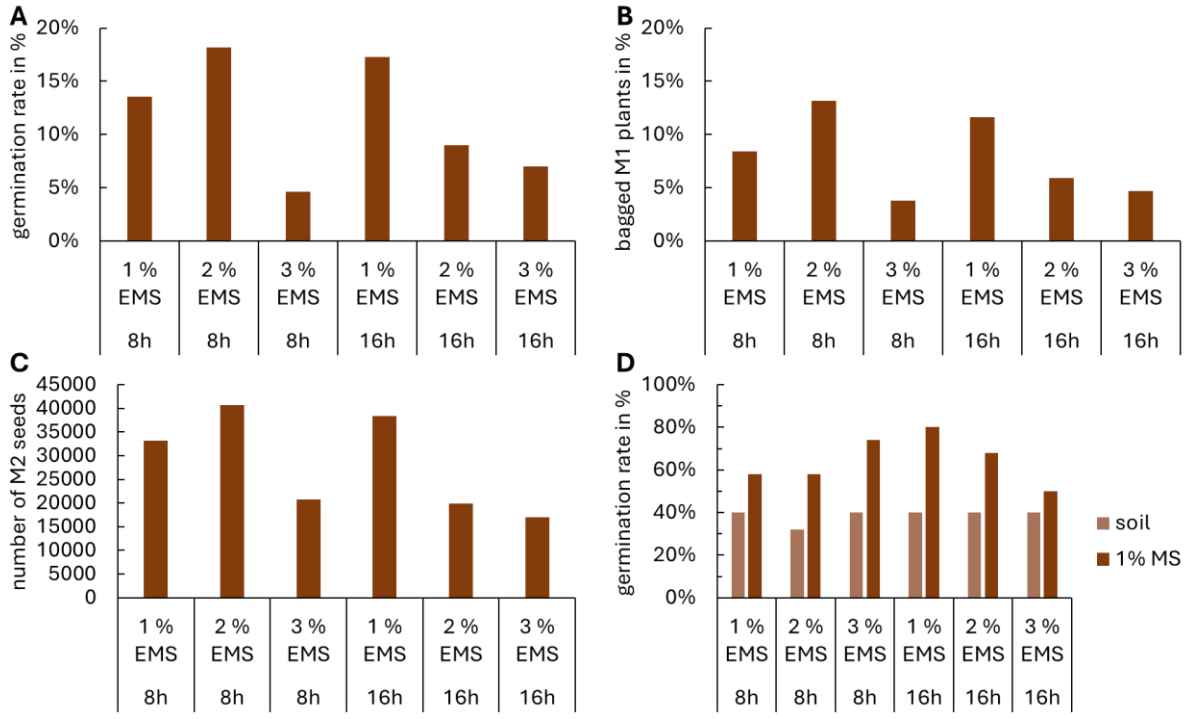

Figure 19: Germination rate of M1 and M2 seeds and grain yield of M1 seeds. A) germination rate of M1 seeds after EMS mutagenesis on 1 % MS, **B)** M1 plants which completed the entire life cycle, **C)** amount of M2 seeds, **D)** germination rate of 50 M2 seeds on soil or 1 % MS. Per EMS treatment 2000 seeds were treated with EMS for 8 or 16 h at a concentration of 1 %, 2 %, or 3 %. M2 seeds were sown onto 1 % MS plates, stratified for six days and transferred to short-day conditions.

After EMS mutagenesis, the germination rate (M1 plants) of the different EMS treatments was determined (Figure 19 A) and as expected, the germination rate decreased with increasing EMS concentration. On average, the number of seedlings decreased from 14 to 5 % when incubated for 8 h in EMS and from 17 to 7 % when incubated for 16 h. However, the germination rate for the treatment with 2 % EMS (8 h) was higher than for the 1 % (8 h) treatment. Unexpectedly, the germination rate was also higher with a longer incubation time (16 h). Not all seedlings were able to complete their whole life cycle (Figure 19 B). Therefore,

the amount of collected M1 plants decreased for the 1 and 2 % EMS treatment by about 3 to 5 % and for the 3 % EMS treatment by 1 to 2 %.

Afterwards, the number of M2 seeds was determined (Figure 19 C). The 1 % EMS treatment resulted in a grain yield of around 33,000 (8 h) and 38,000 (16 h) seeds. Since the germination rate for the 2 % EMS treatment for 8 h was higher than for the other treatments, it is not unexpected that the number of seeds was also higher in comparison. The grain yield was around 40,700 seeds. Correspondingly, the number of seeds was also lower for the treatments with 3% EMS. The grain yield was only 16,900 (16 h) and 20,700 (8 h) seeds.

In a preliminary experiment before the mutant screen (Figure 19 C), the germination rates of 50 seeds on soil or 1 % MS were tested. On soil, the germination rate for the different EMS treatments was around 40 %, and on 1 % MS, between 50 and 80 %. In all cases, the germination rate of seeds sown on 1 % MS was higher than that of seeds sown on soil.

3.8.2 Albino rate is affected by EMS concentration

Since seed germination rates were higher on 1 % MS, the mutant screen and the determination of albinos were performed on plates. To assess the efficiency of the EMS mutagenesis, the number of albinos was determined. For this purpose, M2 seeds were sown on 1 % MS and screened for albinos, since an albino rate of around 1 % reflects an efficient EMS mutagenesis (Lai et al., 2012). For 2 % EMS and 8 hours incubation, 2,708 seedlings, and for 16 hours, 1,653 seedlings were analyzed. For 3 % EMS, all seeds were sown and analyzed (Figure 19 C). For an incubation time of 8 hours, 15,776 seedlings and for 16 hours, 12,484 seedlings were analyzed.

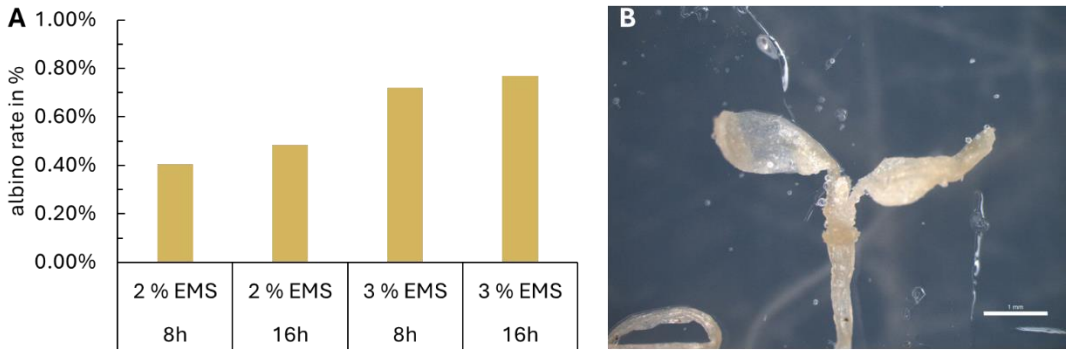

Figure 20: Albino rate of EMS mutagenesis in *C. suecicum*. Displayed are the **A)** albino rate at a concentration of 2 and 3 % EMS and **B)** an overview of an *C. suecicum* albino. Per EMS treatment 2000 seeds were treated with EMS for 8 or 16 h at concentration of 1 %, 2 %, or 3 %. M2 seeds were sown onto 1 % MS plates, stratified for six days and transferred to short-day conditions. Plates were analyzed to identify albinos using the Leica S6E stereo microscope. The Leica MZ16 F fluorescence stereo microscope (z-stack function) was used to image albinos. The scale bar is set to 1 mm.

In Figure 20 A, the albino rate for M2 seeds of the different EMS treatments is shown. At a concentration of 2 % and 8 hours of incubation, the albino rate was 0.41 %. When the seeds were incubated for a total of 16 hours, the amount of observed albinos rose to 0.48 %. At a concentration of 3 % EMS, the number of albinos rose to 0.72 % at an incubation time of 8 hours and 0.77 %, when incubated for 16 hours. The albino rates for the 1 % EMS treatments were not evaluated, because the albino rates of the 2 % EMS treatments were below 0.5 % and therefore, an even lower albino rate was expected for the 1 % treatments.

3.8.3 Identification of bladder cell mutants EMS mutant screen

In the following, the found bladder cell mutants are displayed (Figure 21). One glabrous mutant was found within the 3 % EMS treatment for 8 hours and three glabrous mutants and one bladder cell mutant were found within the 3 % EMS treatment for 16 hours.

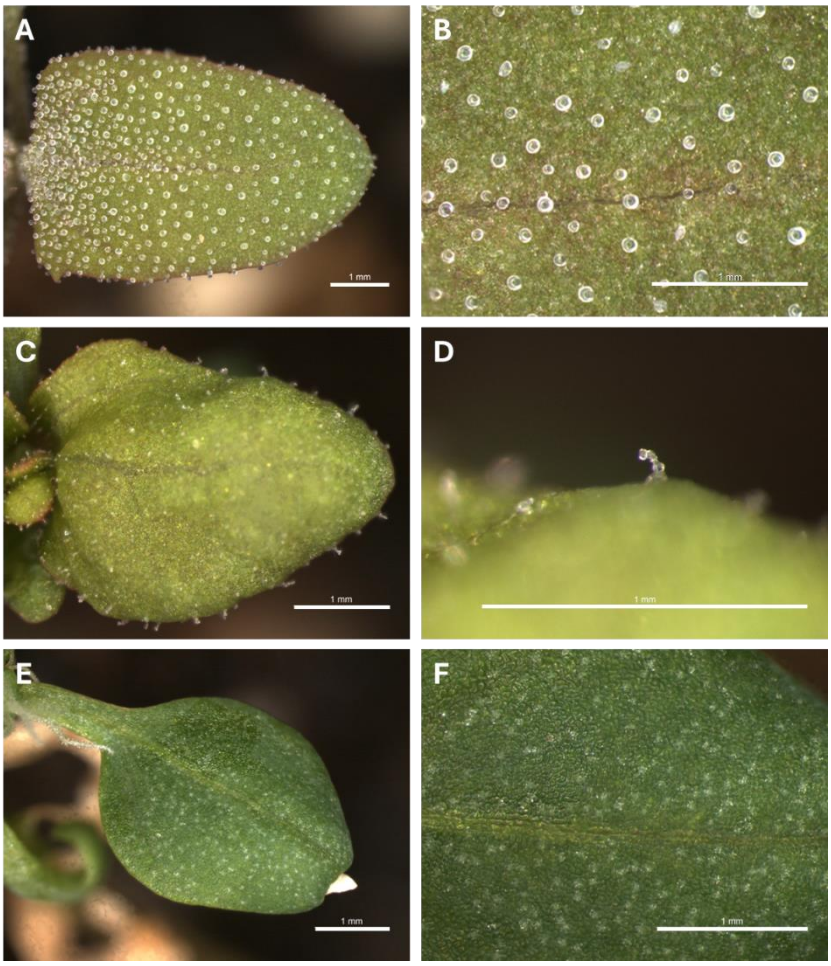

Figure 21: *C. suecicum* bladder cell (EMS) mutants. A) *C. suecicum* wild-type overview, **B)** *C. suecicum* wild-type bladder cells, **C)** bladder cell mutant overview, **D)** mutant bladder cell, **E)** glabrous mutant overview, **F)** glabrous mutant leaf excerpt. The Leica MZ16 F fluorescence stereo microscope (z-stack function) was used to image leaves of *C. suecicum*. The scale bar is set to 1 mm.

The identified bladder cell mutants (Figure 21 C-F) were compared to the wild type (Figure 21 A-B). In the wild type, the leaves were densely covered with round bladder cells (Figure 21 A-B). Density seemed to be higher at the leaf base in comparison to the leaf tip. The bladder cell mutant (Figure 21 C) had a disrupted bladder cell phenotype, the trichomes were elongated and looked as if several cells were stacked on top of each other (Figure 21 D). Compared to the wild type, the amount of trichomes was visually reduced. A glabrous mutant, which lacks bladder cells, was also identified. This type of mutant was identified four times in the EMS screens. Most of them faced challenges during the transition from 1% MS medium to soil and ultimately did not survive. The last one thrived for a few weeks in the plant chamber before unfortunately succumbing to pest activity. No seeds of the mutants could be generated to bring them into the next generation and to carry out genetic analyses. During the time in the plant chamber, the mutant grew very slowly compared to the wild type and was also smaller

and more fragile. It was assumed that not only the bladder cell formation was disturbed but also other important functions.

3.9 Salt stress affects germination in *C. suecicum*

In order to determine the salt resistance of *C. suecicum*, the germination efficiency was analyzed under various salt stress conditions (Figure 22) ranging from 100 mM to 500 mM NaCl. In addition, one set was grown under short-day (8 h light, 16 h darkness) and the other under long-day conditions (16 h light, 8 h darkness) to identify the optimal light duration.

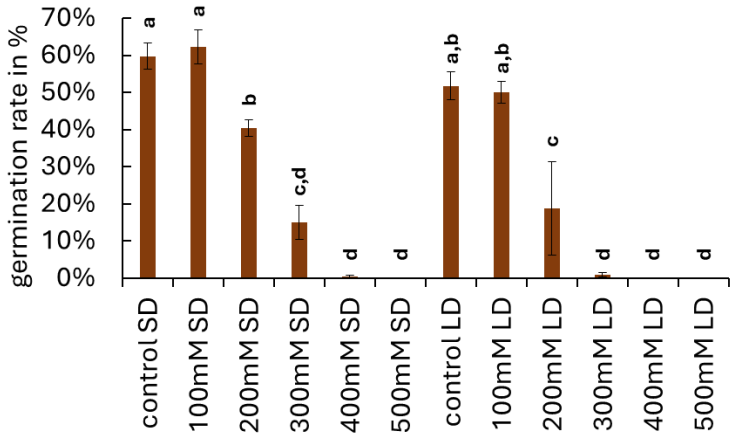

Figure 22: Germination rate of *C. suecicum* under salt stress. Seeds were either germinated under SD or LD conditions and exposed to control (0 mM NaCl) or salt stress conditions (100, 200, 300, 400, 500 mM NaCl). Seeds were sown in petri dishes on Whatman paper, 5 ml NaCl solution was added and the plates were sealed with adhesive tape. The plates were then transferred into a plant chamber set to short-day (SD) or long-day (LD) conditions, 22 °C and a light intensity of 200-250 µmol/m²s. Error bars depict the standard deviation; n = 9 replicates; lowercase letters indicate significance groups; significance was tested using One-way ANOVA with post-hoc Tukey HSD test at a level of $p < 0.05$.

Under short-day conditions and NaCl concentrations of 0 or 100 mM, the germination rate did not differ and ranged between 59 and 60 % (Figure 22). At a concentration of 200 mM NaCl the germination efficiency significantly dropped to 40 %. When the salt concentration increased to 300 mM, the germination rate dropped again by more than half to only 15 %. At a concentration of 400 mM, the seeds hardly germinated (0.4 %) and did not germinate at all when reaching a concentration of 500 mM NaCl. Under long-day conditions and 0 or 100 mM NaCl (Figure 22), the germination rate was around 50 %. With increasing salt concentrations, the germination efficiency dropped significantly to 20 % for 200 mM and 1 % for 300 mM NaCl. At higher NaCl concentrations, no germination was observed. Comparing the short- and long-day conditions, it was noticeable that the germination rate at 200 mM is significantly lower under long-day conditions than under short-day conditions. The germination rate was reduced

by half, from 40 % to around 20 % under long-day conditions. In general, seeds showed the tendency to germinate better under short-day conditions.

3.10 Salt stress affects flowering time and grain yield

The flowering time and grain yield were compared under different salt stress conditions between the tetraploid *C. quinoa* and the diploid *C. suecicum*. Flowering time is defined by the time it takes for bolting to occur, which is characterized by the appearance of the first visible flower bud. Since the previous experiment showed that seeds could no longer germinate at 400 and 500 mM NaCl and that the germination rates were higher under short-day conditions, the salt stress was limited to a concentration of up to 300 mM NaCl and performed under short-day conditions. In addition, the salt stress was started at different times to investigate whether the plant stage played a role in salt tolerance. Seeds or seedlings were treated with salt directly or after one, two or three weeks of growth.

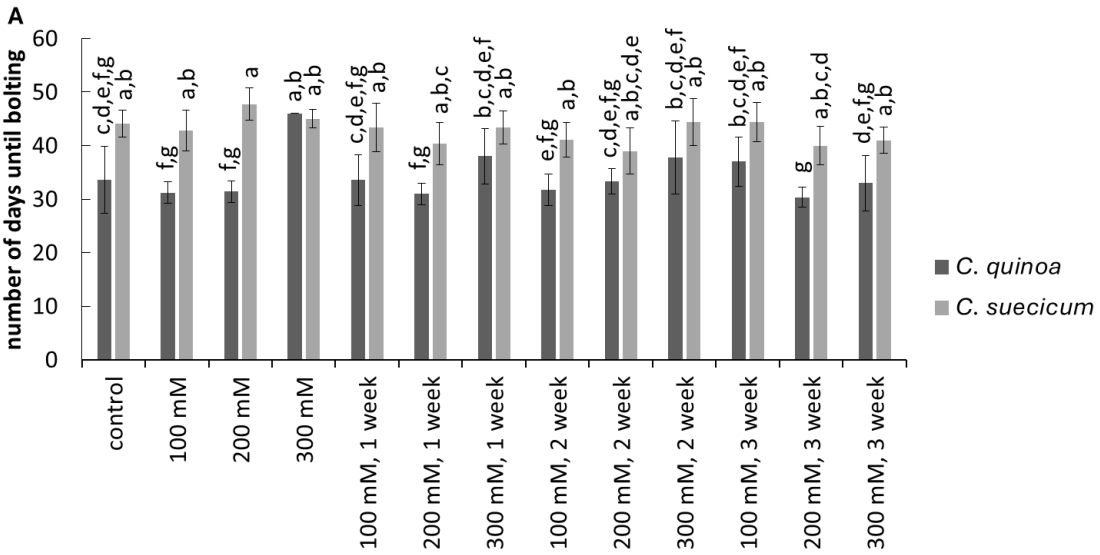

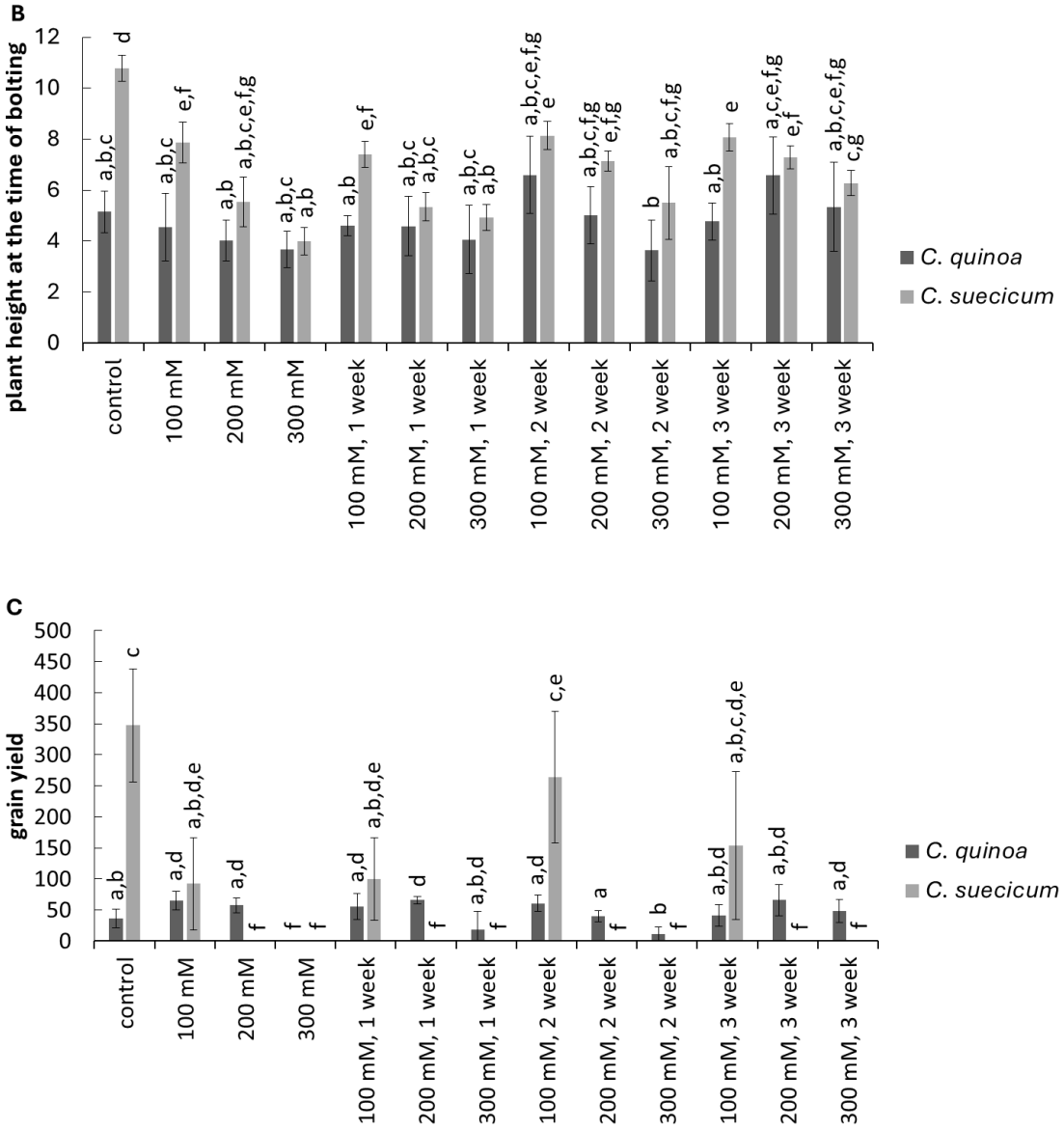

Figure 23: Flowering time and grain yield of *C. quinoa* and *C. suecicum* under salt stress. Seeds/seedlings were either germinated under control (0 mM NaCl) or exposed to salt stress conditions (100, 200, 300 mM NaCl) right from the seed stage or after one, two or three weeks. Plants were watered with the appropriate amount of salt solution three times a week. Displayed are **A)** the number of days until bolting, **B)** the plant height at the time of bolting and **C)** the grain yield. Error bars depict the standard deviation; $n \leq 10$ replicates; lowercase letters indicate significance groups; significance was tested using One-way ANOVA with post-hoc Tukey HSD test at a level of $p < 0.05$ **(A)** or using Welch-ANOVA and Games-Howell post-hoc test at a level of $p < 0.05$ **(B and C)**.

Figure 23 A displays the number of days until bolting. For *C. quinoa* the average number of days was between 31 and 38. Only a few treatments differed significantly from each other. When the seeds were treated with 300 mM NaCl, the plants needed significantly longer (46 days) to reach the flowering stage than the control and seeds treated with 100 or 200 mM NaCl (around 31 days). The direct 300 mM treatment also differed significantly from seedlings treated with 100 or 200 mM NaCl after one and two weeks and when seedlings were treated after three weeks with 200 mM or 300 mM NaCl. On average, under these treatments, the

plants needed around 13 days less to flower. Seedlings treated with 200 mM NaCl after three weeks reached the flowering time fastest, they only needed around 30 days to bolt. Therefore, the treatment was significantly different in comparison to seedlings treated with 300 mM NaCl after one or two weeks and seedlings treated with 100 mM NaCl after three weeks. When looking at the flowering time of *C. suecicum*, it is noticeable that all treatments led to flowering after around 43 days. There were no significant differences. In general *C. suecicum* showed the tendency to need more time to reach the flowering phase in comparison to *C. quinoa*. In some cases, there were significant differences between *C. suecicum* and *C. quinoa* regarding the number of days they took to flower. *C. suecicum* took significantly longer to flower when seeds were treated with 100 or 200 mM NaCl and when seedlings were treated with 100 mM or 200 mM NaCl after one week or 100 mM NaCl after two weeks. The treatment also differed from seedlings exposed to 200 or 300 mM NaCl after three weeks and in comparison to the control treatment. On average, for these different treatments, *C. suecicum* required around 10 additional days to flower.

When the plants had reached flowering time, the height of the plants was also determined (Figure 23 B). For *C. quinoa*, the size of the plants was approximately the same for almost all treatments, the plants reached an average height of 4 to 5 cm. Only seedlings treated with 300 mM NaCl after three weeks were significantly smaller (3.6 cm) than seedlings treated with 200 mM NaCl after three weeks (6.5 cm). For the salt stress treatments in *C. suecicum* it is noticeable that the control plants, which were not treated with salt, were significantly larger compared to all the other treatments. They reached a height of 10.8 cm when flowering. Seeds treated with 200 or 300 mM NaCl and seedlings treated with 200 or 300 mM NaCl after one week were significantly smaller in comparison to treatments with 100 mM NaCl. They only reached a height of 4 to 7 cm. Also, the height of seedlings exposed to 300 mM NaCl after two weeks was significantly smaller (5.5 cm).

When the plants had completed their life cycle, the above-ground material was collected, and the grain yield was determined (Figure 23 C). Some plants did not endure the salt stress treatments until plant material collection. *C. suecicum* was particularly affected, at concentrations of 200 and 300 mM NaCl, none of the plants could be analyzed regarding their grain yield. This was also impossible for *C. quinoa* when salt stress already started in the seed stage at 300 mM NaCl. Looking at *C. quinoa*, it is noticeable that seed production was relatively

low, even without salt stress. Under control conditions, around 36 seeds were produced per plant. Only one salt stress treatment that led to an unexpectedly higher seed production. When seedlings were exposed to 200 mM NaCl after one week, the grain yield rose to around 66 seeds. The lowest number of seeds was determined, when seedlings were treated with 300 mM NaCl after two weeks, on average, only 11 seeds could be collected. For *C. suecicum*, seed production under control conditions was significantly higher than for seeds or seedlings treated with 100 mM NaCl after one week. The grain yield was, on average, 350 seeds for the control and around 100 for the salt stress treatment. For *C. suecicum* the grain yield fluctuated strongly also within a treatment, which was also evident from the high standard deviations. Even though *C. suecicum* seems to produce more seeds than *C. quinoa*, this can only be statistically proven for the control treatment and for seedlings treated with 100 mM after two weeks due to the high standard deviation. For both, the grain yield was above 260.

3.11 Cell size differs among *C. quinoa* and *C. suecicum* and salt stress affects bladder cell density

An analysis of the epidermis and bladder cells of *C. quinoa* and *C. suecicum* (Figure 24) was performed to compare the two species. In addition, the bladder cell density of both species under salt stress conditions was determined. Given that the effects of salt stress on germination became evident at a concentration of 200 mM (Figure 22), the following salt stress experiments were performed with 200 mM NaCl. Therefore, five-day-old seedlings were watered with 200 mM NaCl solution three times a week for a duration of two weeks. Leaf three was analyzed when it reached a size of around 2 cm. The practical work was carried out by Anna Marxer as part of her bachelor thesis.

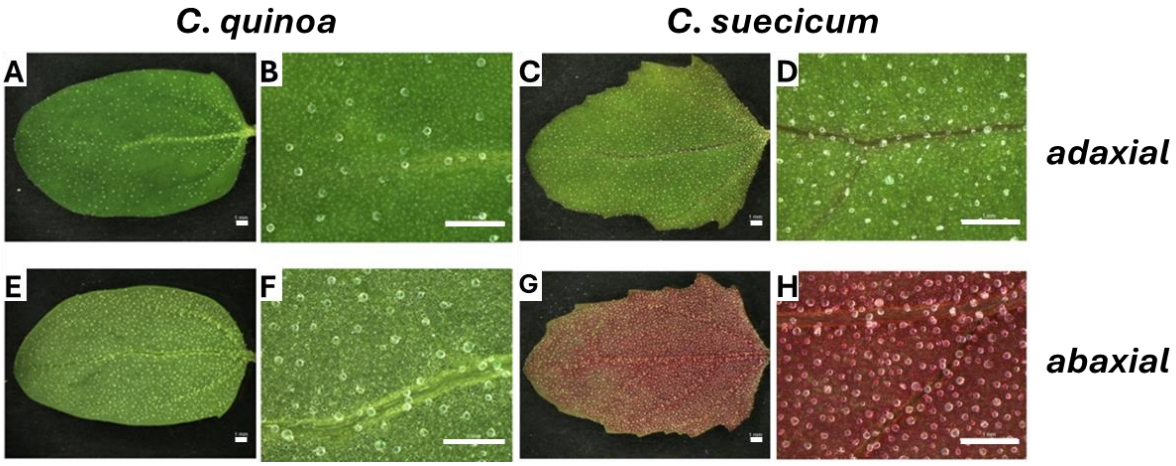

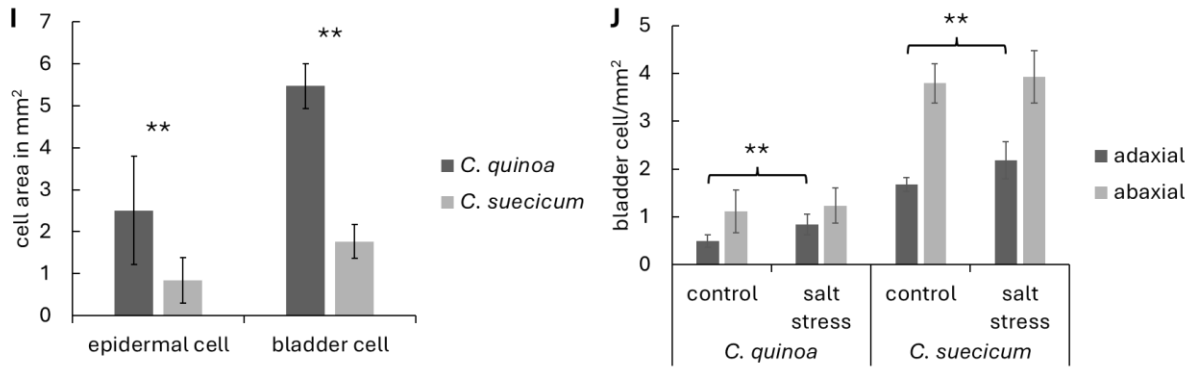

Figure 24: Determination of epidermis and bladder cell area in *C. quinoa* and *C. suecicum* and analysis of the bladder cell density under salt stress. A) overview of the adaxial leaf side of *C. quinoa*, **B)** bladder cells on the adaxial leaf side of *C. quinoa*, **C)** overview of the adaxial leaf side of *C. suecicum*, **D)** bladder cells on the adaxial leaf side of *C. suecicum*, **E)** overview of the abaxial leaf side of *C. quinoa*, **F)** bladder cells on the abaxial leaf side of *C. quinoa*, **G)** overview of the abaxial leaf side of *C. suecicum*, **H)** bladder cells on the abaxial leaf side of *C. suecicum*, **I)** epidermal and bladder cell area and **J)** bladder cell density under 200 mM salt stress. **I)** epidermal cell area n = 300 replicates; bladder cell area *n* = 30 replicates (*C. quinoa*, *n* = 21); **J)** *n* = 30 replicates; ** indicate significant differences; significance was tested using two-tailed Fisher test and a subsequent two-tailed Student t-test at a level of $p < 0.05$; ** $p < 0.01$. Modified from the bachelor thesis by Anna Marxer.

The analysis found that the diploid had more trichomes than *C. quinoa*. *C. suecicum* had about three times as many bladder cells on the adaxial and abaxial leaf sides (Figure 24 A-H). Both species also had more trichomes on the abaxial leaf side (Figure 24 F, H). In addition, the size of the epidermal and bladder cells of the two *Chenopodium* species also differed. In *C. quinoa* both cell types were significantly larger (Figure 24 I). Compared to the diploid, the two cell types were about three times as large. In a first salt stress experiment, the bladder cell density on the adaxial and abaxial leaf sides was determined (Figure 24 J). For both species, only the number of bladder cells on the adaxial leaf side increased significantly. For *C. quinoa,* the bladder cell density increased under salt stress exposure from 0.5 to 0.8 and for *C. suecicum,* the density increased from 1.7 to 2.2 bladder cells per mm^2.

4 Discussion

This study aimed to analyze how plants respond to abiotic stress at the phenotypic and genetic level, with a particular focus on the expression of genes within the *A. thaliana* MBW network. Specifically, light and heat stress treatments were performed, focusing on the trichome patterning trait and its phenotypic plasticity. Additionally, salt stress experiments were conducted in *C. quinoa* and *C. suecicum*, two halophyte species, carrying epidermal bladder cells. Overall, the conducted experiments aimed to provide a deeper understanding of the mechanisms behind the genetic and phenotypic changes contributing to plant stress resistance.

4.1 Light intensity affects trichome patterning and anthocyanin production

An important aspect of this study was the investigation of the phenotypic plasticity of trichomes under low- and high-light conditions. The results showed that constant light stress leads to a change in trichome density (Figure 8), while short-term light stress has no significant effect on trichome number (Figure 7). It was also shown that these changes in light intensity seem to come with additional consequences for plant fitness, since constant low-light stress (30 µmol/m^2s) also significantly affected dry weight and seed production (Figure 6). These results are consistent with other studies showing that dry biomass and seed production were reduced under low-light compared to high-light treatments (Eckardt et al., 1997; Tian & Ye, 2017).

In various studies, it has also been shown that high light stimulates anthocyanin production and plays a role in photoprotection (Huang et al., 2019; Page et al., 2012). This study suggested that constant high-light stress leads to an accumulation of anthocyanin pigments in the leaves of *A. thaliana* after 14 to 16 days (Figure 10).

4.2 Regulatory mechanisms vary under short and long-term stress

Since short-term light stress conditions, in contrast to constant light conditions, did not result in any phenotypic changes regarding trichome patterning, the question arose as to which mechanisms underlie this phenomenon. This different regulation suggests that plants might have developed adaptive strategies to cope with short-term stress conditions without causing phenotypic changes in trichome patterning. During short-term stress, plants might prioritize

direct survival tactics, such as stomata opening/closing or nutrient rearrangement (Desikan et al., 2002; Hildebrandt, 2018; Neill et al., 2008; Wang et al., 2020a). In this regard, Neill and colleagues observed that dehydration of detached leaves induced rapid stomata closing, which might serve to minimize water loss through transpiration in *A. thaliana* (Neill et al., 2008). Another study found that a short-term heat shock resulted in stomata opening, while constant elevated temperatures led to reinforced stomata closing (Wang et al., 2020a). The authors suggested that stomatal opening under short-term heat stress might induce evaporation, which could serve as a cooling effect, while stomata closing under constant increased temperatures might prevent water loss (Wang et al., 2020a). This indicates that a quick stress response, such as stomata opening or closing, is an advantage of sessile organisms to be able to keep up with fluctuating environmental conditions (Neill et al., 2008; Wang et al., 2020a).

Another reason for the varying stress responses under short- and long-term stress could be a different resource allocation. Under long-term stress, resource allocation might shift towards long-term survival strategies, such as root development to access water and nutrients, changing the developmental timing or the production of protective compounds such as anthocyanin (Huang et al., 2019; King et al., 2008; Oh et al., 2011; Page et al., 2012; Xu et al., 2014). A study by Oh and colleagues suggested that in *A. thaliana*, initial drought stress may induce root growth to improve water intake, while severe drought stress inhibits root growth (Oh et al., 2011). Furthermore, it was shown that developmental timing, including flowering time, is crucial for plant reproduction (Amasino et al., 2017). Therefore, flowering time is regulated under stress conditions such as varying light exposure or cold stress (King et al., 2008; Xu et al., 2014). In this context, it was shown that long-term exposure to cold stress promotes flowering, while in contrast, short-term cold stress delayed flowering time in *A. thaliana* (Kim et al., 2004; Seo et al., 2009; Xu et al., 2014). Therefore, flowering time regulation might be an evolutionary adaptation to increase survival rates in plants.

Taken together, it seems reasonable that in evolutionary adaptation to survival in changing environmental conditions, short-term changes do not lead directly to far-reaching changes in the phenotypic appearance. For instance, structures like trichomes cannot be simply degenerated. How the plants use their resources and energy is thus essential to ensure their survival and reproduction (King et al., 2008; Xu et al., 2014). This indicates that a certain

threshold of stress duration or intensity might need to be exceeded in order to lead to a phenotypic change. Research in *A. thaliana* has shown that a threshold temperature of 34 °C was necessary to induce the formation of stress granules in the cytoplasm, independent from stress duration (Hamada et al., 2018). In regard to this and to determine the threshold required to induce a phenotypic response, a stress time series with different light intensities should be performed.

4.3 Light intensity affects trichome- and anthocyanin-specific gene expression

Since the analysis of intercalation as a possible cause of differences in trichome density did not reveal a significant association (Figure 9), other factors, specifically on the expression level, were assumed to play a role. Consequently, the gene expression within the MBW network under short-term and constant light stress was investigated. The results showed altered expression of MBW genes specifically associated with trichome formation as well as anthocyanidin and proanthocyanidin production.

4.3.1 Short- and long-term stress affect gene expression differently

Particularly under short-term light stress, a distinct regulation of MBW genes was observed (Figure 13 and Figure 14). This observation was surprising since short-term stress led to no change in the number of trichomes. The expression of the genes under constant light conditions did not change beyond the specified two-fold difference for most genes. It can be assumed that genetic adaptation is triggered earlier, or it could be possible that short-term stress triggers different signal-pathways than constant stress and therefore, balances the overall gene expression over time. In this context, Yang and colleagues identified changes in hormonal signaling outputs during short-term and continuous stress exposure (Yang et al., 2014). It appears that long-term stressors might be able to induce deeper genetic changes (Chen et al., 2022).

<u>Short-term high light induces the expression of genes related to anthocyanin production</u>

Under short-term low-light conditions (Figure 13 A), a downregulation of most MBW genes was observed. For the anthocyanin trait, *TT8*, *EGL3*, *PAP1*, and *PAP2* expression was negatively affected. This could indicate that the plants tried to save resources by reducing gene expression since light protective mechanisms were not necessary under low light. Different studies showed that anthocyanins did not accumulate under low light (Huang et al., 2019;

Maier & Hoecker, 2015). In contrast, under high-light stress (Figure 13 B), *TT8*, *TT2*, *PAP1* and *PAP2*, and to a smaller extent *EGL3* expression was upregulated. The opposing regulation suggested that anthocyanin production was stimulated under high light in order to accumulate anthocyanins as light protection (Hatier & Gould, 2009; Huang et al., 2019).

Constant low- and high-light stress regulate the expression of *TT8* in opposite directions

Although constant light stress did not affect gene expression related to the anthocyanin trait beyond the two-fold threshold (Figure 11), the expression of *TT8* tends to be upregulated under high-light. An opposite response was observed under low-light stress (Table 7). This suggests that *TT8* might play an important role in anthocyanin synthesis and could partially explain why a phenotypic change in the anthocyanin synthesis was observed under constant high light (Figure 10). However, since the gene expression of *TTG1*, *PAP1*, and *PAP2* also showed a tendency to upregulate under both low- and high-light conditions, these factors alone cannot be the main reason for the visible anthocyanin production.

It is assumed that anthocyanin production is initiated earlier in response to high light, but might not be clearly visible. In this regard, Huang and colleagues showed that a duration of 6 hours of high light (1200 µmol/m^2s) was sufficient to increase the anthocyanin content in *A. thaliana*, whereas a duration of 0.5 hours was not sufficient (Huang et al., 2019). To further investigate this finding, samples for anthocyanin analysis under high-light exposure could be taken several times a day over a period of a few days. This approach would help reveal small, significant differences in the anthocyanin content and determine the required duration of high light to induce anthocyanin production. Additionally, plants could be exposed to various light intensities to find out which intensity is needed to trigger the production of anthocyanins. In this context, it would be interesting to investigate whether prolonged exposure to a medium high-light intensity is able to induce the same response as brief exposure to a stronger high light intensity. This experimental setup could determine whether the duration, the intensity or a combination of both is important for the production of anthocyanins.

Short-term low light reduces trichome patterning-related gene expression

Regarding the trichome trait under short-term stress (Figure 14), a similar gene expression change was observed for genes of the anthocyanin trait. Under low light, almost all genes were downregulated, and under high light, most showed a tendency to upregulation. Under low light, *EGL3*, *GL3*, *MYC1*, *GL1*, *MYB82* and the inhibitors *ETC2*, *ETC3,* and *TCL1* were

especially affected. Therefore, light stress has the potential to alter trichome patterning, but since inhibitors and activators are equally impacted under low light, it is challenging to determine whether the trichome count may be influenced. This might reflect a feedback mechanism, aiming to optimize developmental processes in response to limited light resources. The inhibition of gene expression could help to conserve energy, but this process might also require balancing gene expression to maintain overall levels of gene activity. Under high light, expression changes were not significant, however, especially *EGL3*, *GL3*, *TRY* and *ETC2* tended to be upregulated, whereas *CPC*, *TCL1* and *TCL2* tended to be downregulated. While the expression of the activators was stimulated to a certain extent, which might increase trichome formation, the inhibitors seemed to be regulated in opposite directions. It is known that the mutation of *CPC* leads to a modest increase of trichomes, while the opposite is shown in the *try* mutant (Pesch & Hülskamp, 2011; Schellmann et al., 2002). Accordingly, the opposite regulation of *CPC* and *TRY* gene expression, observed under high light, might lead to an increased number of trichomes. However, a phenotypic analysis of the trichome phenotype did not reveal any significant differences (Figure 7). Nevertheless, these changes in gene expression can provide insights into the internal regulatory mechanism activated in response to abiotic stress. Such expression changes may need to exceed a certain threshold to manifest phenotypic changes, therefore, the performance of additional light stress experiments with varying durations and intensities of stress exposure, could provide a more precise understanding of internal stress regulations in plants.

Constant low light causes increased expression of *ETC2*

Regarding the trichome patterning trait, constant light stress (Figure 12) revealed an increased expression of *ETC2* and a downregulation of *TCL2* under low light, whereas under high light, *ETC2* expression was hardly affected, and *TCL2* expression was also downregulated. Therefore, *ETC2* seems to have a supporting role under low light, whereas *TCL2* might be generally involved in the light response in *A. thaliana*. The upregulation of *ETC2* under low-light conditions may be associated with a reduction in trichome density (Figure 8 C) since it was shown that the *etc2* single mutant carried an increased number of trichomes, whereas overexpression of *ETC2* led to a glabrous phenotype (Kirik et al., 2004b). In general, suppression of inhibitors could induce increased trichome numbers, as shown under high light (Figure 8 C). However, because the expression of *ETC2* was generally particularly low (supplemental Figure 31), conducting light stress experiments in the *etc2* mutant could

provide insights into whether *ETC2* is actually involved in the regulation of trichome density under low-light conditions.

Since expression differences under constant light stress are less affected compared to short-term stress, it could be possible that the plants have already adapted, to these constant conditions, to a certain extent. This adaption might indicate that no further genetic modifications are required for plants to thrive under constant stress since they might have already optimized their physiological processes. Overall, the results support the hypothesis that plants adapt to different light conditions through phenotypic plasticity and genetic regulation to overcome climate change (Somero, 2010; Sultan, 2000).

4.4 Heat stress leads to downregulation of MBW expression

The results of this study clearly demonstrate that heat stress significantly negatively impacts the expression of the MBW genes. Especially since *TTG1* gene expression, the key component of the network, was negatively regulated (Figure 17 and Figure 18), it is suggested that heat stress exposure might affect the various traits in *A. thaliana* (Figure 2). Additionally, other studies have shown that gene expression was downregulated under heat stress. Dobra and colleagues have shown that during a 15-minute heat stress treatment at 40 °C, proteins related to chloroplasts were predominantly downregulated (Dobra et al., 2015). Furthermore, Wang and colleagues found that short- (42 °C, 1 h) and long-term (42/35 °C, day/night, 7 d) heat stress led to a strong downregulation of photosynthesis-related genes in *Rhododendron hainanense* (Wang et al., 2020b). Heat stress thus seems to have a negative effect on the expression of different gene groups.

Heat stress negatively affects the expression of genes related to anthocyanin production

In regard to the regulation of flavonoid biosynthesis (Figure 17), the downregulation of *TT8*, *PAP1* and *PAP2* indicates a potential reduction in anthocyanin production. Therefore, plant development and defense mechanisms might be negatively affected, particularly due to a possible impairment in protection against harmful radiation (Neill & Gould, 2003; Zheng et al., 2021). In this context, a study by Kim and colleagues found that heat stress at 28 °C for 24 hours was able to suppress anthocyanin biosynthesis by degradation of ELONGATED HYPOCOTYL 5 (HY5) in a CONSTITUTIVE PHOTOMORPHOGENIC 1 (COP1) dependent manner. Their analysis included *cop1* and *hy5* mutants, in which anthocyanin biosynthesis and

accumulation remained unaffected (Kim et al., 2017; Park et al., 2017). In regard to the production of proanthocyanidins, the expression of *TT2* was hardly affected. This could indicate that *TT2* expression is not directly affected by heat stress. However, it is important to note that proanthocyanins primarily accumulate in seeds (Debeaujon et al., 2003). Accordingly, young leaves are probably unsuitable plant material for examining their production and the expression of related genes.

Heat stress has the ability to affect trichome patterning

Concerning the trichome patterning trait (Figure 18), heat stress treatment negatively affected gene expression of all different MBW genes, most of them showing a significant downregulation to approximately 50 %. Since inhibitors and activators are equally affected, it is difficult to predict whether the trichome count could be affected, and if so, whether the number of trichomes would increase or decrease. In a study by Okamoto and colleagues, it was demonstrated that heat stress was able to disturb trichome patterning, under constant heat stress conditions (21 days at 26 °C or 30 °C), where distances between trichomes significantly increased compared to standard growth conditions at 22 °C (Okamoto et al., 2020). Since in this study the gene expression of *GL3*, *MYC1*, *TRY* and *CPC*, which are involved in trichome distribution, was significantly downregulated, the analysis of trichome distribution should be part of future studies, considering not only heat stress but also light stress (Payne et al., 2000; Pesch & Hülskamp, 2011; Schnittger et al., 1999; Symonds et al., 2011; Wang et al., 2007; Zhao et al., 2012).

In this study, plants were exposed to heat stress for a short period of time (3 h). Similar to the findings observed under short-term light stress, no significant changes in trichome number could be detected (Figure 15). It is assumed that a longer heat period or grater intensity is necessary to alter the internal genetics of the plant to trigger a phenotypic response. Accordingly, experiments with different heat stress periods should be conducted to determine the required threshold to trigger a change in phenotypic traits. Also, experimental setups with constant heat stress could show how heat affects the phenotypic appearance of plants, including the trichome formation. Further studies are needed to understand how heat stress affects phenotypic characteristics and expression levels.

4.5 Comparison between qPCR and transcriptomic data emphasizes the importance of the experimental design

When comparing the results of this study with published data (Table 8), it was shown that the results were partly similar (Huang et al., 2019; Kilian et al., 2007; Winter et al., 2007). Differences in the setup and stress intensity could explain the varying gene expressions. Kilian and colleagues used a hydroponic system to grow their plants, and they also collected the whole shoot material. In this study, seedlings grew on soil since the root material was not analyzed, and the cotyledons were removed for sampling (Kilian et al., 2007). Furthermore, Huang and colleagues defined high light as a light intensity of 1200 µmol/m^2s and low light as 60 µmol/m^2s. In this thesis, a light intensity of 400 µmol/m^2s was considered as high-light and 30 µmol/m^2s as low-light stress. Therefore, it is not surprising that the expression changes are not identical. Accordingly, the experimental setup and the selected plant material are crucial for the outcome of the experiments.

For further studies, the plant material selected for examination should align with the traits being investigated. Since the intensity and duration of the stress might also play a role in the outcome of the results, a time series of stress would be a better choice for future experiments. Additionally, a transcriptome analysis could be performed focusing on MBW network genes, along with known possible interactors to obtain more comprehensive data on gene expression under heat stress. A transcriptomic analysis could facilitate the identification of additional genes involved in stress regulation in plants. It would be valuable to investigate the expression profiles of potential downstream genes within the network. Suitable downstream targets could be for example the transcription factor GOLDEN2-LIKE 1 (GLK1), which is involved in anthocyanin production or the transcription factor GLABROUS INFLORESCENCE STEMS (GIS), which is assumed to promote trichome formation and might act downstream of TCL1 (Li et al., 2023). Since many different genes, besides the displayed MBW network, are involved in the regulation of the various traits, further studies are needed to unravel this complex mechanism.

4.6 Conclusions on the *Chenopodium* project and future perspectives

The following section summarizes the key findings of the *Chenopodium* project, outlines the challenges encountered throughout the project and provides reasons why the project was ultimately discontinued.

4.6.1 EMS mutagenesis is a suitable tool for gene manipulation in *C. suecicum*

Although it was not possible to propagate the identified glabrous mutants for subsequent genetic analysis, it has been shown that EMS mutagenesis is a suitable method for identifying mutants in *C. suecicum* and that the development of bladder cells is genetically accessible. In the course of this work, the EMS mutagenesis was repeated twice with 3 % EMS, but no viable glabrous mutant could be identified.

Dormancy is one possible cause for germination issues in *C. suecicum*

Furthermore, significant challenges with seed germination led to the decision to discontinue further analysis of mutants exhibiting altered salt bladder phenotypes. This decision was made because the risk of losing the mutants due to germination problems was relatively high. In an attempt to address this issue, it was assumed that the seeds had become dormant. Dormancy is a mechanism that prevents seed germination under unfavorable conditions (Bewley, 1997; Graeber et al., 2012). Therefore, seeds were treated with gibberellic acid, a plant hormone, which is known to stimulate germination and can help to overcame dormancy (Evans et al., 1996; Karssen & Lacka, 1986). Unfortunately, germination rates could not be increased with gibberellic acid treatment (data not shown). Currently, there is limited research focused on seed dormancy in *C. quinoa*, presumably it will become more relevant since the species faces challenges related to preharvest sprouting, which can affect the crop yield (Mares, 1993; McGinty et al., 2021). Other reasons contributing to the poor germination rates might include genetic factors that are inherited through generations, through inbreeding, and affect the germinability of the seeds.

Furthermore, the nutrient supply in the experimental setup might not have been sufficient, since no additional fertilizer was added during the experiment, although *C. quinoa* has a longer life cycle than *A. thaliana* (Sajjad et al., 2014). This lack of nutrients could have influenced the seed quality and their viability. Additionally, the environmental conditions within the plant chamber, such as the humidity, might not have been optimally adapted to the conditions favorable for *C. quinoa* cultivation. The plant chambers are primarily configured for the cultivation of *A. thaliana* and were only adjusted in terms of light intensity and photoperiod (short-day conditions). These settings could also have influenced the germination rate. Ultimately, due to these challenges, the project was discontinued.

4.6.2 Salt stress in *Chenopodium* increases bladder cell density

Salt stress treatment of *C. quinoa* and *C. suecicum* led to a significantly increased bladder cell density on the adaxial leaf side (Figure 24 J). This might indicate that bladder cells contribute to salt resistance in *Chenopodium*, through the possibility of increased salt excretion (Böhm et al., 2018). Since it was observed that *C. suecicum* carried an increased amount of bladder cells in comparison to *C. quinoa* leaves, it was assumed that *C. suecicum* might perform better under salt stress than *C. quinoa*.

Salt stress reduces plant height and seed production in *C. suecicum*

In the context of flowering time, an increased salt concentration of 200 to 300 mM NaCl was found to affect the plant height at the time of bolting and, especially, affected the grain yield, in *C. suecicum* (Figure 23). High salt concentrations (200 to 300 mM) inhibited seed formation in *C. suecicum*, while *C. quinoa* was able to produce a small number of seeds under most salt treatments. However, when salt stress of 300 mM NaCl started at the seed stage, no seeds could be produced in *C. quinoa* either, suggesting that the seed stage might be particularly vulnerable due to the absence of leaves that carry bladder cells. In this context, it was shown that the mechanical removal of bladder cells negatively impacted salt tolerance in *C. quinoa* (Kiani-Pouya et al., 2017). In general, *C. quinoa* seems to perform better under salt stress than *C. suecicum*. This is also supported by other studies which found that *C. quinoa* was able to withstand and propagate under salt concentrations of up to 500 mM NaCl (Koyro & Eisa, 2008). Under these high salt concentrations, germination was hardly possible in *C. suecicum* (Figure 22). However, in the experiment of Koyro and colleagues, saltwater irrigation began three to four weeks after germination and lasted for six weeks. Therefore, the experimental setup differed, since in this study, plants were irrigated with saltwater throughout their entire life cycle.

Ecotypic variation or experimental setup might influence seed production in *C. quinoa*

Former studies on *C. quinoa* from Koyro and colleagues reported grain yields reaching several thousands of seeds. Even with an irrigation of 500 mM NaCl, the grain yield exceeded one hundred seeds (Koyro & Eisa, 2008). In this study, the grain yield of *C. quinoa* was below a hundred seeds across all treatments (Figure 23 C). Therefore, the question of why there are such drastic differences in seed production emerged. One possible explanation might be variations between ecotypes, since they show differences in salinity tolerance (Ruiz-Carrasco

et al., 2011; Ruiz et al., 2016). Ruiz and colleagues revealed that, at a concentration of 300 mM NaCl, the grain yield of the *salares* ecotype (R49) was significantly reduced by 80 % compared to the control, while in contrast, the two coastal lowland ecotypes either showed no impairment (Villarrica; VR) or experienced only a 40 % reduction (VI-1) (Ruiz et al., 2016).

Another reason could be the experimental setup itself. The current setup involved irrigating the plants with a NaCl solution three times a week, until the end of their life cycle. This approach may have caused NaCl to accumulate in the pots over time, and potentially exceeded the intended concentrations of 200 or 300 mM NaCl significantly. To address this issue, it might be beneficial to implement a different irrigation system, such as a hydroponic growth system or incorporating a measuring device to monitor soil salinity in future approaches. These changes could help to maintain the specified salt concentrations throughout the experiment.

Salt resistance mechanism in *C. quinoa*: An insight into the state of research

The understanding of bladder cells and their contribution to salt stress in *C. quinoa* has progressed further in recent years under the work of other scientists. Even though it was demonstrated that the removal of bladder cells affected salt tolerance (Kiani-Pouya et al., 2017) and it was suggested that bladder cells function as storage compartments for sodium and chloride ions (Böhm et al., 2018), the opposite was shown in a glabrous epidermal bladder cell-free (*ebcf*) mutant in *C. quinoa*. This mutant showed no sensitivity to salt stress, leading to the conclusion that the function of bladder cells as a salt dumpster might be exaggerated, since no significant sodium accumulation could be detected in the EBCs (Moog et al., 2022). This mutant, identified in an EMS screen, carried a mutation in the *REDUCED LEVELS OF EBCs* (*REBC*) and *REBC-like1* gene. In another study, the REBC protein was characterized as a novel WD40-protein involved in the formation of bladder cells (Imamura et al., 2020). These findings provide initial insight into the genes responsible for the regulation of bladder cells in *C. quinoa*. However, Imamura and colleagues also showed that the contribution of bladder cells to salt resistance may not be as significant as previously thought. They identified two *rebc* mutants, which showed no significant difference in Na^+ contents of the leaf lamina compared to the wild type (Imamura et al., 2020). However, they found that bladder cells play a role in protection against UV-B radiation (1.5 W/m^2, 4 h), since the *rebc* mutants displayed more damage to the shoot apex and leaves compared to the wild type (Imamura et al., 2020;

Shabala et al., 2012). Furthermore, bladder cells have been shown to be involved in defense mechanism against herbivores. Bladder cells contain defense compound such as saponins and oxalic acid, and in contrast to the wildtype, bladder cell mutants (*ebcf*, *rebc-2*) exhibited severe damage from thrips infestation, with the shoot apices of these mutants dying within 16 days of infestation (LoPresti, 2014; Moog et al., 2023; Otterbach et al., 2021). Accordingly, bladder cells seem to fulfil several functions in *C. quinoa,* highlighting their importance for the overall resilience of the plant.

In conclusion, the research on *Chenopodium* species was both exciting and challenging. Further studies on the gene regulation of bladder cell formation and their function will be valuable in clarifying their mechanism of resistance to drought, salt, UV-B and herbivores. In the future, it may be possible to transfer some of these resistance mechanisms to other species that are vulnerable to such abiotic and biotic stressors, that are exacerbated by climate change. Research successes in this area could make a significant contribution to ensuring food security.

5 Outlook

This study, showed that the expression of the genes specific to the anthocyanin trait, such as *PAP1* and *PAP2*, was upregulated under short-term high-light stress (Figure 13 B). It was also shown that anthocyanin production is stimulated under constant high-light conditions (Figure 10). The increased production of anthocyanidins under constant high-light stress suggests a protective mechanism against oxidative damage and UV radiation. It would be promising to conduct further studies to understand the underlying mechanisms by which light intensity affects phenotypic plasticity and gene expression. Therefore, analyzing the anthocyanin content would be an interesting future research question to determine the stress intensity and duration required to increase anthocyanin production. In addition, two overexpression lines of *PAP1* and *PAP2* were generated during this study but could not be examined further due to time constraints. The analysis of these and available *pap1* and *pap2* mutants could provide insights into the regulatory mechanisms underlying anthocyanin production in response to abiotic stressors and how these genes contribute to changes in expression within the MBW network. Other MBW single mutants would also be interesting candidates to unravel the contribution of each trait to stress tolerance. In this case, it would also be important to examine other traits such as seed coat mucilage and root hair patterning for phenotypic changes to cover all traits of the MBW network, which might be affected by abiotic stress.

In the future, additional abiotic stressors, such as UV-B light and drought could be analyzed regarding their effects on phenotypic variations and gene expression differences. In this context, drought stress might be particularly interesting, since it can be enhanced by heat stress and therefore, often occurs in combination (Thieme et al., 2022). Stress combinations should also be analyzed to simulate more realistic conditions that plants face in natural environments. In this context, field trials under natural conditions could also be implemented to investigate how they affect gene expression and phenotypic plasticity.

It would also be interesting to investigate the mechanism known as priming or stress memory. Here, primed seeds or plants that have been exposed to an initial stress are more resistant to future stress treatments (Cayuela et al., 1996; Hossain et al., 2018; Hossain et al., 2013; Mauch-Mani et al., 2017; Molinier et al., 2006). In this context, research has shown that such stress exposure can alter the genome by the activation of transposable elements or

homologous recombination (Lebel et al., 1993; Walbot, 1992). Furthermore, increased stress resistance can also be induced chemically. For instance, chemical drought-priming has been demonstrated to enhance heat resistance in *A. thaliana* and other species (Conrath et al., 2001; Wang et al., 2015a; Zhang et al., 2019; Zimmerli et al., 2000). For an experimental priming approach, plants could first be exposed to a mild heat stress signal and subsequently facing a more severe heat stress. Furthermore, analyzing different combinations of stressors could also provide insights into whether plants that, for instance, were initially exposed to a heat treatment, initiate beneficial physiological changes in response to high-light stress. The results of these investigations could provide valuable insights into the molecular mechanisms underlying the stress response related to the MBW network and might contribute to the development of plants with improved stress resistance. Future studies should aim to identify specific signaling pathways, which are involved in phenotypic stress response, contributing to improved crop resilience in changing climates.

6 Acknowledgement

First of all, thank you Prof. Dr. Martin Hülskamp for the opportunity to write my thesis in your working group. Thank you for the regular feedback and discussions about my project and also for your support and advice. I have learned a lot under your supervision in the past years.

I also would like to thank Prof. Dr. Ute Höcker, for taking your time to act as my second reviewer and examiner. You have often supported my thesis with helpful comments and suggestions during the lab seminars. I would also like to thank you for providing space in your plant chamber for parts of the salt stress experiments in Quinoa.

Thank you also to Prof. Dr. Michael Bonkowski for taking the chair of the thesis defense committee. Even though I have never worked in your working group myself, I was able to get an impression of your working group from time to time through one of my best friends, whom I met during my studies, Dr. Hüsna Öztoprak. These insights encouraged me to ask you if you could take over the chair of my examination.

Thank you, Prof. Dr. Rainer Hedrich (JMU Würzburg) and Jürgen Hintzsche, for equipping us with seeds from *C. quinoa* and *C. suecicum*.

I would like to thank the entire Hülskamp lab for the pleasant working atmosphere. I really appreciate the support I received within the group. Thank you to my doctoral colleagues and former colleagues: Dr. Hanna Bechtel, Helen Janßen, Dr. Eva Koebke, Dr. Jessica Pietsch, Dr. Lisa Stephan and Andrii Zinchenko. I have learned a lot from you and received so much support in all areas. You built me up again after every setback and also celebrated the successes with me.

I would especially like to thank Dr. Lisa Stephan. You always have the right solutions for every problem and came up with new ideas when I was stuck. I have benefited greatly from your knowledge and expertise. Thank you for all the time you have invested in me and thank you for all your suggestions and comments during my writing phase.

Many thanks also go to Sabine Lohmer, who took over a lot of the preparatory work for the qPCR experiments. Without your help, the experiments would not have progressed so quickly,

which was a great help in my last few weeks in the lab. It was a pleasure to be your bench neighbor in the lab.

I would also like to thank one of my first bachelor students, Anna Marxer, who carried out some of the first experiments in *C. quinoa* and *C. suecicum*.

A big thank you goes to our student helper Andreina Zey. Thank you for taking over some of the preparation steps for my experiments and for supporting me with data collection. You have simplified my laboratory work.

I am grateful for the support of my family and friends, who always have encouraged me since I started my bachelor's degree. Especially, thank you Till for always supporting me and having my back. You always jumped in when I needed help and you also encouraged me after failures. At this point I would also like to thank my colleagues and friends who helped me with sampling for my experiments: Viktoria Bednarski, Yasemin Birbir, Helen Janßen, Birgit Kernebeck, Dr. Hüsna Öztoprak, Dr. Lisa Stephan, Till Vannahme and Andrii Zinchenko. Without you, sampling in this form would not have been possible.

7 References

Abdel Latef, A. (2010). Changes of antioxidative enzymes in salinity tolerance among different wheat cultivars. *Cereal Research Communications, 38*(1), 43-55.

Agbogidi, O. (2011). Global climate change: a threat to food security and environmental conservation. *British Journal of Environment and Climate Change, 1*(3), 74-89.

Ahanger, M. A., & Agarwal, R. M. (2017). Salinity stress induced alterations in antioxidant metabolism and nitrogen assimilation in wheat (Triticum aestivum L) as influenced by potassium supplementation. *Plant Physiol Biochem, 115*, 449-460. doi:10.1016/j.plaphy.2017.04.017

Alharby, H. F., Colmer, T. D., & Barrett-Lennard, E. G. (2014). Salt accumulation and depletion in the root-zone of the halophyte Atriplex nummularia Lindl.: influence of salinity, leaf area and plant water use. *Plant and soil, 382*, 31-41.

Amasino, R. M., Cheung, A. Y., Dresselhaus, T., & Kuhlemeier, C. (2017). Focus on Flowering and Reproduction. *Plant Physiol, 173*(1), 1-4. doi:10.1104/pp.16.01867

Andersen, C. L., Jensen, J. L., & Orntoft, T. F. (2004). Normalization of real-time quantitative reverse transcription-PCR data: a model-based variance estimation approach to identify genes suited for normalization, applied to bladder and colon cancer data sets. *Cancer Res, 64*(15), 5245-5250. doi:10.1158/0008-5472.CAN-04-0496

Appelhagen, I., Thiedig, K., Nordholt, N., Schmidt, N., Huep, G., Sagasser, M., & Weisshaar, B. (2014). Update on transparent testa mutants from Arabidopsis thaliana: characterisation of new alleles from an isogenic collection. *Planta, 240*(5), 955-970. doi:10.1007/s00425-014-2088-0

Arabidopsis Genome Initiative. (2000). Analysis of the genome sequence of the flowering plant Arabidopsis thaliana. *Nature, 408*(6814), 796-815. doi:10.1038/35048692

Aranda, P. S., LaJoie, D. M., & Jorcyk, C. L. (2012). Bleach gel: a simple agarose gel for analyzing RNA quality. *Electrophoresis, 33*(2), 366-369. doi:10.1002/elps.201100335

Aronson, J. A., & Whitehead, E. E. (1989). HALOPH: a data base of salt tolerant plants of the world.

Balkunde, R., Deneer, A., Bechtel, H., Zhang, B., Herberth, S., Pesch, M., Jaegle, B., Fleck, C., & Hulskamp, M. (2020). Identification of the Trichome Patterning Core Network Using Data from Weak ttg1 Alleles to Constrain the Model Space. *Cell Rep, 33*(11), 108497. doi:10.1016/j.celrep.2020.108497

Balkunde, R., Pesch, M., & Hülskamp, M. (2010). Trichome patterning in Arabidopsis thaliana from genetic to molecular models. *Curr Top Dev Biol, 91*, 299-321. doi:10.1016/S0070-2153(10)91010-7

Bennett, M. D., Leitch, I. J., Price, H. J., & Johnston, J. S. (2003). Comparisons with Caenorhabditis (~ 100 Mb) and Drosophila (~ 175 Mb) using flow cytometry show genome size in Arabidopsis to be~ 157 Mb and thus~ 25% larger than the Arabidopsis genome initiative estimate of~ 125 Mb. *Annals of botany, 91*(5), 547-557.

Bewley, J. D. (1997). Seed Germination and Dormancy. *Plant Cell, 9*(7), 1055-1066. doi:10.1105/tpc.9.7.1055

Bhathal, S., Grover, K., & Gill, N. (2015). Quinoa-a treasure trove of nutrients. *Journal of nutrition Research, 3*(1), 45-49.

Bickford, C. P. (2016). Ecophysiology of leaf trichomes. *Functional Plant Biology, 43*(9), 807-814.

Blanca, M. J., Alarcon, R., Arnau, J., Bono, R., & Bendayan, R. (2017). Non-normal data: Is ANOVA still a valid option? *Psicothema, 29*(4), 552-557. doi:10.7334/psicothema2016.383

Böhm, J., Messerer, M., Muller, H. M., Scholz-Starke, J., Gradogna, A., Scherzer, S., Maierhofer, T., Bazihizina, N., Zhang, H., Stigloher, C., Ache, P., Al-Rasheid, K. A. S., Mayer, K. F. X., Shabala, S., Carpaneto, A., Haberer, G., Zhu, J. K., & Hedrich, R. (2018). Understanding the Molecular Basis of Salt Sequestration in Epidermal Bladder Cells of Chenopodium quinoa. *Curr Biol, 28*(19), 3075-3085 e3077. doi:10.1016/j.cub.2018.08.004

Bonales-Alatorre, E., Shabala, S., Chen, Z. H., & Pottosin, I. (2013). Reduced tonoplast fast-activating and slow-activating channel activity is essential for conferring salinity tolerance in a facultative halophyte, quinoa. *Plant Physiol, 162*(2), 940-952. doi:10.1104/pp.113.216572

Bouyer, D., Geier, F., Kragler, F., Schnittger, A., Pesch, M., Wester, K., Balkunde, R., Timmer, J., Fleck, C., & Hulskamp, M. (2008). Two-dimensional patterning by a trapping/depletion mechanism: the role of TTG1 and GL3 in Arabidopsis trichome formation. *PLoS Biol, 6*(6), e141. doi:10.1371/journal.pbio.0060141

Broun, P. (2005). Transcriptional control of flavonoid biosynthesis: a complex network of conserved regulators involved in multiple aspects of differentiation in Arabidopsis. *Curr Opin Plant Biol, 8*(3), 272-279. doi:10.1016/j.pbi.2005.03.006

Cameron, N. M., & Scrosati, R. A. (2023). Mass disappearance of intertidal mussels after an unusual winter cold snap in eastern Canada. *Ecology, 104*(12), e4179. doi:10.1002/ecy.4179

Cayuela, E., Pérez-Alfocea, F., Caro, M., & Bolarin, M. (1996). Priming of seeds with NaCl induces physiological changes in tomato plants grown under salt stress. *Physiologia Plantarum, 96*(2), 231-236.

Chaves, M., & Pereira, J. (1992). Water stress, CO2 and climate change. *Journal of Experimental Botany, 43*(8), 1131-1139.

Chen, X., Ji, Y., Cheng, Y., Hao, Y., Lei, X., Song, G., Qu, Y., & Lei, F. (2022). Comparison between short-term stress and long-term adaptive responses reveal common paths to molecular adaptation. *iScience, 25*(3), 103899. doi:10.1016/j.isci.2022.103899

Conrath, U., Thulke, O., Katz, V., Schwindling, S., & Kohler, A. (2001). Priming as a mechanism in induced systemic resistance of plants. *European Journal of plant pathology, 107*, 113-119.

Cox, B. J. (2020). *EMS mutagenesis in quinoa: Developing a genetic resource*: Brigham Young University.

Dassanayake, M., & Larkin, J. C. (2017). Making Plants Break a Sweat: the Structure, Function, and Evolution of Plant Salt Glands. *Front Plant Sci, 8*, 406. doi:10.3389/fpls.2017.00406

Debeaujon, I., Nesi, N., Perez, P., Devic, M., Grandjean, O., Caboche, M., & Lepiniec, L. (2003). Proanthocyanidin-accumulating cells in Arabidopsis testa: regulation of differentiation and role in seed development. *Plant Cell, 15*(11), 2514-2531. doi:10.1105/tpc.014043

Deneer, A. (2022). *Mathematical modelling of trichome patterning.* Wageningen University and Research,

Desikan, R., Griffiths, R., Hancock, J., & Neill, S. (2002). A new role for an old enzyme: nitrate reductase-mediated nitric oxide generation is required for abscisic acid-induced stomatal closure in Arabidopsis thaliana. *Proc Natl Acad Sci U S A, 99*(25), 16314-16318. doi:10.1073/pnas.252461999

Digiuni, S., Schellmann, S., Geier, F., Greese, B., Pesch, M., Wester, K., Dartan, B., Mach, V., Srinivas, B. P., Timmer, J., Fleck, C., & Hulskamp, M. (2008). A competitive complex formation mechanism underlies trichome patterning on Arabidopsis leaves. *Mol Syst Biol, 4*, 217. doi:10.1038/msb.2008.54

Dobra, J., Cerny, M., Storchova, H., Dobrev, P., Skalak, J., Jedelsky, P. L., Luksanova, H., Gaudinova, A., Pesek, B., Malbeck, J., Vanek, T., Brzobohaty, B., & Vankova, R. (2015). The impact of heat stress targeting on the hormonal and transcriptomic response in Arabidopsis. *Plant Sci, 231*, 52-61. doi:10.1016/j.plantsci.2014.11.005

Dreesen, F. E., De Boeck, H. J., Janssens, I. A., & Nijs, I. (2012). Summer heat and drought extremes trigger unexpected changes in productivity of a temperate annual/biannual plant community. *Environmental and experimental botany, 79*, 21-30.

Eckardt, N. A., Snyder, G. W., Portis, A. R., Jr., & Orgen, W. L. (1997). Growth and photosynthesis under high and low irradiance of Arabidopsis thaliana antisense mutants with reduced ribulose-1,5-bisphosphate carboxylase/oxygenase activase content. *Plant Physiol, 113*(2), 575-586. doi:10.1104/pp.113.2.575

Evans, A. S., Randall, J. M., & Cabin, R. J. (1996). Morphological side effects of using gibberellic acid to induce germination: consequences for the study of seed dormancy. *American Journal of Botany, 83*(5), 543-549.

Flowers, T. J., & Colmer, T. D. (2008). Salinity tolerance in halophytes. *New Phytol, 179*(4), 945-963. doi:10.1111/j.1469-8137.2008.02531.x

Flowers, T. J., Galal, H. K., & Bromham, L. (2010). Evolution of halophytes: multiple origins of salt tolerance in land plants. *Functional Plant Biology, 37*(7), 604-612.

Forghani, F., Wei, S., & Oh, D. H. (2016). A Rapid Multiplex Real-Time PCR High-Resolution Melt Curve Assay for the Simultaneous Detection of Bacillus cereus, Listeria monocytogenes, and Staphylococcus aureus in Food. *J Food Prot, 79*(5), 810-815. doi:10.4315/0362-028X.JFP-15-428

Gonzalez, A., Zhao, M., Leavitt, J. M., & Lloyd, A. M. (2008). Regulation of the anthocyanin biosynthetic pathway by the TTG1/bHLH/Myb transcriptional complex in Arabidopsis seedlings. *Plant J, 53*(5), 814-827. doi:10.1111/j.1365-313X.2007.03373.x

Goto, N., Kumagai, T., & Koornneef, M. (1991). Flowering responses to light-breaks in photomorphogenic mutants of Arabidopsis thaliana, a long-day plant. *Physiologia Plantarum, 83*(2), 209-215.

Graeber, K., Nakabayashi, K., Miatton, E., Leubner-Metzger, G., & Soppe, W. J. (2012). Molecular mechanisms of seed dormancy. *Plant Cell Environ, 35*(10), 1769-1786. doi:10.1111/j.1365-3040.2012.02542.x

Hamada, T., Yako, M., Minegishi, M., Sato, M., Kamei, Y., Yanagawa, Y., Toyooka, K., Watanabe, Y., & Hara-Nishimura, I. (2018). Stress granule formation is induced by a threshold temperature rather than a temperature difference in Arabidopsis. *Journal of Cell Science, 131*(16), jcs216051.

Handley, R., Ekbom, B., & Ågren, J. (2005). Variation in trichome density and resistance against a specialist insect herbivore in natural populations of Arabidopsis thaliana. *Ecological Entomology, 30*(3), 284-292.

Hatier, J.-H. B., & Gould, K. S. (2009). Anthocyanin function in vegetative organs. *Anthocyanins: Biosynthesis, functions, and applications*, 1-19.

He, W., Yan, K., Zhang, Y., Bian, L., Mei, H., & Han, G. (2021). Contrasting photosynthesis, photoinhibition and oxidative damage in honeysuckle (Lonicera japonica Thunb.) under iso-osmotic salt and drought stresses. *Environmental and experimental botany, 182*, 104313.

Heitkam, T., Weber, B., Walter, I., Liedtke, S., Ost, C., & Schmidt, T. (2020). Satellite DNA landscapes after allotetraploidization of quinoa (Chenopodium quinoa) reveal unique A and B subgenomes. *Plant J, 103*(1), 32-52. doi:10.1111/tpj.14705

Hildebrandt, T. M. (2018). Synthesis versus degradation: directions of amino acid metabolism during Arabidopsis abiotic stress response. *Plant Mol Biol, 98*(1-2), 121-135. doi:10.1007/s11103-018-0767-0

Hossain, M. A., Li, Z.-G., Hoque, T. S., Burritt, D. J., Fujita, M., & Munné-Bosch, S. (2018). Heat or cold priming-induced cross-tolerance to abiotic stresses in plants: key regulators and possible mechanisms. *Protoplasma, 255*, 399-412.

Hossain, M. A., Mostofa, M. G., & Fujita, M. (2013). Cross protection by cold-shock to salinity and drought stress-induced oxidative stress in mustard (Brassica campestris L.) seedlings. *Molecular Plant Breeding, 4*.

Huang, J., Zhao, X., & Chory, J. (2019). The Arabidopsis Transcriptome Responds Specifically and Dynamically to High Light Stress. *Cell Rep, 29*(12), 4186-4199 e4183. doi:10.1016/j.celrep.2019.11.051

Hülskamp, M. (2004). Plant trichomes: a model for cell differentiation. *Nat Rev Mol Cell Biol, 5*(6), 471-480. doi:10.1038/nrm1404

Hülskamp, M., Misra, S., & Jurgens, G. (1994). Genetic dissection of trichome cell development in Arabidopsis. *Cell, 76*(3), 555-566. doi:10.1016/0092-8674(94)90118-x

Imamura, T., Yasui, Y., Koga, H., Takagi, H., Abe, A., Nishizawa, K., Mizuno, N., Ohki, S., Mizukoshi, H., & Mori, M. (2020). A novel WD40-repeat protein involved in formation of epidermal bladder cells in the halophyte quinoa. *Commun Biol, 3*(1), 513. doi:10.1038/s42003-020-01249-w

IUCN. (2024). The IUCN Red List of Threatened Species. Version 2024-1. https://www.iucnredlist.org.

Jacob, P., Brisou, G., Dalmais, M., Thevenin, J., van der Wal, F., Latrasse, D., Suresh Devani, R., Benhamed, M., Dubreucq, B., Boualem, A., Lepiniec, L., Immink, R. G. H., Hirt, H., & Bendahmane, A. (2021). The Seed Development Factors TT2 and MYB5 Regulate Heat Stress Response in Arabidopsis. *Genes (Basel), 12*(5). doi:10.3390/genes12050746

Jacobsen, S.-E., Mujica, A., & Jensen, C. (2003). The resistance of quinoa (Chenopodium quinoa Willd.) to adverse abiotic factors. *Food reviews international, 19*(1-2), 99-109.

Jaegle, B. (2015). *Natural variation of a gene network regulating trichome patterning, seed coat mucilage and proanthocyanidin production in Arabidopsis thaliana.* Universität zu Köln,

Jäger, K., Fabian, A., Tompa, G., Deak, C., Hohn, M., Olmedilla, A., Barnabas, B., & Papp, I. (2011). New phenotypes of the drought-tolerant cbp20 Arabidopsis thaliana mutant have changed epidermal morphology. *Plant Biol (Stuttg), 13*(1), 78-84. doi:10.1111/j.1438-8677.2010.00343.x

Jarvis, D. E., Ho, Y. S., Lightfoot, D. J., Schmockel, S. M., Li, B., Borm, T. J., Ohyanagi, H., Mineta, K., Michell, C. T., Saber, N., Kharbatia, N. M., Rupper, R. R., Sharp, A. R., Dally, N., Boughton, B. A., Woo, Y. H., Gao, G., Schijlen, E. G., Guo, X., Momin, A. A., Negrao, S., Al-Babili, S., Gehring, C., Roessner, U., Jung, C., Murphy, K., Arold, S. T., Gojobori, T., Linden, C. G., van Loo, E. N., Jellen, E. N., Maughan, P. J., & Tester, M. (2017). The genome of Chenopodium quinoa. *Nature, 542*(7641), 307-312. doi:10.1038/nature21370

Jeong, S. W., Das, P. K., Jeoung, S. C., Song, J. Y., Lee, H. K., Kim, Y. K., Kim, W. J., Park, Y. I., Yoo, S. D., Choi, S. B., Choi, G., & Park, Y. I. (2010). Ethylene suppression of sugar-induced anthocyanin pigmentation in Arabidopsis. *Plant Physiol, 154*(3), 1514-1531. doi:10.1104/pp.110.161869

Kahle, M., Kempf, M., Martin, B., & Glaser, R. (2022). Classifying the 2021 'Ahrtal'flood event using hermeneutic interpretation, natural language processing, and instrumental data analyses. *Environmental Research Communications, 4*(5), 051002.

Karssen, C., & Lacka, E. (1986). *A revision of the hormone balance theory of seed dormancy: studies on gibberellin and/or abscisic acid-deficient mutants of Arabidopsis thaliana.* Paper presented at the Plant Growth Substances 1985: Proceedings of the 12th International Conference on Plant Growth Substances, Held at Heidelberg, August 26–31, 1985.

Kataria, S., Jajoo, A., & Guruprasad, K. N. (2014). Impact of increasing Ultraviolet-B (UV-B) radiation on photosynthetic processes. *J Photochem Photobiol B, 137*, 55-66. doi:10.1016/j.jphotobiol.2014.02.004

Khan, A., & Rayner, G. D. (2003). Robustness to non-normality of common tests for the many-sample location problem. *Journal of Applied Mathematics and Decision Sciences, 7*, 187-206.

Kiani-Pouya, A., Roessner, U., Jayasinghe, N. S., Lutz, A., Rupasinghe, T., Bazihizina, N., Bohm, J., Alharbi, S., Hedrich, R., & Shabala, S. (2017). Epidermal bladder cells confer salinity stress tolerance in the halophyte quinoa and Atriplex species. *Plant Cell Environ, 40*(9), 1900-1915. doi:10.1111/pce.12995

Kilian, J., Whitehead, D., Horak, J., Wanke, D., Weinl, S., Batistic, O., D'Angelo, C., Bornberg-Bauer, E., Kudla, J., & Harter, K. (2007). The AtGenExpress global stress expression data set: protocols, evaluation and model data analysis of UV-B light, drought and cold stress responses. *Plant J, 50*(2), 347-363. doi:10.1111/j.1365-313X.2007.03052.x

Kim, H. J., Hyun, Y., Park, J. Y., Park, M. J., Park, M. K., Kim, M. D., Kim, H. J., Lee, M. H., Moon, J., Lee, I., & Kim, J. (2004). A genetic link between cold responses and flowering time through FVE in Arabidopsis thaliana. *Nat Genet, 36*(2), 167-171. doi:10.1038/ng1298

Kim, S., Hwang, G., Lee, S., Zhu, J.-Y., Paik, I., Nguyen, T. T., Kim, J., & Oh, E. (2017). High ambient temperature represses anthocyanin biosynthesis through degradation of HY5. *Frontiers in Plant Science, 8*, 1787.

King, R. W., Hisamatsu, T., Goldschmidt, E. E., & Blundell, C. (2008). The nature of floral signals in Arabidopsis. I. Photosynthesis and a far-red photoresponse independently regulate flowering by increasing expression of FLOWERING LOCUS T (FT). *J Exp Bot, 59*(14), 3811-3820. doi:10.1093/jxb/ern231

Kirik, V., Lee, M. M., Wester, K., Herrmann, U., Zheng, Z., Oppenheimer, D., Schiefelbein, J., & Hulskamp, M. (2005). Functional diversification of MYB23 and GL1 genes in trichome morphogenesis and initiation. *Development, 132*(7), 1477-1485. doi:10.1242/dev.01708

Kirik, V., Simon, M., Huelskamp, M., & Schiefelbein, J. (2004a). The ENHANCER OF TRY AND CPC1 gene acts redundantly with TRIPTYCHON and CAPRICE in trichome and root hair cell patterning in Arabidopsis. *Dev Biol, 268*(2), 506-513. doi:10.1016/j.ydbio.2003.12.037

Kirik, V., Simon, M., Wester, K., Schiefelbein, J., & Hulskamp, M. (2004b). ENHANCER of TRY and CPC 2 (ETC2) reveals redundancy in the region-specific control of trichome development of Arabidopsis. *Plant Mol Biol, 55*(3), 389-398. doi:10.1007/s11103-004-0893-8

Kolano, B., McCann, J., Orzechowska, M., Siwinska, D., Temsch, E., & Weiss-Schneeweiss, H. (2016). Molecular and cytogenetic evidence for an allotetraploid origin of Chenopodium quinoa and C. berlandieri (Amaranthaceae). *Mol Phylogenet Evol, 100*, 109-123. doi:10.1016/j.ympev.2016.04.009

Koncz, C., & Schell, J. (1986). The promoter of TL-DNA gene 5 controls the tissue-specific expression of chimaeric genes carried by a novel type of Agrobacterium binary vector. *Molecular and General Genetics MGG, 204*, 383-396.

Koornneef, M. (1981). The complex syndrome of ttg mutants. *Arabid. Inf.Serv., 18*, 45-51.

Koubouris, G., Kavroulakis, N., Metzidakis, I., Vasilakakis, M., & Sofo, A. (2015). Ultraviolet-B radiation or heat cause changes in photosynthesis, antioxidant enzyme activities and pollen performance in olive tree. *Photosynthetica, 53*, 279-287.

Koyro, H.-W., & Eisa, S. S. (2008). Effect of salinity on composition, viability and germination of seeds of Chenopodium quinoa Willd. *Plant and soil, 302*, 79-90.

Kozioł, M. J. (1992). Chemical composition and nutritional evaluation of quinoa (Chenopodium quinoa Willd.). *Journal of food composition and analysis, 5*(1), 35-68.

Kramer, U. (2015). Planting molecular functions in an ecological context with Arabidopsis thaliana. *Elife, 4*. doi:10.7554/eLife.06100

Kurata, T., Ishida, T., Kawabata-Awai, C., Noguchi, M., Hattori, S., Sano, R., Nagasaka, R., Tominaga, R., Koshino-Kimura, Y., Kato, T., Sato, S., Tabata, S., Okada, K., & Wada, T. (2005). Cell-to-cell movement of the CAPRICE protein in Arabidopsis root epidermal cell differentiation. *Development, 132*(24), 5387-5398. doi:10.1242/dev.02139

Lai, K. S., Kaothien-Nakayama, P., Iwano, M., & Takayama, S. (2012). A TILLING resource for functional genomics in Arabidopsis thaliana accession C24. *Genes Genet Syst, 87*(5), 291-297. doi:10.1266/ggs.87.291

Larkin, J. C., Young, N., Prigge, M., & Marks, M. D. (1996). The control of trichome spacing and number in Arabidopsis. *Development, 122*(3), 997-1005. doi:10.1242/dev.122.3.997

Lebel, E. G., Masson, J., Bogucki, A., & Paszkowski, J. (1993). Stress-induced intrachromosomal recombination in plant somatic cells. *Proc Natl Acad Sci U S A, 90*(2), 422-426. doi:10.1073/pnas.90.2.422

Lee, H., Calvin, K., Dasgupta, D., Krinner, G., Mukherji, A., Thorne, P., Trisos, C., Romero, J., Aldunce, P., & Barrett, K. (2023). *Climate change 2023: synthesis report. Contribution of working groups I, II and III to the sixth assessment report of the intergovernmental panel on climate change*: The Australian National University.

Lee, M. M., & Schiefelbein, J. (1999). WEREWOLF, a MYB-related protein in Arabidopsis, is a position-dependent regulator of epidermal cell patterning. *Cell, 99*(5), 473-483. doi:10.1016/s0092-8674(00)81536-6

Lepiniec, L., Debeaujon, I., Routaboul, J. M., Baudry, A., Pourcel, L., Nesi, N., & Caboche, M. (2006). Genetics and biochemistry of seed flavonoids. *Annu Rev Plant Biol, 57*, 405-430. doi:10.1146/annurev.arplant.57.032905.105252

Li, B., Suzuki, J. I., & Hara, T. (1998). Latitudinal variation in plant size and relative growth rate in Arabidopsis thaliana. *Oecologia, 115*(3), 293-301. doi:10.1007/s004420050519

Li, S. F., Milliken, O. N., Pham, H., Seyit, R., Napoli, R., Preston, J., Koltunow, A. M., & Parish, R. W. (2009). The Arabidopsis MYB5 transcription factor regulates mucilage synthesis, seed coat development, and trichome morphogenesis. *Plant Cell, 21*(1), 72-89. doi:10.1105/tpc.108.063503

Li, Y., Lei, W., Zhou, Z., Li, Y., Zhang, D., & Lin, H. (2023). Transcription factor GLK1 promotes anthocyanin biosynthesis via an MBW complex-dependent pathway in Arabidopsis thaliana. *J Integr Plant Biol, 65*(6), 1521-1535. doi:10.1111/jipb.13471

Liakoura, V., Stefanou, M., Manetas, Y., Cholevas, C., & Karabourniotis, G. (1997). Trichome density and its UV-B protective potential are affected by shading and leaf position on the canopy. *Environmental and experimental botany, 38*(3), 223-229.

Liang, G., He, H., Li, Y., Ai, Q., & Yu, D. (2014). MYB82 functions in regulation of trichome development in Arabidopsis. *J Exp Bot, 65*(12), 3215-3223. doi:10.1093/jxb/eru179

Lin, Q., & Aoyama, T. (2012). Pathways for epidermal cell differentiation via the homeobox gene GLABRA2: update on the roles of the classic regulator. *J Integr Plant Biol, 54*(10), 729-737. doi:10.1111/j.1744-7909.2012.01159.x

LoPresti, E. F. (2014). Chenopod salt bladders deter insect herbivores. *Oecologia, 174*(3), 921-930. doi:10.1007/s00442-013-2827-0

Maier, A., & Hoecker, U. (2015). COP1/SPA ubiquitin ligase complexes repress anthocyanin accumulation under low light and high light conditions. *Plant Signal Behav, 10*(1), e970440. doi:10.4161/15592316.2014.970440

Mandák, B., Trávníček, P., Paštová, L., & Kořínková, D. (2012). Is hybridization involved in the evolution of the Chenopodium album aggregate? An analysis based on chromosome counts and genome size estimation. *Flora-Morphology, Distribution, Functional Ecology of Plants, 207*(7), 530-540.

Mares, D. (1993). Pre-harvest sprouting in wheat. I. Influence of cultivar, rainfall and temperature during grain ripening. *Australian Journal of Agricultural Research, 44*(6), 1259-1272.

Marhold, K. (2006). IAPT/IOPB chromosome data 1. *Taxon, 55*(2), 443-445.

Martin, B., Ramiro, M., Martinez-Zapater, J. M., & Alonso-Blanco, C. (2009). A high-density collection of EMS-induced mutations for TILLING in Landsberg erecta genetic background of Arabidopsis. *BMC Plant Biol, 9*, 147. doi:10.1186/1471-2229-9-147

Masucci, J. D., Rerie, W. G., Foreman, D. R., Zhang, M., Galway, M. E., Marks, M. D., & Schiefelbein, J. W. (1996). The homeobox gene GLABRA2 is required for position-dependent cell differentiation in the root epidermis of Arabidopsis thaliana. *Development, 122*(4), 1253-1260. doi:10.1242/dev.122.4.1253

Mauch-Mani, B., Baccelli, I., Luna, E., & Flors, V. (2017). Defense Priming: An Adaptive Part of Induced Resistance. *Annu Rev Plant Biol, 68*, 485-512. doi:10.1146/annurev-arplant-042916-041132

McGinty, E. M., Murphy, K. M., & Hauvermale, A. L. (2021). Seed Dormancy and Preharvest Sprouting in Quinoa (Chenopodium quinoa Willd.). *Plants (Basel), 10*(3). doi:10.3390/plants10030458

Meinke, D. W., Cherry, J. M., Dean, C., Rounsley, S. D., & Koornneef, M. (1998). Arabidopsis thaliana: a model plant for genome analysis. *Science, 282*(5389), 662, 679-682. doi:10.1126/science.282.5389.662

Merila, J., & Hendry, A. P. (2014). Climate change, adaptation, and phenotypic plasticity: the problem and the evidence. *Evol Appl, 7*(1), 1-14. doi:10.1111/eva.12137

Molinier, J., Ries, G., Zipfel, C., & Hohn, B. (2006). Transgeneration memory of stress in plants. *Nature, 442*(7106), 1046-1049. doi:10.1038/nature05022

Moog, M. W., Trinh, M. D. L., Nørrevang, A. F., Bendtsen, A. K., Wang, C., Østerberg, J. T., Shabala, S., Hedrich, R., Wendt, T., & Palmgren, M. (2022). The epidermal bladder cell-free mutant of the salt-tolerant quinoa challenges our understanding of halophyte crop salinity tolerance. *New phytologist, 236*(4), 1409-1421.

Moog, M. W., Yang, X., Bendtsen, A. K., Dong, L., Crocoll, C., Imamura, T., Mori, M., Cushman, J. C., Kant, M. R., & Palmgren, M. (2023). Epidermal bladder cells as a herbivore defense mechanism. *Curr Biol, 33*(21), 4662-4673 e4666. doi:10.1016/j.cub.2023.09.063

Morales, L. O., Brosche, M., Vainonen, J., Jenkins, G. I., Wargent, J. J., Sipari, N., Strid, A., Lindfors, A. V., Tegelberg, R., & Aphalo, P. J. (2013). Multiple roles for UV RESISTANCE LOCUS8 in regulating gene expression and metabolite accumulation in Arabidopsis under solar ultraviolet radiation. *Plant Physiol, 161*(2), 744-759. doi:10.1104/pp.112.211375

Morohashi, K., Zhao, M., Yang, M., Read, B., Lloyd, A., Lamb, R., & Grotewold, E. (2007). Participation of the Arabidopsis bHLH factor GL3 in trichome initiation regulatory events. *Plant Physiol, 145*(3), 736-746. doi:10.1104/pp.107.104521

Murashige, T., & Skoog, F. (1962). A Revised Medium for Rapid Growth and Bio Assays with Tobacco Tissue Cultures. *Physiologia Plantarum, 15*(3), 473-497. doi:DOI 10.1111/j.1399-3054.1962.tb08052.x

Nabati, J., Kafi, M., Nezami, A., Moghaddam, P. R., Ali, M., & Mehrjerdi, M. Z. (2011). Effect of salinity on biomass production and activities of some key enzymatic antioxidants in kochia (Kochia scoparia). *Pakistan Journal of Botany, 43*(1), 539-548.

Naidoo, G., & Rughunanan, R. (1990). Salt tolerance in the succulent, coastal halophyte, Sarcocornia natalensis. *Journal of Experimental Botany, 41*(4), 497-502.

Neill, S., Barros, R., Bright, J., Desikan, R., Hancock, J., Harrison, J., Morris, P., Ribeiro, D., & Wilson, I. (2008). Nitric oxide, stomatal closure, and abiotic stress. *J Exp Bot, 59*(2), 165-176. doi:10.1093/jxb/erm293

Neill, S. O., & Gould, K. S. (2003). Anthocyanins in leaves: light attenuators or antioxidants? *Funct Plant Biol, 30*(8), 865-873. doi:10.1071/FP03118

Nesi, N., Debeaujon, I., Jond, C., Pelletier, G., Caboche, M., & Lepiniec, L. (2000). The TT8 gene encodes a basic helix-loop-helix domain protein required for expression of DFR and BAN genes in Arabidopsis siliques. *Plant Cell, 12*(10), 1863-1878.

Oh, J. E., Kwon, Y., Kim, J. H., Noh, H., Hong, S. W., & Lee, H. (2011). A dual role for MYB60 in stomatal regulation and root growth of Arabidopsis thaliana under drought stress. *Plant Mol Biol, 77*(1-2), 91-103. doi:10.1007/s11103-011-9796-7

Okamoto, S., Negishi, K., Toyama, Y., Ushijima, T., & Morohashi, K. (2020). Leaf Trichome Distribution Pattern in Arabidopsis Reveals Gene Expression Variation Associated with Environmental Adaptation. *Plants (Basel), 9*(7). doi:10.3390/plants9070909

Otterbach, S. L., Khoury, H., Rupasinghe, T., Mendis, H., Kwan, K. H., Lui, V., Natera, S. H. A., Klaiber, I., Allen, N. M., Jarvis, D. E., Tester, M., Roessner, U., & Schmockel, S. M. (2021). Characterization of epidermal bladder cells in Chenopodium quinoa. *Plant Cell Environ, 44*(12), 3606-3622. doi:10.1111/pce.14181

Page, M., Sultana, N., Paszkiewicz, K., Florance, H., & Smirnoff, N. (2012). The influence of ascorbate on anthocyanin accumulation during high light acclimation in Arabidopsis thaliana: further evidence for redox control of anthocyanin synthesis. *Plant Cell Environ, 35*(2), 388-404. doi:10.1111/j.1365-3040.2011.02369.x

Palomino, G., Hernández, L. T., & de la Cruz Torres, E. (2008). Nuclear genome size and chromosome analysis in Chenopodium quinoa and C. berlandieri subsp. nuttalliae. *Euphytica, 164*, 221-230.

Park, Y. J., Lee, H. J., Ha, J. H., Kim, J. Y., & Park, C. M. (2017). COP1 conveys warm temperature information to hypocotyl thermomorphogenesis. *New Phytol, 215*(1), 269-280. doi:10.1111/nph.14581

Pattanaik, S., Patra, B., Singh, S. K., & Yuan, L. (2014). An overview of the gene regulatory network controlling trichome development in the model plant, Arabidopsis. *Front Plant Sci, 5*, 259. doi:10.3389/fpls.2014.00259

Payne, C. T., Zhang, F., & Lloyd, A. M. (2000). GL3 encodes a bHLH protein that regulates trichome development in arabidopsis through interaction with GL1 and TTG1. *Genetics, 156*(3), 1349-1362. doi:10.1093/genetics/156.3.1349

Perazza, D., Herzog, M., Hülskamp, M., Brown, S., Dorne, A.-M., & Bonneville, J.-M. (1999). Trichome cell growth in Arabidopsis thaliana can be derepressed by mutations in at least five genes. *Genetics, 152*(1), 461-476.

Pesch, M., & Hülskamp, M. (2004). Creating a two-dimensional pattern de novo during Arabidopsis trichome and root hair initiation. *Curr Opin Genet Dev, 14*(4), 422-427. doi:10.1016/j.gde.2004.06.007

Pesch, M., & Hülskamp, M. (2009). One, two, three...models for trichome patterning in Arabidopsis? *Curr Opin Plant Biol, 12*(5), 587-592. doi:10.1016/j.pbi.2009.07.015

Pesch, M., & Hülskamp, M. (2011). Role of TRIPTYCHON in trichome patterning in Arabidopsis. *BMC Plant Biol, 11*, 130. doi:10.1186/1471-2229-11-130

Pfaffl, M. W., Tichopad, A., Prgomet, C., & Neuvians, T. P. (2004). Determination of stable housekeeping genes, differentially regulated target genes and sample integrity: BestKeeper--Excel-based tool using pair-wise correlations. *Biotechnol Lett, 26*(6), 509-515. doi:10.1023/b:bile.0000019559.84305.47

Pietsch, J. (2022). *Cross-regulatory interactions of trichome patterning genes in Arabidopsis thaliana and related species.* Universität zu Köln,

Qin, C., Ahanger, M. A., Zhou, J., Ahmed, N., Wei, C., Yuan, S., Ashraf, M., & Zhang, L. (2020). Beneficial role of acetylcholine in chlorophyll metabolism and photosynthetic gas exchange in Nicotiana benthamiana seedlings under salinity stress. *Plant Biol (Stuttg), 22*(3), 357-365. doi:10.1111/plb.13079

Ramsay, N. A., & Glover, B. J. (2005). MYB-bHLH-WD40 protein complex and the evolution of cellular diversity. *Trends Plant Sci, 10*(2), 63-70. doi:10.1016/j.tplants.2004.12.011

Rengasamy, P. (2010). Soil processes affecting crop production in salt-affected soils. *Functional Plant Biology, 37*(7), 613-620.

Rerie, W. G., Feldmann, K. A., & Marks, M. D. (1994). The GLABRA2 gene encodes a homeo domain protein required for normal trichome development in Arabidopsis. *Genes Dev, 8*(12), 1388-1399. doi:10.1101/gad.8.12.1388

Rizza, F., Badeck, F., Cattivelli, L., Lidestri, O., Di Fonzo, N., & Stanca, A. (2004). Use of a water stress index to identify barley genotypes adapted to rainfed and irrigated conditions. *Crop science, 44*(6), 2127-2137.

RStudioTeam. (2015). RStudio: Integrated Development for R. *RStudio Inc., Boston, MA*.

Ruales, J., & Nair, B. M. (1992). Nutritional quality of the protein in quinoa (Chenopodium quinoa, Willd) seeds. *Plant Foods Hum Nutr, 42*(1), 1-11. doi:10.1007/BF02196067

Ruales, J., & Nair, B. M. (1993). Content of fat, vitamins and minerals in quinoa (Chenopodium quinoa, Willd) seeds. *Food Chemistry, 48*(2), 131-136.

Ruiz-Carrasco, K., Antognoni, F., Coulibaly, A. K., Lizardi, S., Covarrubias, A., Martinez, E. A., Molina-Montenegro, M. A., Biondi, S., & Zurita-Silva, A. (2011). Variation in salinity tolerance of four lowland genotypes of quinoa (Chenopodium quinoa Willd.) as assessed by growth, physiological traits, and sodium transporter gene expression. *Plant Physiol Biochem, 49*(11), 1333-1341. doi:10.1016/j.plaphy.2011.08.005

Ruiz, K. B., Aloisi, I., Del Duca, S., Canelo, V., Torrigiani, P., Silva, H., & Biondi, S. (2016). Salares versus coastal ecotypes of quinoa: Salinity responses in Chilean landraces from contrasting habitats. *Plant Physiol Biochem, 101*, 1-13. doi:10.1016/j.plaphy.2016.01.010

Sajjad, A., Munir, H., Ahmed Anjum, S., Tanveer, M., & Rehman, A. (2014). Growth and development of chenopodium quinoa genotypes at different sowing dates. *Journal of Agricultural Research (03681157), 52*(4).

Schellmann, S., Schnittger, A., Kirik, V., Wada, T., Okada, K., Beermann, A., Thumfahrt, J., Jurgens, G., & Hulskamp, M. (2002). TRIPTYCHON and CAPRICE mediate lateral inhibition during trichome and root hair patterning in Arabidopsis. *EMBO J, 21*(19), 5036-5046. doi:10.1093/emboj/cdf524

Schiefelbein, J. (2003). Cell-fate specification in the epidermis: a common patterning mechanism in the root and shoot. *Curr Opin Plant Biol, 6*(1), 74-78. doi:10.1016/s136952660200002x

Schnittger, A., Folkers, U., Schwab, B., Jurgens, G., & Hulskamp, M. (1999). Generation of a spacing pattern: the role of triptychon in trichome patterning in Arabidopsis. *Plant Cell, 11*(6), 1105-1116. doi:10.1105/tpc.11.6.1105

Schofield, R., & Kirkby, M. (2003). Application of salinization indicators and initial development of potential global soil salinization scenario under climatic change. *Global Biogeochemical Cycles, 17*(3).

Seo, E., Lee, H., Jeon, J., Park, H., Kim, J., Noh, Y. S., & Lee, I. (2009). Crosstalk between cold response and flowering in Arabidopsis is mediated through the flowering-time gene SOC1 and its upstream negative regulator FLC. *Plant Cell, 21*(10), 3185-3197. doi:10.1105/tpc.108.063883

Shabala, L., Mackay, A., Tian, Y., Jacobsen, S. E., Zhou, D., & Shabala, S. (2012). Oxidative stress protection and stomatal patterning as components of salinity tolerance mechanism in quinoa (Chenopodium quinoa). *Physiol Plant, 146*(1), 26-38. doi:10.1111/j.1399-3054.2012.01599.x

Shabala, S., Bose, J., & Hedrich, R. (2014). Salt bladders: do they matter? *Trends Plant Sci, 19*(11), 687-691. doi:10.1016/j.tplants.2014.09.001

Shabala, S., & Mackay, A. (2011). Ion transport in halophytes. In *Advances in botanical research* (Vol. 57, pp. 151-199): Elsevier.

Shetty, D. (2024). A lack of quality statistics is hiding the real heatwave death toll. *BMJ, 385*.

Short, F. T., & Neckles, H. A. (1999). The effects of global climate change on seagrasses. *Aquatic Botany, 63*(3-4), 169-196.

Silver, N., Best, S., Jiang, J., & Thein, S. L. (2006). Selection of housekeeping genes for gene expression studies in human reticulocytes using real-time PCR. *BMC Mol Biol, 7*, 33. doi:10.1186/1471-2199-7-33

Singh, P., & Mustapha, A. (2014). Development of a real-time PCR melt curve assay for simultaneous detection of virulent and antibiotic resistant Salmonella. *Food Microbiol, 44*, 6-14. doi:10.1016/j.fm.2014.04.014

Skiljaica, A., Jagic, M., Vuk, T., Leljak Levanic, D., Bauer, N., & Markulin, L. (2022). Evaluation of reference genes for RT-qPCR gene expression analysis in Arabidopsis thaliana exposed to elevated temperatures. *Plant Biol (Stuttg), 24*(2), 367-379. doi:10.1111/plb.13382

Sletvold, N., & Ågren, J. (2012). Variation in tolerance to drought among Scandinavian populations of Arabidopsis lyrata. *Evolutionary Ecology, 26*, 559-577.

Smaoui, A., Barhoumi, Z., Rabhi, M., & Abdelly, C. (2011). Localization of potential ion transport pathways in vesicular trichome cells of Atriplex halimus L. *Protoplasma, 248*(2), 363-372. doi:10.1007/s00709-010-0179-8

Somero, G. N. (2010). The physiology of climate change: how potentials for acclimatization and genetic adaptation will determine 'winners' and 'losers'. *J Exp Biol, 213*(6), 912-920. doi:10.1242/jeb.037473

Srikanth, S., Lum, S. K. Y., & Chen, Z. (2016). Mangrove root: adaptations and ecological importance. *Trees, 30*, 451-465.

Stephan, L., Tilmes, V., & Hulskamp, M. (2019). Selection and validation of reference genes for quantitative Real-Time PCR in Arabis alpina. *PLoS One, 14*(3), e0211172. doi:10.1371/journal.pone.0211172

Storchova, H., Drabesova, J., Chab, D., Kolar, J., & Jellen, E. N. (2015). The introns in FLOWERING LOCUS T-LIKE (FTL) genes are useful markers for tracking paternity in

tetraploid Chenopodium quinoa Willd. *Genetic Resources and Crop Evolution, 62*(6), 913-925. doi:10.1007/s10722-014-0200-8

Sultan, S. E. (2000). Phenotypic plasticity for plant development, function and life history. *Trends Plant Sci, 5*(12), 537-542. doi:10.1016/s1360-1385(00)01797-0

Suo, B., Seifert, S., & Kirik, V. (2013). Arabidopsis GLASSY HAIR genes promote trichome papillae development. *J Exp Bot, 64*(16), 4981-4991. doi:10.1093/jxb/ert287

Symonds, V. V., Hatlestad, G., & Lloyd, A. M. (2011). Natural allelic variation defines a role for ATMYC1: trichome cell fate determination. *PLoS Genet, 7*(6), e1002069. doi:10.1371/journal.pgen.1002069

Talbot, C. J., Bennett, E. M., Cassell, K., Hanes, D. M., Minor, E. C., Paerl, H., Raymond, P. A., Vargas, R., Vidon, P. G., & Wollheim, W. (2018). The impact of flooding on aquatic ecosystem services. *Biogeochemistry, 141*, 439-461.

Thieme, M., Brechet, A., Bourgeois, Y., Keller, B., Bucher, E., & Roulin, A. C. (2022). Experimentally heat-induced transposition increases drought tolerance in Arabidopsis thaliana. *New Phytol, 236*(1), 182-194. doi:10.1111/nph.18322

Thomson, W., Faraday, C., & Oross, J. (1988). Salt glands. In 'Solute transport in plant cells and tissues'.(Eds D Baker, J Hall) pp. 498–537. In: Longman: Harlow, UK.

Tian, M., & Ye, S. (2017). Design of Light-Sensitive NMDARs by Genetically Encoded Photo-Cross-Linkers. *Methods Mol Biol, 1677*, 185-197. doi:10.1007/978-1-4939-7321-7_10

Tigue, K. (2024). Clean Energy Debate Reignites After Texas Endures Another Brutal Cold Snap. *InsideClimate News*, NA-NA.

Tominaga-Wada, R., Ishida, T., & Wada, T. (2011). New insights into the mechanism of development of Arabidopsis root hairs and trichomes. *Int Rev Cell Mol Biol, 286*, 67-106. doi:10.1016/B978-0-12-385859-7.00002-1

Tominaga-Wada, R., & Wada, T. (2017). Extended C termini of CPC-LIKE MYB proteins confer functional diversity in Arabidopsis epidermal cell differentiation. *Development, 144*(13), 2375-2380. doi:10.1242/dev.149542

Traas, J., Hulskamp, M., Gendreau, E., & Hofte, H. (1998). Endoreduplication and development: rule without dividing? *Curr Opin Plant Biol, 1*(6), 498-503. doi:10.1016/s1369-5266(98)80042-3

Trenberth, K. E. (2011). Changes in precipitation with climate change. *Climate research, 47*(1-2), 123-138.

Valladares, F., & Niinemets, Ü. (2008). Shade tolerance, a key plant feature of complex nature and consequences. *Annual Review of Ecology, Evolution, and Systematics, 39*(1), 237-257.

Vandesompele, J., De Preter, K., Pattyn, F., Poppe, B., Van Roy, N., De Paepe, A., & Speleman, F. (2002). Accurate normalization of real-time quantitative RT-PCR data by geometric averaging of multiple internal control genes. *Genome Biol, 3*(7), RESEARCH0034. doi:10.1186/gb-2002-3-7-research0034

Walbot, V. (1992). Reactivation of Mutator transposable elements of maize by ultraviolet light. *Molecular and General Genetics MGG, 234*, 353-360.

Walker, A. R., Davison, P. A., Bolognesi-Winfield, A. C., James, C. M., Srinivasan, N., Blundell, T. L., Esch, J. J., Marks, M. D., & Gray, J. C. (1999). The TRANSPARENT TESTA GLABRA1 locus, which regulates trichome differentiation and anthocyanin biosynthesis in Arabidopsis, encodes a WD40 repeat protein. *Plant Cell, 11*(7), 1337-1350.

Wang, L., Ma, K. B., Lu, Z. G., Ren, S. X., Jiang, H. R., Cui, J. W., Chen, G., Teng, N. J., Lam, H. M., & Jin, B. (2020a). Differential physiological, transcriptomic and metabolomic responses of Arabidopsis leaves under prolonged warming and heat shock. *BMC Plant Biol, 20*(1), 86. doi:10.1186/s12870-020-2292-y

Wang, S., Kwak, S. H., Zeng, Q., Ellis, B. E., Chen, X. Y., Schiefelbein, J., & Chen, J. G. (2007). TRICHOMELESS1 regulates trichome patterning by suppressing GLABRA1 in Arabidopsis. *Development, 134*(21), 3873-3882. doi:10.1242/dev.009597

Wang, X., Li, Z., Liu, B., Zhou, H., Elmongy, M. S., & Xia, Y. (2020b). Combined Proteome and Transcriptome Analysis of Heat-Primed Azalea Reveals New Insights Into Plant Heat Acclimation Memory. *Front Plant Sci, 11*, 1278. doi:10.3389/fpls.2020.01278

Wang, X., Vignjevic, M., Liu, F., Jacobsen, S., Jiang, D., & Wollenweber, B. (2015a). Drought priming at vegetative growth stages improves tolerance to drought and heat stresses occurring during grain filling in spring wheat. *Plant Growth Regulation, 75*, 677-687.

Wang, X., Wang, X., Hu, Q., Dai, X., Tian, H., Zheng, K., Wang, X., Mao, T., Chen, J. G., & Wang, S. (2015b). Characterization of an activation-tagged mutant uncovers a role of GLABRA2 in anthocyanin biosynthesis in Arabidopsis. *Plant J, 83*(2), 300-311. doi:10.1111/tpj.12887

Winter, D., Vinegar, B., Nahal, H., Ammar, R., Wilson, G. V., & Provart, N. J. (2007). An "Electronic Fluorescent Pictograph" browser for exploring and analyzing large-scale biological data sets. *PLoS One, 2*(8), e718. doi:10.1371/journal.pone.0000718

Xiao, K., Mao, X., Lin, Y., Xu, H., Zhu, Y., Cai, Q., Xie, H., & Zhang, J. (2017). Trichome, a functional diversity phenotype in plant. *Mol Biol, 6*(1), 183.

Xie, F., Xiao, P., Chen, D., Xu, L., & Zhang, B. (2012). miRDeepFinder: a miRNA analysis tool for deep sequencing of plant small RNAs. *Plant Mol Biol*. doi:10.1007/s11103-012-9885-2

Xu, C., & Min, J. (2011). Structure and function of WD40 domain proteins. *Protein Cell, 2*(3), 202-214. doi:10.1007/s13238-011-1018-1

Xu, M. Y., Zhang, L., Li, W. W., Hu, X. L., Wang, M. B., Fan, Y. L., Zhang, C. Y., & Wang, L. (2014). Stress-induced early flowering is mediated by miR169 in Arabidopsis thaliana. *J Exp Bot, 65*(1), 89-101. doi:10.1093/jxb/ert353

Yan, A., Pan, J., An, L., Gan, Y., & Feng, H. (2012). The responses of trichome mutants to enhanced ultraviolet-B radiation in Arabidopsis thaliana. *Journal of Photochemistry and Photobiology B: Biology, 113*, 29-35.

Yang, C., Liu, J., Dong, X., Cai, Z., Tian, W., & Wang, X. (2014). Short-term and continuing stresses differentially interplay with multiple hormones to regulate plant survival and growth. *Mol Plant, 7*(5), 841-855. doi:10.1093/mp/ssu013

Yuan, F., Leng, B., & Wang, B. (2016). Progress in Studying Salt Secretion from the Salt Glands in Recretohalophytes: How Do Plants Secrete Salt? *Front Plant Sci, 7*, 977. doi:10.3389/fpls.2016.00977

Zeng, F., Shabala, S., Maksimovic, J. D., Maksimovic, V., Bonales-Alatorre, E., Shabala, L., Yu, M., Zhang, G., & Zivanovic, B. D. (2018). Revealing mechanisms of salinity tissue tolerance in succulent halophytes: A case study for Carpobrotus rossi. *Plant Cell Environ, 41*(11), 2654-2667. doi:10.1111/pce.13391

Zhang, B., & Schrader, A. (2017). TRANSPARENT TESTA GLABRA 1-Dependent Regulation of Flavonoid Biosynthesis. *Plants (Basel), 6*(4). doi:10.3390/plants6040065

Zhang, F., Gonzalez, A., Zhao, M., Payne, C. T., & Lloyd, A. (2003). A network of redundant bHLH proteins functions in all TTG1-dependent pathways of Arabidopsis. *Development, 130*(20), 4859-4869. doi:10.1242/dev.00681

Zhang, X., Wang, X., Zhuang, L., Gao, Y., & Huang, B. (2019). Abscisic acid mediation of drought priming-enhanced heat tolerance in tall fescue (Festuca arundinacea) and Arabidopsis. *Physiol Plant, 167*(4), 488-501. doi:10.1111/ppl.12975

Zhao, H., Wang, X., Zhu, D., Cui, S., Li, X., Cao, Y., & Ma, L. (2012). A single amino acid substitution in IIIf subfamily of basic helix-loop-helix transcription factor AtMYC1 leads to trichome and root hair patterning defects by abolishing its interaction with partner proteins in Arabidopsis. *J Biol Chem, 287*(17), 14109-14121. doi:10.1074/jbc.M111.280735

Zhao, M., Morohashi, K., Hatlestad, G., Grotewold, E., & Lloyd, A. (2008). The TTG1-bHLH-MYB complex controls trichome cell fate and patterning through direct targeting of regulatory loci. *Development, 135*(11), 1991-1999. doi:10.1242/dev.016873

Zheng, X. T., Yu, Z. C., Tang, J. W., Cai, M. L., Chen, Y. L., Yang, C. W., Chow, W. S., & Peng, C. L. (2021). The major photoprotective role of anthocyanins in leaves of Arabidopsis thaliana under long-term high light treatment: antioxidant or light attenuator? *Photosynth Res, 149*(1-2), 25-40. doi:10.1007/s11120-020-00761-8

Zimmerli, L., Jakab, G., Metraux, J. P., & Mauch-Mani, B. (2000). Potentiation of pathogen-specific defense mechanisms in Arabidopsis by beta -aminobutyric acid. *Proc Natl Acad Sci U S A, 97*(23), 12920-12925. doi:10.1073/pnas.230416897

8 Appendix

8.1 Intercalation in MBW mutants

Benjamin Jaegle investigated intercalating trichomes in various MBW mutants as part of his doctoral thesis. A section of the results is shown below (Figure 25). Intercalation was tracked over four days and the percentage of intercalating trichomes is shown in yellow.

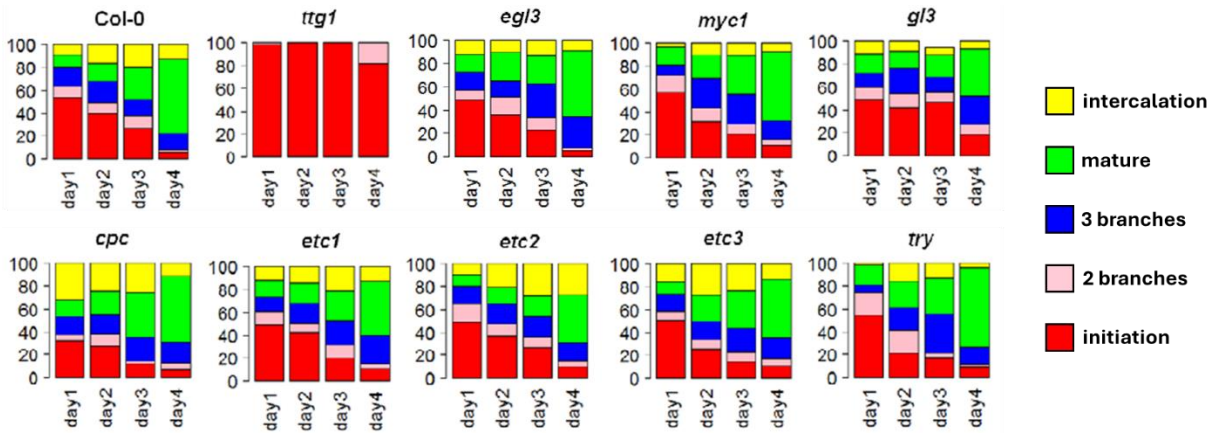

Figure 25: Types of developed trichomes over the course of four days in different MBW mutants. Leaf observation started when the number of mature trichomes ranged between one and six. The y-axis represents the respective share of the trichome stage in percent. Intercalating trichomes are shown in yellow. Modified from Jaegle, 2015.

8.2 Trichome intercalation under various light conditions

Representative images of the intercalation evaluation of trichomes are shown below (Figure 26). Col-0 leaves were exposed to control (120 µmol/m²s) or light stress conditions (30, 60, 90 and 400 µmol/m²s). Leaf three was analyzed when reaching a size of 300 to 400 µm. Intercalation trichomes, developing above the initiation zone, are marked with a red x.

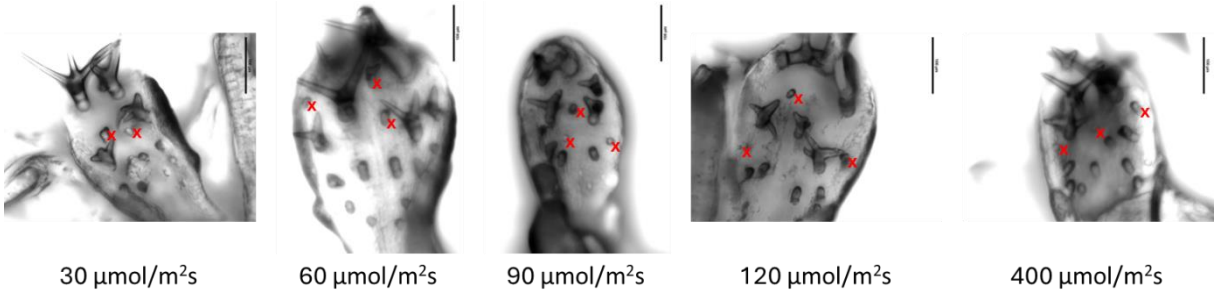

Figure 26: Intercalating trichomes under various light conditions. Intercalating trichomes are marked with a red x. The scale bar is set to 100 µm.

8.3 The trichome number does not increase over time

The number of trichomes was determined two additional weeks after the initial analysis (Figure 27) to investigate whether it increases over time. Since plant development progresses more slowly under low-light conditions, trichome formation could be specifically delayed under these conditions. The number of trichomes from the first analysis was compared to an additional analysis after two more weeks, when the same leaves were counted for a second time. It was shown that the number of trichomes does not differ between the first and second count. Therefore, no further trichomes are formed, even under low-light conditions.

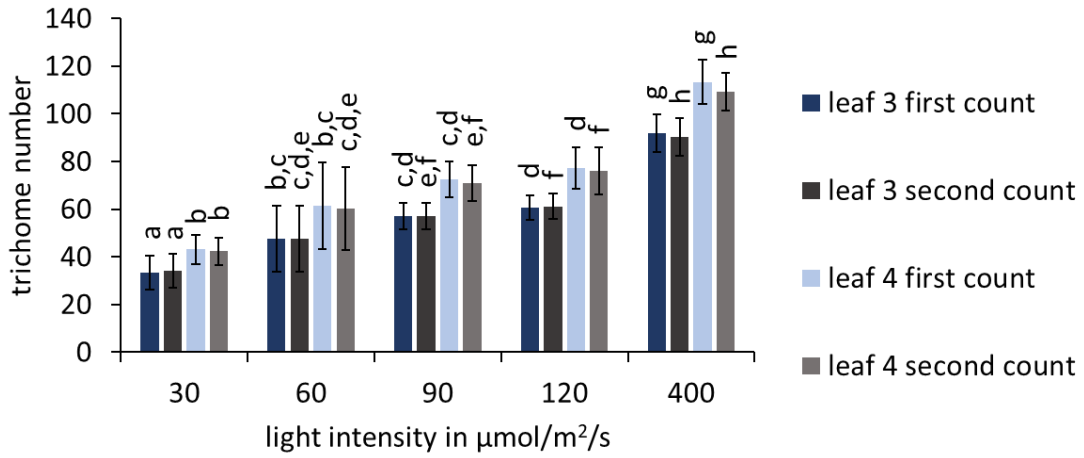

Figure 27: Number of trichomes after two additional weeks. Comparison of trichome number between the first and second counting event. Plants were either grown under low-light (30, 60, 90 µmol/m²s), control (120 µmol/m²s) or high-light (400 µmol/m²s) conditions after stratification. Error bars depict the standard deviation; n ≥ 20 replicates; lowercase letters indicate significance groups; significance was tested using Welch-ANOVA and Games-Howell post-hoc test at a level of $p < 0.05$.

8.4 qPCR analysis of young *A. thaliana* leaves under different stress regimes

Met curve plots, normalized relative expression differences and expression change data can be found in the following figures and the table.

8.4.1 Melt curve plots of primer pairs tested for efficiency during this study

To ensure that the selected primer pairs are suitable for qPCR analysis, the melt curve plots (Figure 28), provided by the QuantStudioTM Design & Analysis Software, were evaluated during the efficiency testing. Melt curve plots showing a single tight peak, exclude the occurrence of primer dimers, which would be visible as an additional or a wavy shape of the peak. In the melt curve plot the derivative reporter (−Rn') is plotted against the temperature in C°, which visualized the maximum rate of change in fluorescence during the temperature rise (Forghani et al., 2016; Singh & Mustapha, 2014).

Melt Curve Plot MYB5

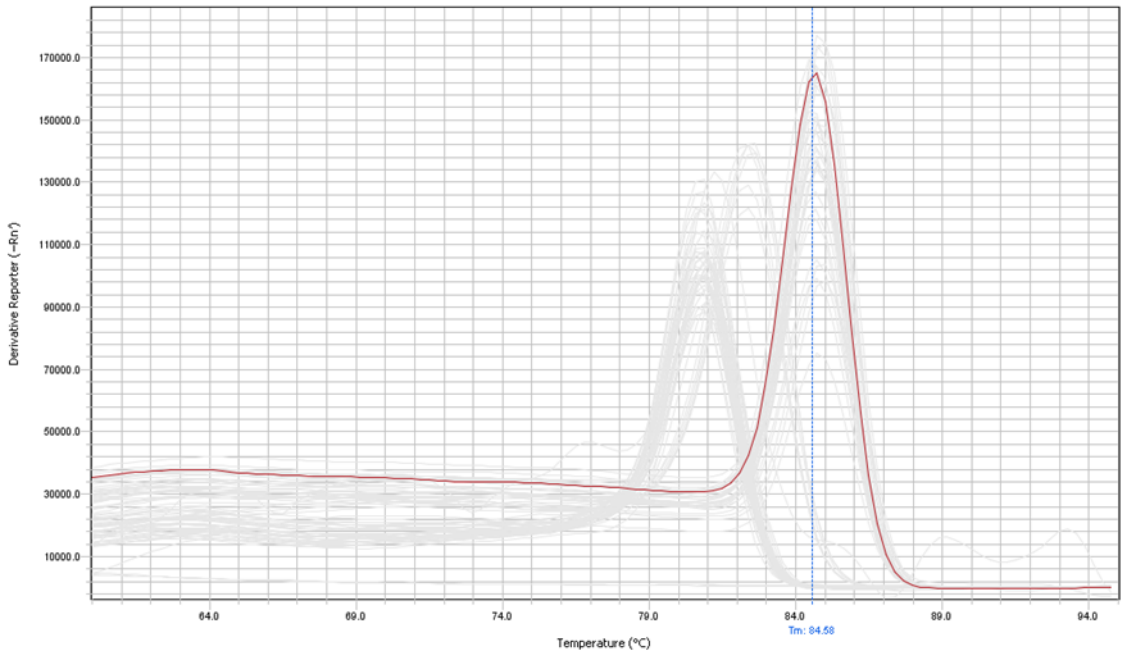

Melt Curve Plot MYB82

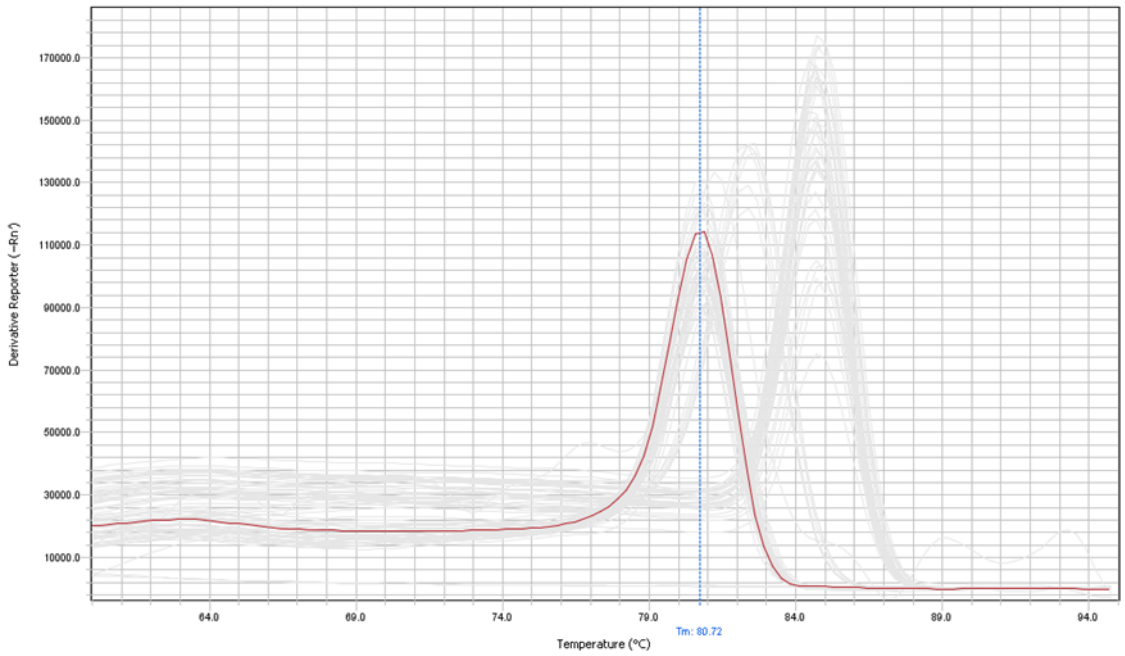

Melt Curve Plot PAP1

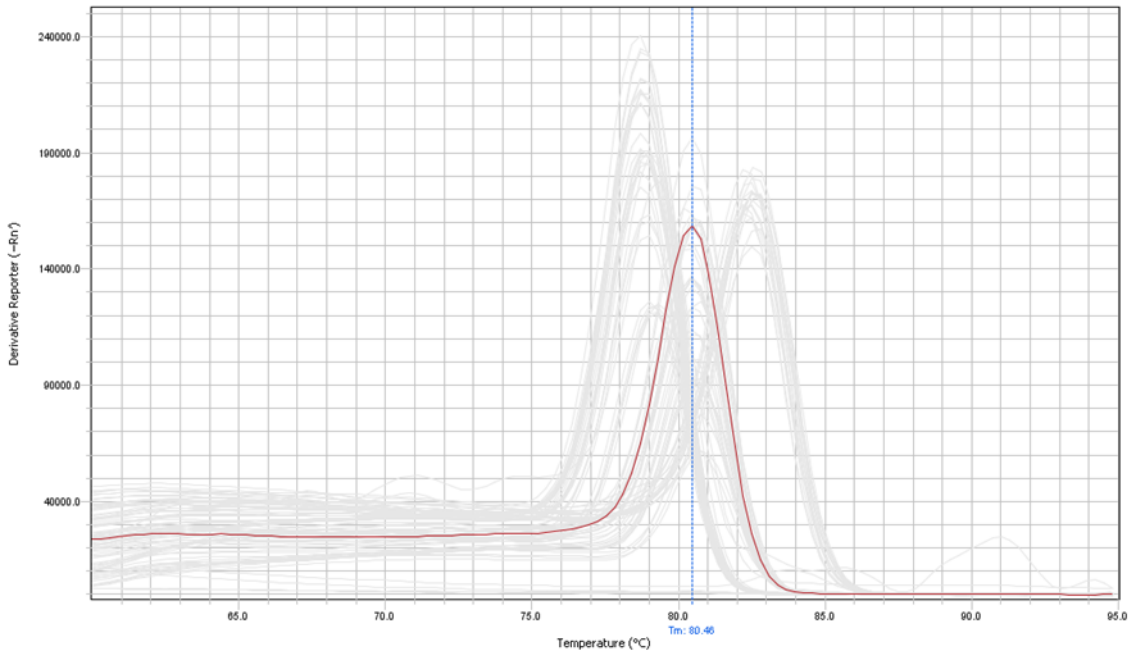

Melt Curve Plot PAP2

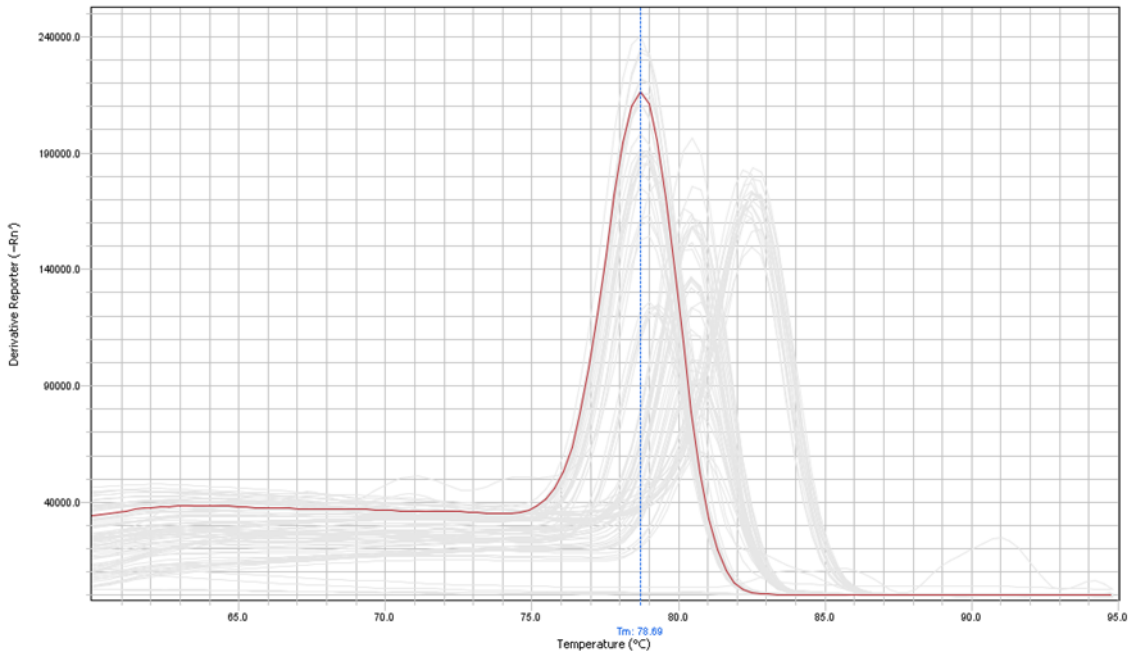

Melt Curve Plot TT2

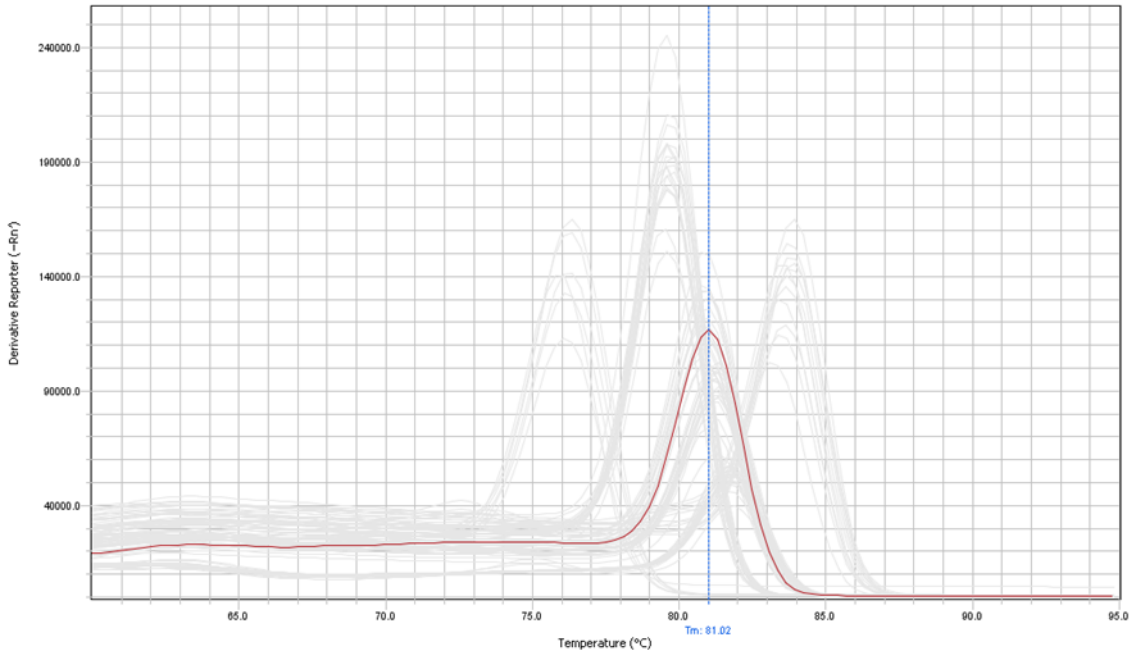

Melt Curve Plot TT8

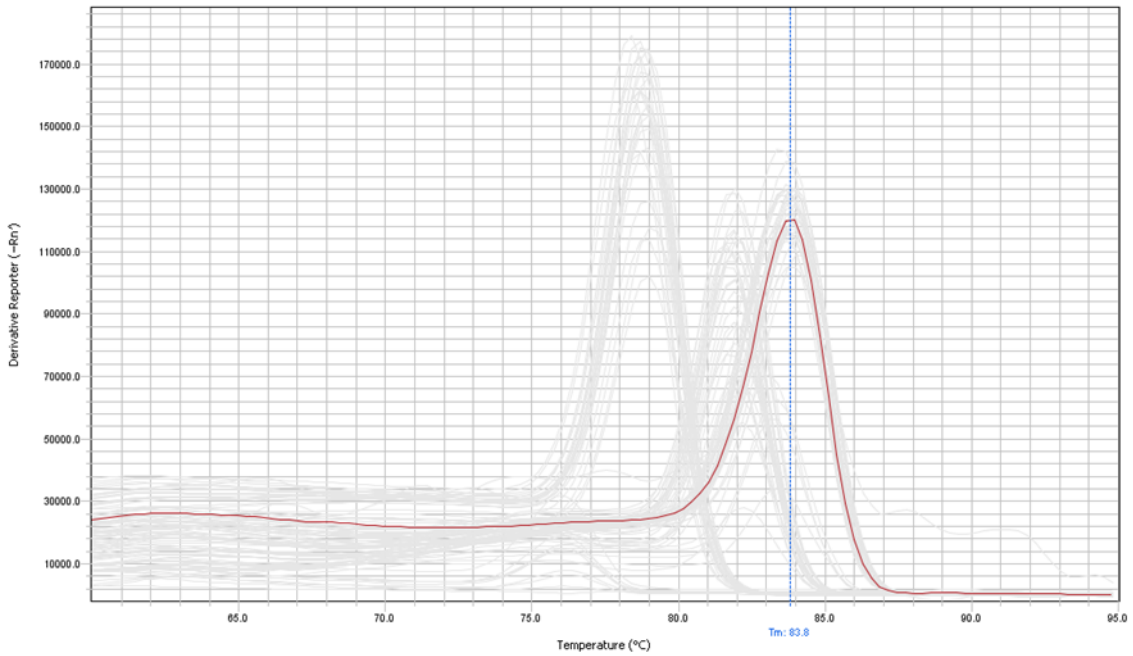

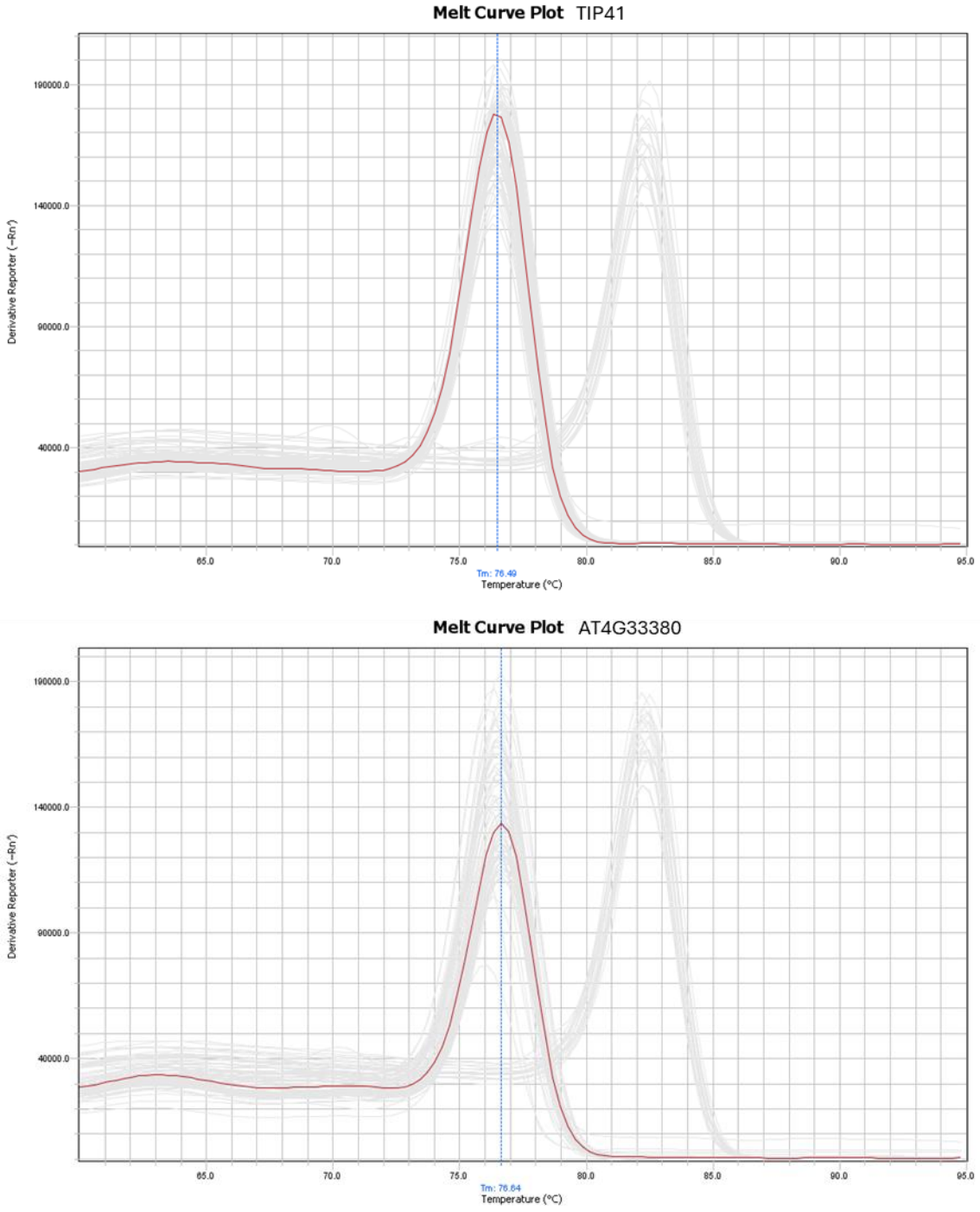

Figure 28: Melt curve plots of MYB5, MYB82, PAP1, PAP2, TT2, TT8, TIP41 and AT4g33380. Melt curve plots were extracted from the QuantStudioTM Design & Analysis Software.

8.4.2 Normalized relative expression differences of stress treated Col-0 plants

The following shows the normalized expression differences for Col-0 under different abiotic stress conditions such as different light intensity and heat (38 °C). The sampling was based on the plant stage, as the plants grow slower or faster under constant low- (30 µmol/m^{2}s) or high-light (400 µmol/m^{2}s), therefore the same day is not suitable for sampling. For the stress treatments with low- or high-light the plants were either grown under the conditions from the

start or were transferred from the control conditions (120 µmol/m^{2}s) to the low- or high-light conditions and stressed for 6 hours. The heat samples were first grown under control conditions and then stressed in an incubator for 3 hours at 38 °C, and afterwards returned to control conditions for 3 hours. Kilian and colleagues showed that this time point after heat stress had the most expression changes (Kilian et al., 2007). All samples were harvested at the same time of the day.

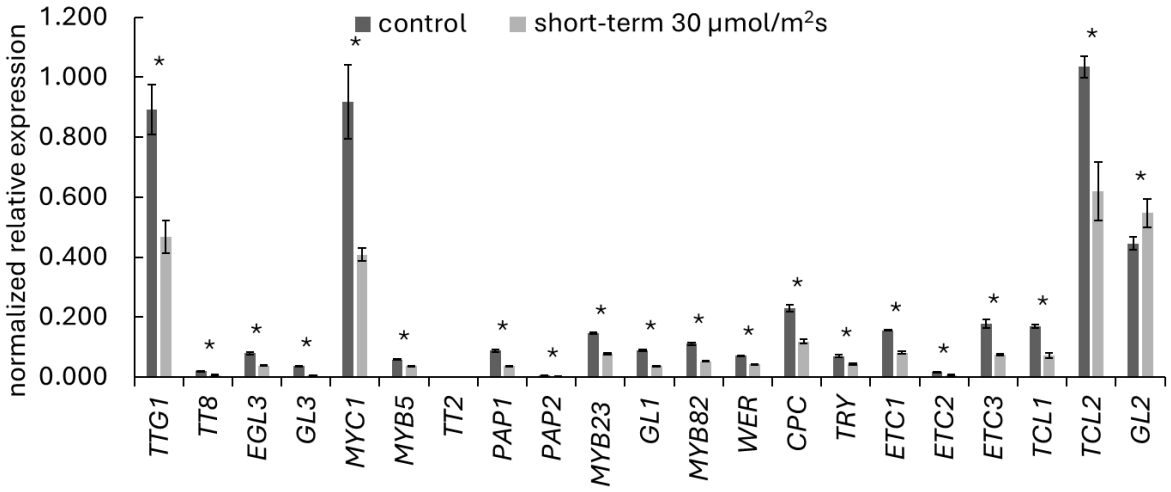

Figure 29: Relative expression differences under 6 hours low-light conditions. cDNA from control and stress treated young Col-0 leaves (40 single plants per rep), harvested after eight days at 22 ± 2 °C and control (120 µmol/m^{2}s) or short-term stress conditions (6 h at 30 µmol/m^{2}s), were tested for the expression of the MBW genes via qPCR. All values were normalized to the two reference genes *TIP41* and *AT4G33380*. Error bars depict the standard deviation; *n* = 3 replicates; * indicate significant differences; significance was tested using Mann Whitney U test at a level of $p < 0.1$.

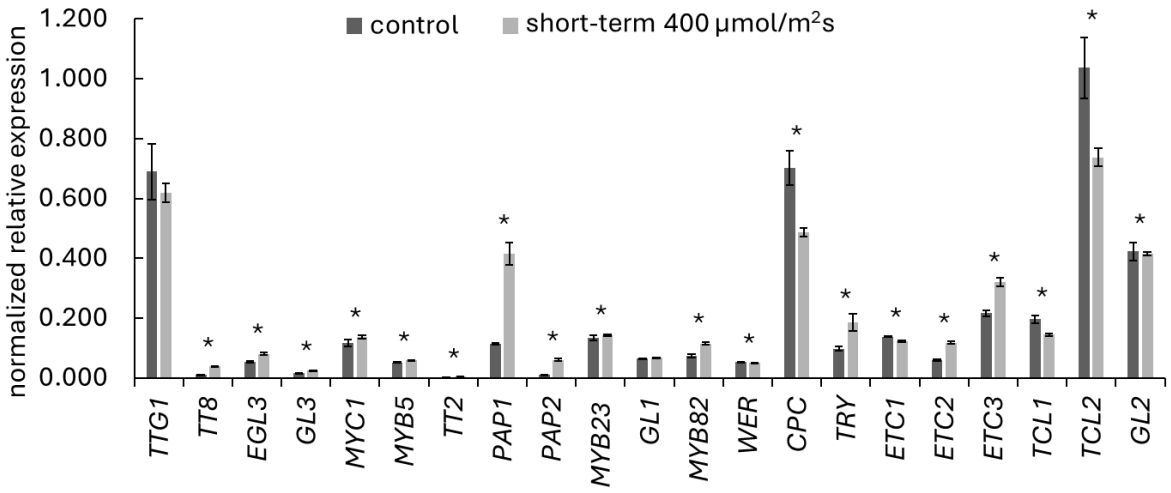

Figure 30: Relative expression differences under 6 hours high-light conditions. cDNA from control and stress treated young Col-0 leaves (40 single plants per rep), harvested after eight days at 22 ± 2 °C and control (120 µmol/m^{2}s) or short-term stress conditions (6 h at 400 µmol/m^{2}s), were tested for the expression of the MBW genes via qPCR. All values were normalized to the two reference genes *TIP41* and *AT4G33380*. Error bars depict the standard deviation; *n* = 3 replicates; * indicate significant differences; significance was tested using Mann Whitney U test at a level of $p < 0.1$.

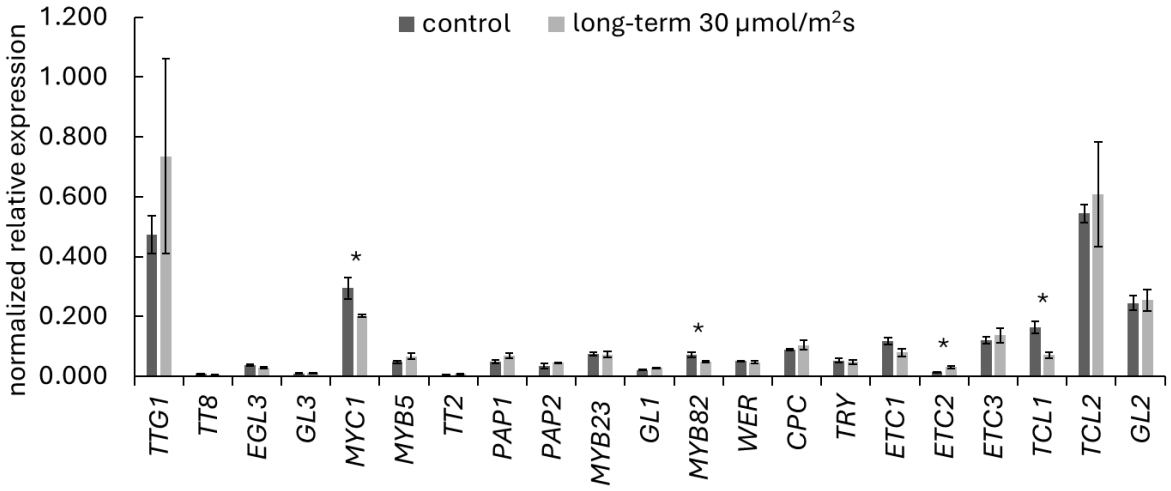

Figure 31: Relative expression differences under twelve days low-light conditions. cDNA from control and stress treated young Col-0 leaves (40 single plants per rep), harvested after eight (control) or twelve (stress) days at 22 ± 2 °C and 120 (control) or 30 (stress) µmol/m²s, were tested for the expression of the MBW genes via qPCR. All values were normalized to the two reference genes *TIP41* and *AT4G33380*. Error bars depict the standard deviation; *n* = 3 replicates; * indicate significant differences; significance was tested using Mann Whitney U test at a level of $p < 0.1$.

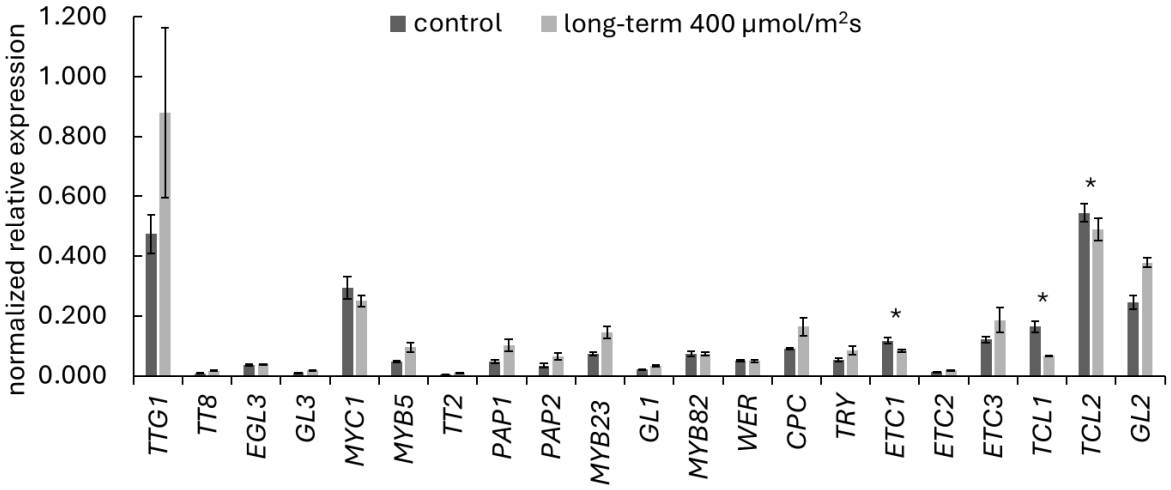

Figure 32: Relative expression differences under six days high-light conditions. cDNA from control and stress treated young Col-0 leaves (40 single plants per rep), harvested after eight (control) or six (stress) days at 22 ± 2 °C and 120 (control) or 400 (stress) µmol/m²s, were tested for the expression of the MBW genes via qPCR. All values were normalized to the two reference genes *TIP41* and *AT4G33380*. Error bars depict the standard deviation; *n* = 3 replicates; * indicate significant differences; significance was tested using Mann Whitney U test at a level of $p < 0.1$.

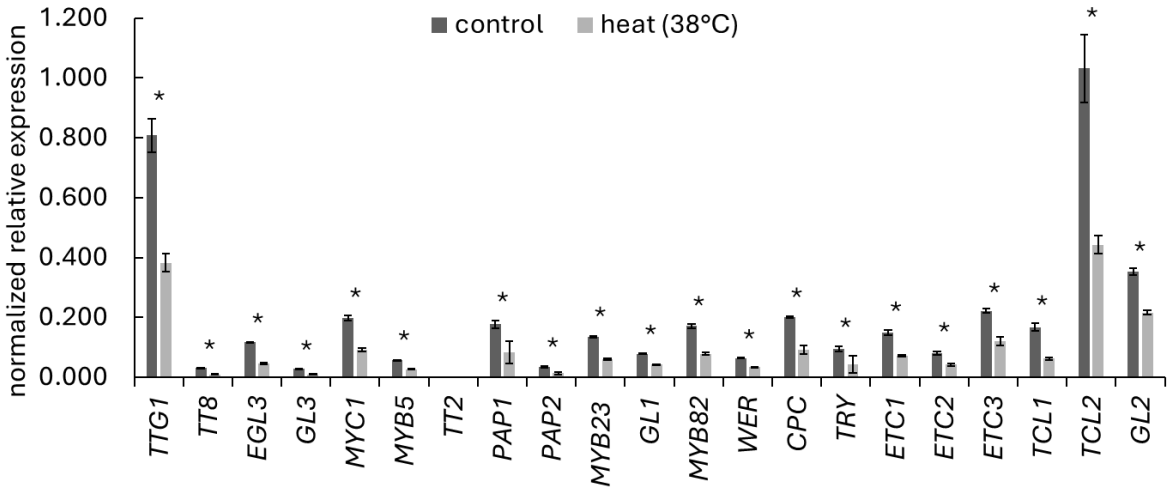

Figure 33: Relative expression differences under 3 hours heat stress. cDNA from control and stress treated young Col-0 leaves (40 single plants per rep), harvested after eight days at 22 ± 2 °C and 120 µmol/m²s (control) or heat stress conditions (3 h at 38°C, 3 h back to control conditions), were tested for the expression of the MBW genes via qPCR. All values were normalized to the two reference genes *PSB33* and *AT4G33380*. Error bars depict the standard deviation; *n* = 3 replicates; * indicate significant differences; significance was tested using Mann Whitney U test at a level of $p < 0.1$.

8.4.3 Expression change

By calculating the fold change, the expression change was determined for the different stress treatments compared to control conditions.

Table 9: Expression changes within the various stress experiments. WD40 (blue), bHLH (light green), R2R3-MYB (orange), inhibitors (red), *GL2* (grey), green background = significant differences and at least doubling of expression, light red background = significant differences and at least halving of expression. *n* = 3 replicates; significance was tested using Mann Whitney U test at a level of $p < 0.1$.

expression change	short-term light 30 µmol/m²s	short-term light 400 µmol/m²s	long-term light 30 µmol/m²s	long-term light 400 µmol/m²s	short-term heat 38 °C
TTG1	0.525	0.898	1.552	1.441	0.474
TT8	0.347	3.867	0.615	1.542	0.290
EGL3	0.475	1.518	0.808	0.833	0.394
GL3	0.155	1.655	1.142	1.483	0.342
MYC1	0.445	1.186	0.687	0.851	0.459
MYB5	0.633	1.138	1.414	1.620	0.467
TT2	0.667	2.959	1.872	1.558	0.852
PAP1	0.416	3.673	1.410	1.677	0.477
PAP2	0.414	5.431	1.299	1.500	0.424
MYB23	0.528	1.058	0.989	1.578	0.442
GL1	0.426	1.042	1.287	1.231	0.538
MYB82	0.470	1.548	0.663	0.798	0.460
WER	0.589	0.935	0.933	0.787	0.524
CPC	0.519	0.694	1.166	1.439	0.452
TRY	0.619	1.888	0.900	1.261	0.452
ETC1	0.519	0.886	0.678	0.546	0.484
ETC2	0.433	1.954	2.218	1.010	0.530

ETC3	0.420	1.478	1.128	1.229	0.541
TCL1	0.424	0.739	0.433	0.310	0.377
TCL2	0.599	0.711	1.118	0.715	0.430
GL2	1.227	0.981	1.037	1.258	0.612

8.5 *C. quinoa* number of leaves at the time of bolting

To determine the flowering time, the number of leaves at the time of bolting was recorded in *C. quinoa*. Figure 34 showed that the number of leaves, for most treatments, was consistent, only when seeds were treated with 300 mM NaCl, a significantly lower number of leaves was observed. The number of seeds was reduced to eight, while on average the number of leaves was around 13 at the time of bolting.

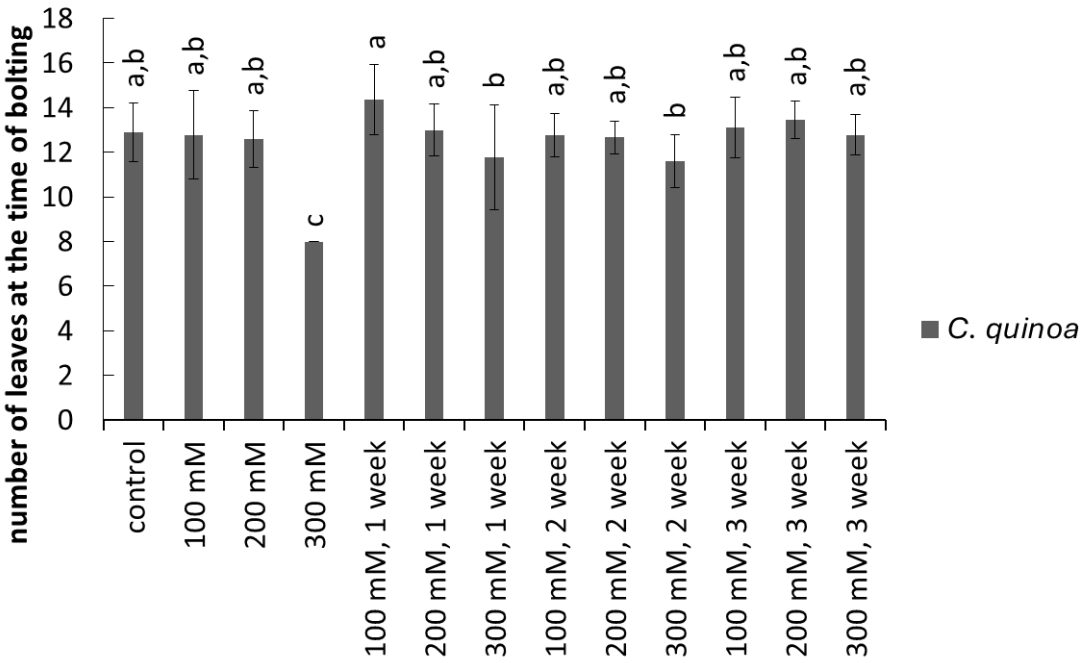

Figure 34: Flowering time in *C. quinoa* under salt stress. Seeds/seedlings were either germinated under control (0 mM NaCl) or exposed to salt stress conditions (100, 200, 300 mM NaCl) right from the seed stage or after one, two or three weeks. Plants were watered with the appropriate amount of salt solution three time a week. Displayed is the number of leaves at the time of bolting. Error bars depict the standard deviation; n = 10 replicates; lowercase letters indicate significance groups; significance was tested using One-way ANOVA with post-hoc Tukey HSD test at a level of $p < 0.05$.

9 Declaration of academic integrity

„Hiermit versichere ich an Eides statt, dass ich die vorliegende Dissertation selbstständig und ohne die Benutzung anderer als der angegebenen Hilfsmittel und Literatur angefertigt habe. Alle Stellen, die wörtlich oder sinngemäß aus veröffentlichten und nicht veröffentlichten Werken dem Wortlaut oder dem Sinn nach entnommen wurden, sind als solche kenntlich gemacht. Ich versichere an Eides statt, dass diese Dissertation noch keiner anderen Fakultät oder Universität zur Prüfung vorgelegen hat; dass sie - abgesehen von unten angegebenen Teilpublikationen und eingebundenen Artikeln und Manuskripten - noch nicht veröffentlicht worden ist sowie, dass ich eine Veröffentlichung der Dissertation vor Abschluss der Promotion nicht ohne Genehmigung des Promotionsausschusses vornehmen werde. Die Bestimmungen dieser Ordnung sind mir bekannt. Darüber hinaus erkläre ich hiermit, dass ich die Ordnung zur Sicherung guter wissenschaftlicher Praxis und zum Umgang mit wissenschaftlichem Fehlverhalten der Universität zu Köln gelesen und sie bei der Durchführung der Dissertation zugrundeliegenden Arbeiten und der schriftlich verfassten Dissertation beachtet habe und verpflichte mich hiermit, die dort genannten Vorgaben bei allen wissenschaftlichen Tätigkeiten zu beachten und umzusetzen. Ich versichere, dass die eingereichte elektronische Fassung der eingereichten Druckfassung vollständig entspricht."

Teilpublikationen:

- keine -

Köln, 31.08.2024

Unterschrift: Barbara Paffendorf